Analysis of the Effect of Corrosion on the Surface Chemistry of Mild Steel Exposed to Biofuel

THESIS

Timothy D. Plourde, Captain, USAF

AFIT-ENV-MS-19-M-193

DEPARTMENT OF THE AIR FORCE
AIR UNIVERSITY

AIR FORCE INSTITUTE OF TECHNOLOGY

Wright-Patterson Air Force Base, Ohio

The views expressed in this thesis are those of the author and do not reflect the official policy or position of the United States Air Force, Department of Defense, or the United States Government.

AFIT/GEM/ENV/19M

ANALYSIS OF THE EFFECT OF CORROSION ON THE SURFACE CHEMISTRY OF MILD STEEL EXPOSED TO BIOFUEL

THESIS

Presented to the Faculty

Department of Systems & Engineering Management

Graduate School of Engineering and Management

Air Force Institute of Technology

Air University

Air Education and Training Command

In Partial Fulfillment of the Requirements for the

Degree of Master of Science in Engineering Management

Timothy D. Plourde, BS

Captain, USAF

January, 2019

AFIT/GEM/ENV/19M

ANALYSIS OF THE EFFECT OF CORROSION ON THE SURFACE CHEMISTRY OF MILD STEEL EXPOSED TO BIOFUEL

Timothy D. Plourde, BS
Captain, USAF

Approved:

_____	_____
Jeremy M. Slagley, PhD (Chairman)	Date
_____	_____
Daniel L. Felker, PhD (Member)	Date
_____	_____
Andrew Hoisington, Lt Col, USAF (Member)	Date
_____	_____
Caitlin Bojanowski, PhD (Member)	Date

Abstract

The use of biofuels in society is steadily becoming more prevalent. Through this proliferation a concern regarding the role of the fungus *Byssochlamys nivea* in microbially induced corrosion has surfaced. Through the use of X-ray Photoelectron Spectroscopy (XPS) and Scanning Electron Microscope (SEM) technology, this thesis focused on attempting to determine what effect, if any, *Byssochlamys nivea* has on the corrosion of mild steel. For this analysis, samples were placed in environments that simulated the conditions of fuel tanks containing the biofuel B20, water, and spores of *Byssochlamys nivea* for varying lengths of time. However, due to a variety of complicating factors involving the development of the samples analyzed in this thesis, no clear determination can be drawn about the influence of *Byssochlamys nivea* on mild steel. Some evidence may point towards microbially induced corrosion occurring in the form of iron reduction, however no conclusive statements on such a matter can be claimed, due to the lack of a comparable control. As such, the findings of this thesis ultimately describe the methods by which future researchers should carry out the preparation and execution of the experiment and analysis of samples in order to successfully identify any microbially influenced corrosion in mild steel that results from direct influence from the fungus *Byssochlamys nivea*.

Dedicated to my Wife,
whose love and compassion has rekindled
a once dormant flame of passion within me.

Acknowledgments

I would like to thank all of the members of my committee for taking time to review my thesis and for providing advice and support. In particular, I would like to thank Dr. Bojanowski and the staff at AFRL for their assistance in developing samples and experiments. Additionally, I would like to express my appreciation towards Dr. Slagley for the opportunity to work on such an interesting topic and with such amazing people. Likewise, I would like to extend my sincere gratitude to Dr. Felker for his ceaseless support and wisdom. His endless time and effort in the laboratory teaching me about the XPS and the SEM was extremely appreciated and helped me make significant contributions towards completing my thesis. Finally, and most importantly, I am extremely grateful towards my wife Shoko. Without her constant love, emotional support, and patience, I would not be who I am today.

Timothy D. Plourde

Table of Contents

Page

List of Figures

Page

List of Tables

List of Equations

ANALYSIS OF THE EFFECT OF CORROSION ON THE SURFACE CHEMISTRY OF FUEL LINES CONTAINING BIOFUEL

I. Introduction

Background

The United States Air Force (USAF) owns and operates approximately $1.77 billion of real property fuel tanks (US Air Force, 2016). Considering both the substantial amount of money associated with these assets, as well as their inherent importance to the mission of the Air Force, these resources are considerably important to both the USAF and the Department of Defense (DoD). Through the operation of this fuel infrastructure, water will eventually enter into the system; this typically occurs through the infrastructure being exposed to precipitation or through the condensation of water in the air (J. S. Lee, Ray, & Little, 2010). When this occurs, microorganisms begin to propagate in between the interface that forms between the water and fuel, which occurs due to the well-known fact that petrochemicals have lower densities than water. This environment is beneficial for certain microorganisms to grow in, as the interface provides easy access to the nutrients necessary for the survival of these organisms. This is because nutrients from the fuel dissolve into the water, allowing for both a medium for the microorganisms to grow, while also providing the right chemical environment for these organisms to thrive (J. S. Lee et al., 2010). Upon analysis of the types of microorganisms within these environments, a myriad of species were discovered to exist within the interface (Blake W. Stamps, Caitlin

L. Bojanowski, Carrie A. Drake, Heather S. Nunn, Lloyd, James G. Floyd, Katelyn A. Berberich, Abby R. Neal, & Stevenson, 2018). However, one species of organism that was found consistently within these environments, was the fungus *Byssochlamys nivea,* which was identified within multiple fuel tanks at CONUS USAF bases.

Problem Statement

This thesis focuses on the concern associated with the existence of fungi within fuel tanks is that with the growth of microbes comes the potential for microbially induced corrosion which could influence both the amount of and the types of corrosion occurring within the system (Videla & Characklis, 1992). There are two main concerns with the occurrence of this corrosion. The first is that any corrosion occurring within the fuel tanks or the fuel lines could lead to the oxides spalling off of the metal and entering into the fuel (EPA, 2016). This could potentially cause damage to the equipment using the fuel. If this spalling is not captured by the filtration systems within the infrastructure, they could enter the internal combustion engine of the equipment. These have the potential to cause damage to internal combustion engines (Hussin, Ismail, & Mustapa, 2016). The other issue involved with this corrosion is the deterioration of the fuel infrastructure through the gradual erosion of metal. If corrosion occurs over prolonged durations, it is likely that the corrosion will eventually cause the infrastructure to fail. This would not only incur a financial cost, as the infrastructure would need to be repaired or rebuilt, but it could potentially raise far greater concerns involving national security, as these pieces of infrastructure are critical to the use of equipment which allow the aircraft owned by the USAF to undergo their operations. Therefore, the purpose of this research is to determine

how the introduction of the fungus *Byssochlamys nivea* over a varying span of time affects the amount and the type of corrosion that occurs within samples of a mild steel similar in nature to the metal used for fuel infrastructure.

Research Questions

This thesis focused on two primary questions, the first question is in regard to the types of oxide formed on a mild steel sample when that sample is introduced into an environment compromised of Bushnell-Haas Broth (BH), B20 biofuel, and the fungus *Byssochlamys nivea*. In particular, this research is attempting to discover the effect that the fungus *Byssochlamys nivea* has on mild steel through the process of microbially induced corrosion. The second question this research is attempting to answer is how does the amount of time that mild steel is introduced to an environment containing BH, B20 biofuel, and the fungus *Byssochlamys nivea*, affect the types iron oxides produced as a result of corrosion.

Research Focus

This research was primarily focused on the corrosion that occurs over time when a sample of mild steel is subjected to an environment, which mimics the interaction between fuel and the bottom water often found in fuel tanks. The fuel being considered for this research is B20 Diesel fuel (B20), a standardized mixture of 20% plant and animal based bio-fuel, and 80% diesel fuel (Eljuri, 2016). Furthermore, BH is composed of water and salts and was therefore chosen to simulate the water found within fuel tanks. The reason that BH was chosen was that BH has been found to be an effective medium for allowing organisms that degrade hydrocarbons to grow (Zimbro, Power, Miller, Wilson, & Johnson,

2009). Ultimately, this research aims to determine how the introduction of the fungus *Byssochlamys nivea* affects the corrosion occurring on mild steel submerged in an environment of BH and B20. Figure 1 displays the difference between a normal mild steel coupon, and one that has been submerged in standard deionized (DI) water for a total of four weeks in a sealed test tube. As can be seen in the Figure, corrosion has occurred on the coupon submerged in water with two different types of corrosion being visible, the first being a type of reddish-brown oxide that spalled off and floated to the surface of the water while it was submerged, and the second a darker black oxide that uniformly covers the lower half of the coupon. This is quite different from the corrosion seen in Figure 2, which displays an example of the corrosion that occurred during the experiment. However, it should be noted that the corroded sample in Figure 2 was also placed within a shaking incubator that rotated at 60 rotations per minute (RPM) at 27°C, which could potentially account for some differences, due to increased amounts of oxygen exposed to the environment, or from causing oxide to spall off. Furthermore, this sample was also subjected to BH as opposed to DI water, which could account for differences as well. SEM images of the corrosion occuring in DI water can be seen on the right side in Figure 1.

Materials and Equipment

This research required the use of an Scienta Omicron instrument with an Argus CU analyzer and XM1000 monochromatic X-ray source X-Ray Photoelectric Spectrometer (XPS) and a Zeiss EVO10 Scanning Electron Microscope (SEM).

The X-Ray Photoelectric Spectrometer is necessary to analyze the contents of the sample in terms of volumetric percentage of iron and iron oxides while the SEM is necessary to visually observe the samples.

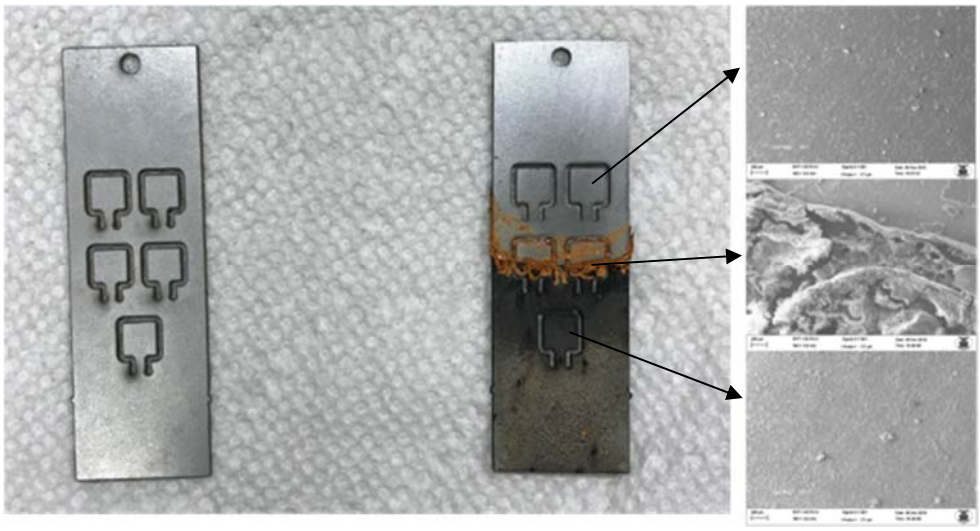

Figure 1: Mild Steel Coupon Exposed to Air and Mild Steel Coupon Exposed to DI Water for 4 Weeks (Left), SEM Images of DI Water Exposed Coupon (Right) displaying the unexposed surface (Top Image), the interface (Middle Image), and the DI water submerged surface (Bottom Image)

Methodology

This research was conducted by analyzing the exposed samples and control via XPS. The samples analyzed were prepared by cutting a sheet of mild steel into rectangular coupons, the interiors of those were then cut again to form a total of five samples per coupon for a total of twenty samples. Figure 2 displays an image of a rectangular coupon that was subjected to the experiment. Following the initial preparation of the mild steel, the coupons were then subjected to further preparation. This consisted of sanding down the coupons with P1500 grit sandpaper, degreased with ethanol, and subsequently sterilized via submersion in isopropyl alcohol for a total of 15 minutes. After 15 minutes had passed,

the coupons were removed from the isopropyl alcohol and any excess alcohol was subject to combustion via a Bunsen burner. Following this, the coupons were placed into conical test tubes which were then filled with enough BH to cover the lowest sample. After this, spores from the fungus *Byssochlamys nivea* were introduced into the conical test tube via pipetting. The next step involved pipetting a enough B20 fuel into the conical test tube so that the interface between the two solutions formed on the middle sample.

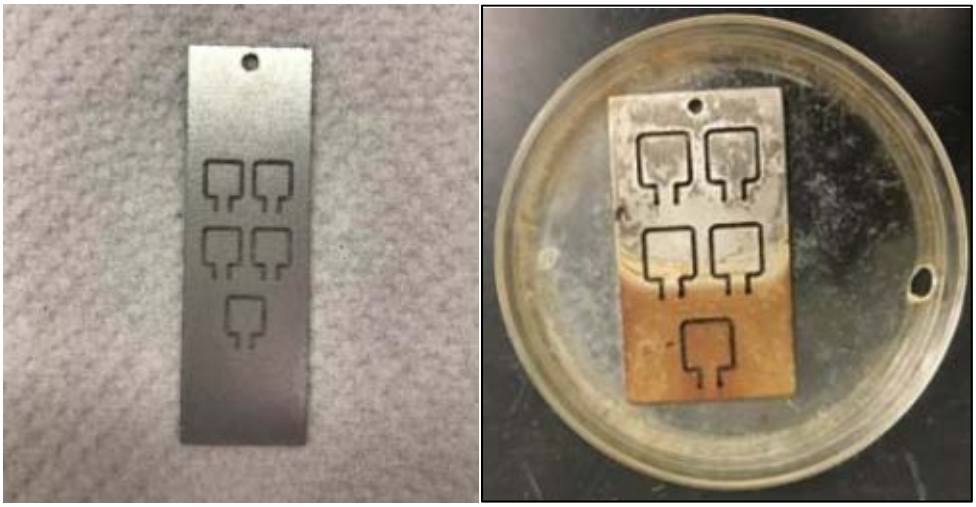

Figure 2: Mild Steel Coupon before experiment (Left) and Mild Steel Coupon after experiment (Right)

Then, the prepared samples were placed in a shaking incubator set at 27 °C and 60 RPM, the length of time that each coupon was subjected to this environment varied between either two weeks or four weeks depending on the coupon. Once the coupons had been subjected to their respective environments for their designated amount of time, the coupons were removed and situated within individual petri dishes and subsequently placed within a desiccator. The next step involved the analysis of the surface chemistry of the samples, which was completed through the use of XPS. However, the individual samples first needed to be removed from the coupons. This was done by cutting the ends of the

samples with a rotary cutting tool and gently plying the metal until the ends fractured, which allowed for the sample to be removed from the coupon. Then the samples were placed on a steel mount designed to fit within the XPS instrument, in order to prepare the sample for analysis. To prevent the samples from falling into the instrument or moving during the analysis, the samples were held to the mount with tantalum wire held over the sample and fused to the steel mount with a spot welder, an example of this can be seen in Figure 3. The sample mount was then inserted into the instrument and the pressure in the chamber was reduced to an ultra-high vacuum. The samples were then analyzed with monochromatic Al Kα radiation with an energy of 1486.7 eV. This method analyzed the sample across a 200nm by 300nm rectangle, which, depending on the angle of the radiation can penetrate up to approximately 100 Å (Briggs & Grant, 2003). Due to the phenomenon known as the photoelectric effect, the energy of the radiation causes electrons in the material to excite and escape into a vacuum that is held within the instrument (Einstein, 1905). These electrons are then collected in an analyzer and CasaXPS Software (Casa software Ltd, 2009) was used to determine the intensity and the binding energy associated with those electrons.

Upon completion of the analysis, a graph of the intensity and binding energy of the electrons within the analyzed sample was developed. Further analysis of intensities and binding energies were performed to determine the composition of the samples.

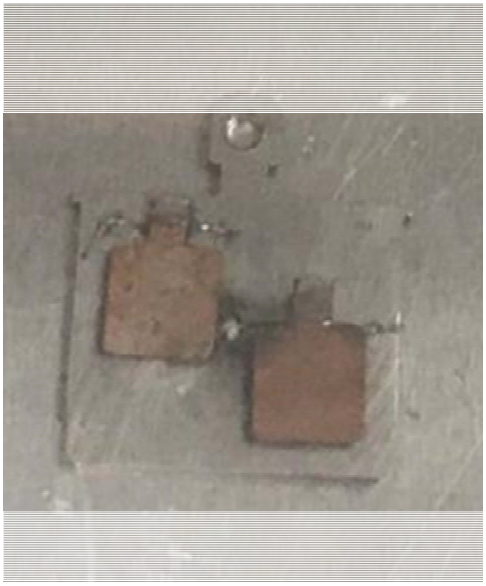

Figure 3: Sample Mounting with Tantalum Wire

Assumptions/Limitations

There are several assumptions involved with this study; the first is that the mild steel being used is assumed to be similar to the type of metal with which fuel tank infrastructure would be constructed. This must be done for the experiment to remain consistent across trials. Another assumption that must be made is that the water medium adequately simulates the water that would be seen in typical fuel tanks. It is likely that the water medium used does not perfectly imitate the water found in fuel tanks and must be assumed that BHis similar in nature to the water substitute for this study. Additionally, typical fuel tank microbial environments contain a vast selection of microbes (Rauch et al., 2006), considering that this research was only conducted using a single species of fungus it is likely that the corrosion that occurs within a fuel tank would be different than the corrosion that occurred in these experiments. Furthermore, the experiments conducted for this analysis were conducted under conditions that were not held consistent, including

differences in the ways the samples were prepared, as well as some samples being introduced to experimentation before analysis. Therefore, the results of this study are limited regarding direct effects of microbially induced corrosion on the mild steel coupons.

Scope

The focus of this study is noteworthy because it acts as a first step towards allowing the DoD to understand the type of corrosion occurring within microbially contaminated fuel tanks and how potentially damaging that corrosion is due to the fungi. Knowing this could allow the DoD to make more informed decisions regarding preventative maintenance or have better judgment surrounding the service life of fuel tanks containing B20 fuel, and likely fuel tanks containing other types of fuel. This research is slightly limited in scope, as the environment within a fuel tank typically consists of a myriad of fungi and bacteria (Rauch et al., 2006). However, for the purposes of investigative research, a single species is an ideal starting point in order to accurately identify the corrosion that occurs due to that particular species. Further research is required to determine both the effect of other species, as well as how multi-species communities will affect the corrosion of mild steel.

Other Support

This research required the support of Air Force Research Laboratory (AFRL) to provide spores of the fungus *Byssochlamys nivea,* BH, and other materials required to conduct the experiment, such as conical tubes and pipetting instruments.

Preview

The outcomes of this experiment varied depending on which environments the samples were submerged within. This section will display the outcome of the control test and one of the conducted experiments. Figures 4 and 5 demonstrate the output of two separate samples that were analyzed by XPS. The Fe2p section displays the binding energy of electrons associated with the core level 2p orbital of iron and iron oxides (Grosvenor, Kobe, Biesinger, & McIntyre, 2004). Figure 4 is the output of the Fe2p section of the analysis for a piece of mild steel which was not subjected to the experiment and acts as a reference. Figure 5 shows the analysis of the interface between sump water (McNamara et al., 2005). The steel sample was submerged in the experiment for two weeks, prepared by the University of Akron (UA). Table 1 shows the percent compositions of iron and iron oxides found within the two samples. It can be observed that unlike the unexposed sample, the sample submerged in the solution has less pure iron within it. This is logically sound, as the environment that the control was subjected to was far less likely to oxidize than the environment of the other sample, given that the experimental sample was subjected to conditions conducive to corrosion. When considering the percent composition of oxide, the amount of FeO found in the unexposed is 17.63% greater than the exposed sample.

Similarly, there was 28.72% more Fe_2O_3 in the control compared to the exposed sample. Furthermore, FeOOH increased by 45.61% in the experimental sample from 0% in the unexposed sample. Also, the amount of Fe_3O_4 increased by 7.66% from the control to the interface sample. Considering how rust typically consists of FeOOH and Fe_3O_4 (Landolt, 2007) the data gathered clearly displays that a significant amount of corrosion did occur, as the total volume percent change of those two oxides increased dramatically.

Images taken from an SEM for both the unexposed control sample and the two-week sample from the University of Akron can be seen in Figure 6 and Figure 7. Figure 6 shows an example of pitting that occurs on the control sample, this displays that the surface of the samples is not uniform and therefore the corrosion that occurs on the samples will not be uniform as well.

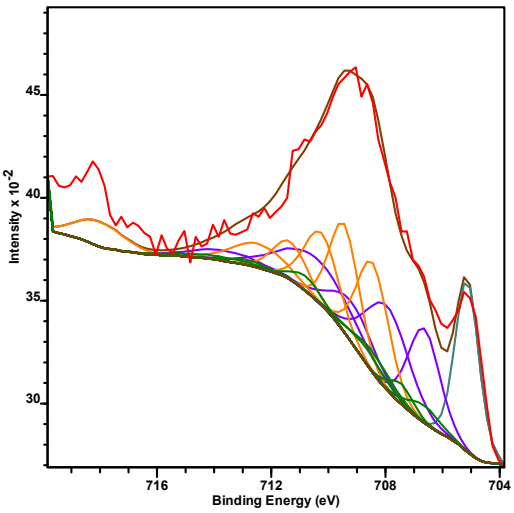

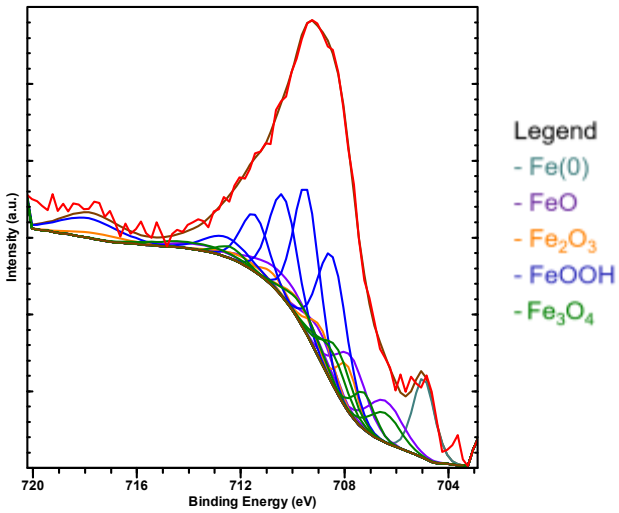

Figure 4: Analysis of Control Fe2p **Figure 5: Analysis of UA 2 Week Interface Fe2p**

Table 1: Percentages of Components of Iron Oxides

Name	Fe(0)	FeO	Fe_2O_3	FeOOH	Fe_3O_4
Control	12.51	37.51	39.70	0.00	10.28
UA B20 2 Week (Interface)	5.62	19.88	10.98	45.61	17.94

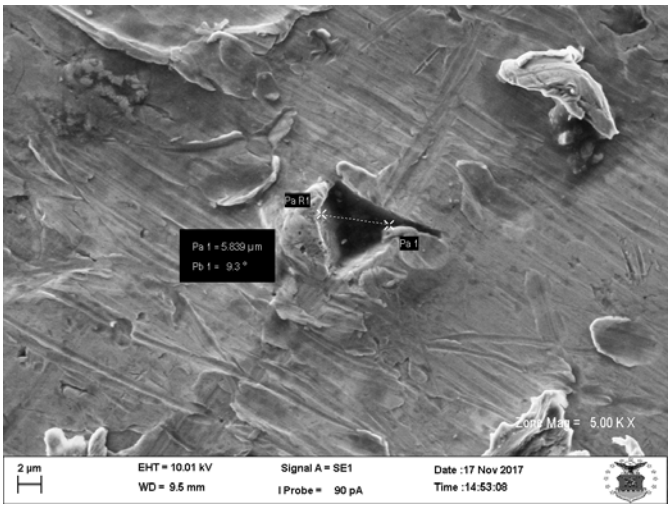

Figure 6: SEM Image of the Control Sample

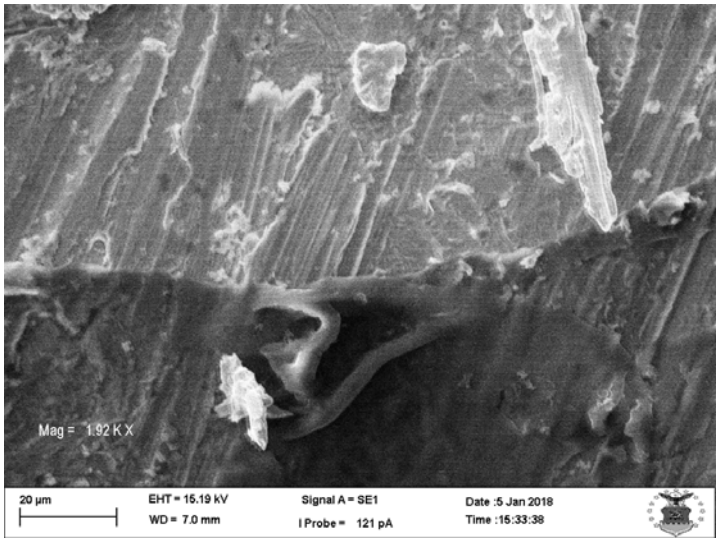

Figure 7: SEM Image of Biological Interface of the University of Akron 2-week Sample

II. Literature Review

Introduction

Corrosion is an endemic issue to society which, as of 2002, cost the United States approximately 3.1% of its GDP which amounted to a total $276 billion, of which approximately 20% has been attributed to biocorrosion (Gu, 2014). Adjusted for inflation in 2018, this value equates to approximately $426 billion. Specifically, the report indicates that the average annual cost associated with corrosion within gas and liquid transmission pipelines is around $7 billion (Gerhardus H. Koch & Brongers, 2002). Often found within this infrastructure is a host of various microorganisms which live at the interface between fuel and water (Rauch et al., 2006) which enters into the system either through precipitation or through moisture condensing into the fuel (J. S. Lee et al., 2010). This is because certain microorganisms found in nature can thrive within this environment, taking nutrients from both solutions in order to grow and sustain their population (J. S. Lee et al., 2010). In this environment, the growth of microorganisms eventually encounters the metallic interior of the fuel tanks and can cause microbially induced corrosion.

Key Terms:

Biodiesel B20:

Biodiesel B20, also referred to as B20, is a mixture of petroleum diesel fuel and biofuel derived from vegetable oil. Specifically, B20 consists of 80% petroleum diesel fuel and 20% vegetable fatty methyl esters (Prince, Haitmanek, & Lee, 2008).

Byssochlamys nivea:

Byssochlamys nivea is a strain of fungus that is frequently found growing within fuel tanks containing B20 fuel. This is evident from an excursion completed by the Air Force Research Laboratory (AFRL) to Barksdale Air Force Base, where this fungus was found to be growing within several separate fuel tanks that contained B20 fuel (Blake W. Stamps, Caitlin L. Bojanowski, Carrie A. Drake, Heather S. Nunn et al., 2018).

Microbially Induced Corrosion (MIC):

MIC is the corrosion that occurs due to the growth of, or existence of, microbes on the surface of a metal. There are a multitude of types of microbes which can cause MIC to occur, but the main types are sulfide reducers, iron or manganese oxidizers, iron reducers, sulfide oxidizers, acid producing bacteria and fungi, and slime forming bacteria (Kip & Van Veen, 2015). The existence of these microbes will then drive an oxidation reaction. For example, in environments where anaerobic fermentation occurs, the products of that reaction are usually organic acids. This acid then creates a substantially different pH between the bottom of the biofilm and the remainder of the fluid in this environment, this pH difference then drives corrosion (Gu, 2014). Similarly, fungi have been observed to produce organic acids as well, which can result in the formation of pitting at grain boundaries, which are defined as boundaries that separate crystals

within the metal that have different crystallographic orientations (Callister & Rethwisch, 2009). Which results in a similar mechanism of corrosion driven by differences in pH on the surface of the metal (Beech & Gaylarde, 1999).

X-Ray Photoelectron Spectroscopy (XPS):

XPS is a method of analyzing the surface of a sample utilizing X-rays and electrons ejected from a surface via the photoelectric effect. In this method, a variable rectangular area dependent on the configuration of the instrument which ranges from a few centimeters to approximately 200 nanometers, is struck with X-rays, which penetrate into the sample (Briggs & Grant, 2003). This energy excites electrons within the sample which ultimately causes electrons to be removed from the surface hit by the X-ray, this phenomenon is known as the photoelectric effect (Einstein, 1905). These electrons are guided into an analyzer, which is connected to a computer utilizing software to display two factors. The first factor is the binding energy of the electron, and the second factor is the amount, or intensity, of the collected electrons (Casa software Ltd, 2009). Every element has a specific binding energy, also known as ionization energy, which is the minimum amount of energy required for an electron to be removed from an atom (Levine, 1983). As a result, using this display of intensity and binding energy, it becomes possible to use statistics to ascertain the elements and compounds found within a sample (Proctor & Sherwood, 1982).

Aluminum Kα Radiation:

A form of radiation that is emitted from an aluminum target after being bombarded with electrons. This radiation is then focused in a quartz crystal and used to analyze samples. (Briggs & Grant, 2003).

Justification for Research:

When corrosion occurs within fuel tanks or fuel lines there is a chance that the oxide that forms will flake and fall off the metal, in a process known as spalling (Meyers & Taylor Aimone, 1983). In the event that a piece of oxide spalls off the metal undergoing corrosion, it can act as a detrimental agent to the fuel infrastructure through a variety of means. The first concern associated with this oxide spalling, is that these flakes of oxide can potentially pass through the filtration system attached to the fuel infrastructure (EPA, 2016) and enter the internal combustion engines that are powered by this fuel, potentially damaging the engine (Hussin et al., 2016). The second concern relates to how this corrosion degrades the infrastructure itself, namely the fuel tanks and the fuel lines. This corrosion creates significant potential to reduce the working life cycle of the fuel tanks and fuel lines, through the gradual erosion of structural metal in the infrastructure which can result in leaks.

Scope of the Review Method of Gathering Information:

Therefore, this literature review will cover the history of both biologically induced corrosion, focusing on MIC, as well as the history of the method of analysis, X-ray Photoelectron Spectroscopy. The purpose of which is to explain the history of this research, as well as provide justification for the use of XPS to analyze the effects of MIC on mild steel by a fungus such as *Byssochlamys nivea*.

Chronology

Anti-Fouling Efforts in Ancient Greece:

The earliest known recorded reference to biological growth having an effect on the quality of a material was written on a papyrus from 412 B.C. which indicated that the ancient Greeks used an anti-fouling paint made of arsenic, sulfur, and oil (WHOI, 1952). The purpose of this paint was to cause the wood on the hull of a ship to "never spoil from the action of the sun, winds, or salt water." This has been interpreted to refer to the natural degradation associated with the exposure of wood to the environment and the degradation caused by the growth of organisms such as barnacles and weeds on ships. In the 4th century B.C, Plutarch also rightly stated that the existence of biological growth on a ship has a reducing effect on the speed of the ship, thus marking one of the first instances in recorded history of the effect of biologicals on manmade material (WHOI, 1952).

Biological Protection for Ships in the British Royal Navy:

As time progressed, mankind's understanding of the effect that biology can have on equipment and infrastructure steadily increased. One of the most notable examples of this was in 1758, when the British began experimenting with the use of copper sheeting to prevent the fouling of wood on their ships. The first experiment involved the frigate *H.M.S. Alarm* where the hull of the ship was coated with copper and sent on a voyage to the West Indies. When the ship returned, the copper was removed and the planks on the hull analyzed for damage caused by biological growth. Upon observation, it was noted that the copper was found to have prevented fouling and that the planks were in surprisingly good condition, this was a result of what we now know as copper's innate capability to resist biological growth (Grass, Rensing, & Solioz, 2011). Due to the success of this experiment, by the end of the 18th century, it became common practice within the Royal Navy to coat the hulls of all ships with copper, rendering all ships to be resistant to wood fouling (WHOI, 1952).

Early Experiments with Photons:

The next important part of the chronology of this research involves the discovery of photons and the photoelectric effect. This is primarily because the use of XPS relies heavily on the understanding of the photoelectric effect and how photons can be used to excite electrons which then escape into a vacuum. A photon is an elementary unit of electromagnetic radiation which displays the properties of a wave-particle duality. Ultimately, this means that a photon has the properties of both a particle and a wave and will therefore have unique interactions with matter.

The discovery of the photoelectric effect happened in the late 19th century when Heinrich Hertz conducted an experiment by irradiating a pair of metal electrodes with ultraviolet light and seeing how the voltage of the spark between them changed (Klassen, 2008). When Hertz observed a change in voltage, he then concluded that the radiation striking the metal must have resulted in the flow of electrons, and thus the basic principles of the photoelectric effect regarding electromagnetic radiation and the movement of electrons was discovered.

Einstein's Three Step Model of the Photoelectric Effect:

In 1905, Einstein published his "On a Heuristic Point of View Concerning the Creation and Conversion of Light," for which he would later go on to receive the Nobel Prize. In this publication, his famous three step model was proposed, where the actual mechanisms that occurred during the photoelectric effect were described (Einstein, 1905). In the three-step model, the electrons are first excited into higher energy levels by the introduced electromagnetic energy which then creates a vacancy where those electrons once were. This then leads to the second step, where an electron is transported to the surface of the metal. Then the final step in this process involves the electron escaping into the vacuum. This discovery was crucial to the development of XPS as an analytical science, as it was proof that electrons were emitted after being subjected to electromagnetic radiation, the use of which is a key component regarding the functionality of an X-ray spectrometer (Briggs & Grant, 2003).

Gaines and the Observation of Microbially Induced Corrosion

One of the earliest scientists to suggest the possibility of MIC was a man named Richard Gaines. In his 1910 paper, Gaines describes the observation of corrosion on the foundation structure of a bridge which exhibited peculiar pits. After confirmation from the naturalist Wilton Brown that these pits were not what would be expected during typical rusting, the pits were visually inspected. From this inspection, it was determined that an organism must have played a role in this corrosion. This was confirmed when the existence of the bacterial *Gallionella ferruginea* was discovered in large concentrations in samples of the rust after they were observed by a bacteriologist. Gaines then determined that the production of an acid must have served as the means by which these bacteria oxidized the iron. (Gaines, 1910)

Rutherford and the Relation between Kinetic and Electron Binding Energies

Earnest Rutherford is well known for his work on the structure of the atom, but he plays a role in the development of XPS as an analytical science as well. In particular, he published a paper in 1914 which laid the foundation for the fundamental equation of XPS analysis, relating the kinetic energy of β-rays and electron binding energy:

$$E_\beta = hv - E_b \qquad \text{Eq(1)}$$

Where E_β is the kinetic energy of the β-rays, h is Plank's constant, v is the frequency of the waves, and E_b is the binding energy of the electrons. It would later be discovered that this relation holds true for x-ray radiation as well, and is

therefore critical to the use of XPS as a means of analysis (Stuewer, 1983). Controlling the frequency and kinetic energy of the electromagnetic radiation used in XPS allows the binding energy of the returned electrons to be determined, from which the spectra of a sample can be analyzed, and the chemical constituents of that sample can be determined.

Moseley, Rawlinson, and Robinson's Early Experiments:

During this time, some of the earliest experiments of XPS were designed by H. Moseley, H. Robinson, and W. Rawlinson. In particular, Moseley had a large contribution towards finalizing the basic design of an X-ray spectrometer while Rawlinson and Robinson contributed greatly to the development of the β-ray spectrums associated with pure elements such as aluminum, silver, gold and lead (Jenkin, Leckey, & Liesegang, 1977; Rutherford, Robinson, & Rawlinson, 1914) .

Progress in XPS as an Analytical Science During the Mid 20th Century:

The first to identify x-ray spectroscopy as a potential means of chemical analysis was Ralph Steinhardt in 1951, where he proposed that the peaks of an observed spectra could be used for quantitative analysis to determine the chemical composition of a sample (Steinhardt & Serfass, 1951). This proposal is widely agreed upon to have been the start of using XPS as an analytical tool. Building upon this new development, Kai Siegbhan began to use XPS to determine the spectra of copper and copper oxides in the late 1950's (Sokolowski, Nordling, & Siegbahn, 1958). This acted as proof that XPS could be used for the analysis of oxides, which is significant as a key component of this research is to determine in what concentrations iron oxides exist after MIC. It was also around this time that the use

of less intense X-ray sources were beginning to be used for analysis. Most notably, monochromatic magnesium and aluminum Kα radiation began to be used. This resulted in two major contributions to the science, the first was that elements with lower atomic numbers, previously unobservable due to the intense radiation were now observable. The second benefit was a dramatically increased resolution of the spectra allowed for a better understanding of the composition of a sample (Briggs & Grant, 2003).

Peter Sherwood and Statistical Interpretation of Spectra:

In Peter Sherwood's 1982 and 1996 papers, he describes the mechanisms to explain the composition of a given sample based on the spectra obtained from subjecting a sample to XPS. This involves a detailed statistical analysis of the data in order to determine the percent composition of the spectra (Proctor & Sherwood, 1982; Sherwood, 1996).

2004 Grosvenor article:

However, it was not until 2004 that the spectra of iron oxides and iron itself was determined. In Grosvenor's 2004 article titled, "Investigation of multiplet splitting of Fe 2p XPS spectra and bonding in iron compounds," the ranges of binding energies for each multiplet region of each oxide is described. From this research, it became possible to determine through the use of XPS what type of iron oxides had formed on a sample and how much of the sample remained as pure iron (Grosvenor, Kobe, Biesinger, & McIntyre, 2004). This is important because this research is trying to identify what types of iron oxides occur.

XPS Analysis of Microbially Induced Corrosion on Stainless Steel:

An example of the use of XPS to analyze the effects of MIC on steel can be seen in the 2007 article "Microbiologically influenced corrosion of 304 stainless steel by aerobic Pseudomonas NCIMB 2021 bacteria: AFM and XPS study" from S.J Yuan and S.O Pehkonen. In this study, the researchers determined the effect of the biofilm formed by the bacteria *Pseudomonas* had on the surface chemistry of 304 stainless steel. Ultimately the researchers used XPS to confirm that the introduced bacteria did indeed make changes to the surface of the exposed samples. This was shown through an increased amount of iron oxides on the surface, while the percent composition of elemental iron and chromium decreased (Yuan & Pehkonen, 2007). The corrosion occurring in the samples analyzed for the research in this thesis would likely see similar results, primarily regarding increased amounts of iron oxide as well as a decreased amount of elemental iron. Though the metal used during the 2007 experiment is different from the mild steel used for this thesis, the general trend likely remains consistent. The research done by Yang demonstrates the use of XPS as an appropriate means to analyze MIC.

Alternative Views:

Though this literature review has focused on demonstrating that XPS is a viable means of analyzing MIC, there are many of ways in which MIC can be identified. Methods such as Atomic Force Microscopy (AFM), Energy-Dispersive Analysis of X-rays (EDAX) in conjunction with a Scanning Electron Microscope (SEM), X-ray Diffraction (XRD), and Electron Microprobe Analysis (EMPA) have all been identified as viable means of observing the effects of biotic and abiotic

sulfide films on steel (Herrera & Videla, 2005). Therefore, it can be argued that these methods should be considered for analyzing MIC, either in addition to XPS or without it. While XPS is indeed a viable method of analysis, it can be limited in capability considering how little it is capable of penetrating into samples, which leaves it suitable to only thin scaling deposits of less than 1 micrometer (Beech & Gaylarde, 1999).

Source Types:

The sources in this literature review include books, journal articles, government studies, and government statutes. This was done to provide a wide breadth of sources to support the information in this review.

Conclusion

Interpretation:

From this review, it is clear that XPS is a viable means for analyzing iron oxides and the effect that biocorrosion has on steel. This is because XPS as a method of analytical science is preceded by a long history involving the understanding of the photoelectric effect and of the identification and production of the binding energy spectra of multiple elements and compounds. Specifically, the multiple oxides of iron have been analyzed and their spectra determined, allowing for the conducted research to reliably determine the percent composition of mild steel subjected to MIC.

Trend Identification:

As previously mentioned, there are a myriad of types of microbes that can cause MIC (Kip & Van Veen, 2015), but there seem to be general categories by which MIC could be defined. Each of these categories have specific types of iron oxides that form as a result of MIC of steel, and could therefore be useful towards ultimately determining what type of corrosion is occurring as a consequence of the existence of the fungus *Byssochlamys nivea* on mild steel.

Indirect Corrosion from Biofilms:

Though not a direct cause of corrosion, the existence of a biofilm as a result of the natural processes of microbes can induce an anaerobic environment. This reduced concentration underneath the biofilm can result in the creation of an anode, with the surrounding areas not covered with a biofilm then acting as a cathode. This environment then inevitably begins the process of an oxidation reduction reaction, resulting in the formation of corrosion. However, the products associated with this type of corrosion would not be dissimilar to the corrosion not associated with MIC, and would be difficult to observe through XPS. (Hamilton, 2003). In mild steel, these products would likely be, like normal oxidation of rusting, FeOOH and Fe_3O_4.

Sulfate Reducing:

What may likely be the most studied and well understood mechanism of MIC is that of microbes that are sulfate reducing. In this scenario, microbes that are in an anaerobic environment, which is likely considering that these microbes often form biofilms (W. Lee, Lewandowski, Nielsen, & Hamilton,

1995) that prevent the flow of oxygen (Hamilton, 2003) begin to use hydrogen sulfide as an electron acceptor (Costello, 1974). Ultimately, this reaction results in the production of an iron sulfide corrosion product (Hamilton, 2003). Considering the environment for this thesis consists of part diesel fuel, it is not unreasonable to consider this possibility, as sulfur can be found in diesel (Bücker et al., 2014). Therefore, the identification of iron sulfide with XPS would be a key indicator if this type of corrosion had occurred in the experiments conducted in this thesis.

Iron Reducing:

The process of iron reduction is fairly simple, in that it involves reducing Fe_2O_3 to FeO. This is a process that will drive corrosion, due to the transfer of electrons involved in this reduction and has been observed in both bacteria (Johnson & McGinness, 1991), as well as fungi (Ottow, Ottow, & Von Klopotek, 1969). Due to the fact that this method of corrosion has specifically been observed in fungi, it is an ideal type of corrosion to look for with XPS analysis for the experiments in this thesis. The results of such analysis would likely display higher concentrations of FeO, and lower concentrations of Fe_2O_3.

Difficulties:

One of the most significant difficulties associated with XPS is the extreme sensitivity that comes with the analysis of such a small area. The XPS analysis in this thesis was conducted with a resolution of approximately 200 nm which could only penetrates up to 100 Å depending on the angle of the x-rays (Briggs & Grant,

2003). Therefore, any potential contamination or improper preparation can result in observing unintended constituents residing on the sample. If the analysis happens to occur on a part that has been contaminated or contains unintended constituents, it is very likely that the results of the data will not accurately reflect the true nature of the sample. Furthermore, even analysis that occurs on areas that have not been contaminated could still be affected if any part of the sample has been contaminated (Briggs & Grant, 2003). Keeping the sample uncontaminated becomes difficult when considering the multitude steps involved in sample preparation, as will be discussed in the methodology section.

Concluding comments:

X-ray spectroscopy has a well-established history which can been used to analyze MIC. As such, this research is an effective and justifiable means of analyzing the contents of mild steel introduced to biofilm of the fungus *Byssochlamys nivea.* Ideally, the analysis in this thesis should be able to provide some insight into whether or not MIC is occurring, as well identify the types of MIC occurring, based on the products identified in the XPS analysis.

III. Methodology

Introduction

The purpose of this research is to gain an understanding of the effect that the MIC caused by the fungus *Byssochlamys nivea* has on mild steel. This is important because this fungus is commonly found within fuel tanks containing biodiesel B20 and is responsible for MIC, which can cause significant damage to the tanks. In the interest of protecting the infrastructure associated with the biodiesel B20, specifically fuel lines and fuel tanks, this research is an important step towards understanding the types and amounts of oxide produced as a result of MIC.

Theory

The determination of the effect that MIC has on mild steel will allow for future efforts involving either the prevention of corrosion or the repair of that corrosion. This can be determined via X-ray Photoelectron Spectroscopy (XPS), which is an established method of determining the percent composition of iron oxides within a sample (Grosvenor et al., 2004).

Procedure

This procedure is meant to explain how the experiment associated with this research was conducted, as well as explain the reasoning for the steps involved in completing this experiment. A total of twelve coupons were prepared by two separate parties, the first being researchers at the University of Akron (UA), and the second being researchers at the

Air Force Research Laboratory (AFRL) at Wright Patterson Air Force Base. Three coupons, each with three different types of samples were prepared by UA, while a single coupon containing three different types of samples was prepared by AFRL.

The procedures followed by both institutes were similar but differed in certain areas, which will be clarified in this procedure. However, the first step for both institutes involved growing spores of the fungus *Byssochlamys nivea*. This was done at AFRL by introducing the strain of *Byssochlamys nivea* to a potato dextrose agar with a plastic sterile loop and allowing the fungus to incubate for approximately one week, or until spores were present. AFRL used potato dextrose agar to grow *Byssochlamys nivea* because it was known to be a viable way to produce spores as it is a good medium to grow fungus in (Zimbro et al., 2009). However, UA used Hestrin Schramm agar (Hestrin & Schramm, 1954), which took a similar length of time to grow an appropriate number of spores. After adequate growth of *Byssochlamys nivea* occurred, the spores were removed from the potato dextrose agar. This was done by introducing 4mL of Phosphate buffer saline (PBS) containing 0.05% (w/v) Tween 80 to the agar surface and gently scraping the surface with a sterile spreading rod. This allowed for to the spores of *Byssochlamys nivea* to be separated from the agar and resulted in them being suspended in a liquid medium which was then removed via pipetting.

This solution containing the spores was then pipetted into a conical test tube and centrifuged at 10K relative centrifugal force (RCF) for 10 minutes to collect and concentrate the spores. After centrifuging the spores were in a pellet at the bottom of the tube, a pipet was used to remove the PBS supernatant leaving only the spore peleet at the bottom of the tube. The spore pellet was then resuspended in 5 mL PBS without tween and

centrifuged again as a washing step. This process was repeated twice more and the final spore pellet was resuspended in 5 mL PBS. Following this, the concentration of spores was determined through a process of dilution and visual observation with an optical microscope and hemocytometer, this provided a reference for the number of spores per milliliter used in the experiment.

The next step involved sanding coupons of mild steel, as seen in Figure 8, with 1500 grit sandpaper to remove any potential oxidation, this created a uniform surface which is readily available to be corroded. The intent of which was to induce a clearer effect of microbially induced corrosion. When this was completed, the coupons were placed in a desiccator to prevent as much corrosion as possible until the experiment was ready to begin. Furthermore, prior to beginning the experiment the mild steel coupons were degassed in methanol for five minutes and then sonicated in methanol for one hour. Once this was finished, the coupons were left to dry in order to ensure all methanol had evaporated in order to increase the accuracy of XPS analysis. The justification for this was that this would remove any particulates that are on the steel that could potentially interfere with the experiment.

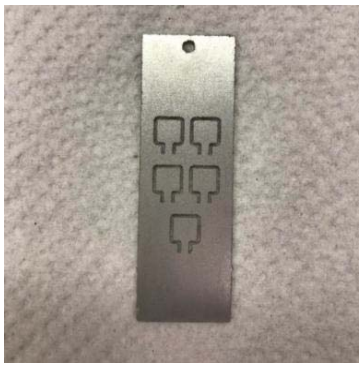

Figure 8: Example of Mild Steel Coupon used in Experiment

The next step was to ensure that the mild steel coupons were sterilized. At AFRL this was done via submerging the coupons in isopropyl alcohol for a total of 10 minutes, however at the UA, ethanol was used instead. The steel was then removed and subjected to the open flame on a Bunsen burner to remove the remaining alcohol via combustion. When this was complete, the mild steel coupon was placed within a conical test tube. The purpose of this was to reduce as many variables as possible, sterilizing the mild steel coupons helped to reduce the risk of contamination from other microorganisms during the experiment which could have altered the results of the experiment. This was done to a total of four mild steel coupons which were then placed into four separate conical tubes. Three of these conical tubes were part of the experiment at UA, and one was part of the experiment at AFRL. At UA, each conical tube was then filled with enough artificial sump water (McNamara et al., 2005) to cover one half of the middle sample. At AFRL, a similar procedure was followed, however instead of artificial sump water, Bushnell Hass broth (BH) was used. The amount of liquid was recorded and then each conical tube received the same amount of liquid to reduce variability in the experiment. The liquid was brought to this level so that the biofilm of *Byssochlamys nivea* would form on the middle sample. At AFRL, the BH was then inoculated via pipetting the available spores into the BH. Following this, enough B20 biodiesel was inserted into the conical test tube to cover the middle sample, but also left the top sample free from contact with the liquid. This method differs slightly from the procedure done at the UA, where the B20 biodiesel was introduced to the coupon before inoculation occurred. However, a similar amount of B20 was added, so that the top coupon was exposed only to the air. At UA, only two of the samples were inoculated with *Byssochlamys nivea*, leaving one control. This allows for conclusions to

be drawn about the nature of biocorrosion on the interface of the sample by comparing the control to the inoculated samples. The way these environments were developed allows for a total of three different types of samples per coupon to be created. The first is a sample that is introduced to only BH or artificial sump water. The second is one where the interface between the water substitute and fuel forms directly on the middle sample, which is important as it is where the fungus will grow and could be observed for MIC. Lastly, this environment created a third sample that was only exposed to air.

After the environments were completed, all conical tubes were placed into a shaking incubator that rotated at 60 RPM and was held at 27°C. The use of a shaking incubator, as well as a rotation speed of 60 RPM allowed for each sample on the coupon to be homogenous. The temperature was chosen at 27°C as it was shown in previous trials to be an ideal temperature for the growth for this fungus. The coupons were then left in the shaking incubator for varying amounts of time. The single experiment done by AFRL was subjected to these conditions for two weeks. However, the sterile coupon and one inoculated coupon from UA were subjected to these environments for two weeks, with the final coupon remaining in the incubator for four weeks. These time intervals for the removal of the coupons were decided because they would provide a time frame to observe the progress of biocorrosion.

After the predetermined amount of time had elapsed and the coupons had been removed from the shaking incubator, the B20 biodiesel was pipetted out and disposed of properly. The biofilms were then removed with a sterile cotton swab. Following this, the remaining water substitute was pipetted out and disposed of properly. The solution in each conical tube was removed this way to prevent potential cross contamination as any cross

contamination could affect the results of the analysis. The coupon was then removed and placed a sterile petri dish, where it was transported to the Air Force Institute of Technology where the XPS analysis would take place. However, it should be noted that these experiments were prepared approximately 4 months prior to analysis and were kept in a desiccator. Therefore, it is likely that the surface chemistry of the samples changed during this time, due to the exposure of these coupons to oxygen or moisture in the atmosphere. However, this effect was mitigated by placing the coupons in a desiccator.

Once the coupons arrived at the location they would be analyzed at, the Air Force Institute of Technology, the samples were removed from the coupons with a Dremel tool. Each sample was cut on the narrow band, as can be seen on the bottom of each sample in Figure 1. After a sample was cut, they were removed using forceps by gently plying the metal until the narrow band fractured. At this point, the samples were placed into individual sterile petri dishes. Great care was taken to keep note of the petri dishes to ensure that the proper sample was catalogued. The first coupon to have its samples removed was the inoculated sample from UA which was exposed to its environment for two weeks. The second coupon was the two week inoculated experiment coupon from AFRL, the third was the four week coupon developed by UA, and the last was the sterile coupon from UA. No samples were removed from their coupons until the analysis of their predecessors was complete.

Following the removal of the samples from the coupon, the samples were mounted onto the mounts designed for the XPS instrument. The first attempt to do so involved carbon tape, however as the first sample to be analyzed, the water exposed sample from UA, was inserted into the XPS, the oxide prevented a strong adhesion to the carbon tape

which resulted in the sample falling into the instrument. After this incident, all sample mounting was done using a spot welder and tantalum wire. With the configuration of the XPS instrument, only one sample mount could fit into the instrument at a time. Therefore, because only two samples could fit onto one sample mount at a time, and there were three total samples to be analyzed per coupon, two separate sample mounts were used to fit all the samples. When all samples were mounted appropriately, the first sample mount was placed inside the XPS instrument and brought to a high-vacuum pressure. While this was being done, the remaining sample mount was kept in a desiccator. After the sample mounts are under the appropriate high vacuum pressure, they were analyzed using the XPS instrument which was set to use Al Kα monochromatic radiation. Once the analysis was complete, the sample mount in the instrument was switched with the sample mount in the desiccator. This process was completed for every coupon in the same order as the samples were removed. The data gathered from this analysis was then converted into a CasaXPS file and subsequently analyzed using CasaXPS. This was done through the methods of analysis identified by Sherwood (Proctor & Sherwood, 1982; Sherwood, 1996) and Grosvenor (Grosvenor et al., 2004). Ultimately, this was accomplished through curve fitting the spectra gathered from the samples. The purpose of which was to determine the percent composition of the elements and compounds within the samples, the results of which can be seen in the next section.

IV. Analysis and Results

Chapter Overview

The focus of this chapter was to present the findings from the conducted experiments in terms of percent composition of iron and iron oxides. The data presented in this chapter was gathered using X-ray Photoelectric Spectroscopy (XPS) and this data was analyzed through the software CasaXPS (Casa software Ltd, 2009). This methodology is described in further detail in Chapter 3 using the peak parameters defined in Grosvenor's 2004 paper (Grosvenor et al., 2004). The samples which were analyzed for this thesis were developed through a joint effort by the University of Akron (UA) and the Air Force Research Laboratory (AFRL).

Results

Control Sample:

The first of the samples analyzed was a sample of mild steel exposed to room temperature and atmospheric conditions. This sample was removed from the same sheet of metal as the later samples analyzed during this research. Figure 9 displays the output of binding energy associated with iron and iron oxides resulting from the control sample being subjected to XPS. This figure contains the curve fitting linked with the suspected compounds within this region, namely, elemental iron (Fe (0)), ferrous oxide (FeO), ferric oxide (Fe_2O_3), anhydrous iron oxide-hydroxide (FeOOH), and ferrosol-ferric oxide (Fe_3O_4). The percent composition of these components can be seen in Table 2. From this analysis, it was found that 12.51% of the sample were Fe (0), 37.51% FeO, 39.70% Fe_2O_3, 0.00% FeOOH,

and 10.28% Fe_3O_4. A Scanning Electron Microscope (SEM) micrograph of this sample can be seen in Figure 10 This micrograph shows an example of pitting prior that was present before experimentation. This provides evidence of a non-uniform surface, which could result in corrosion occurring in different areas or at different rates. This data was collected over 54 minutes.

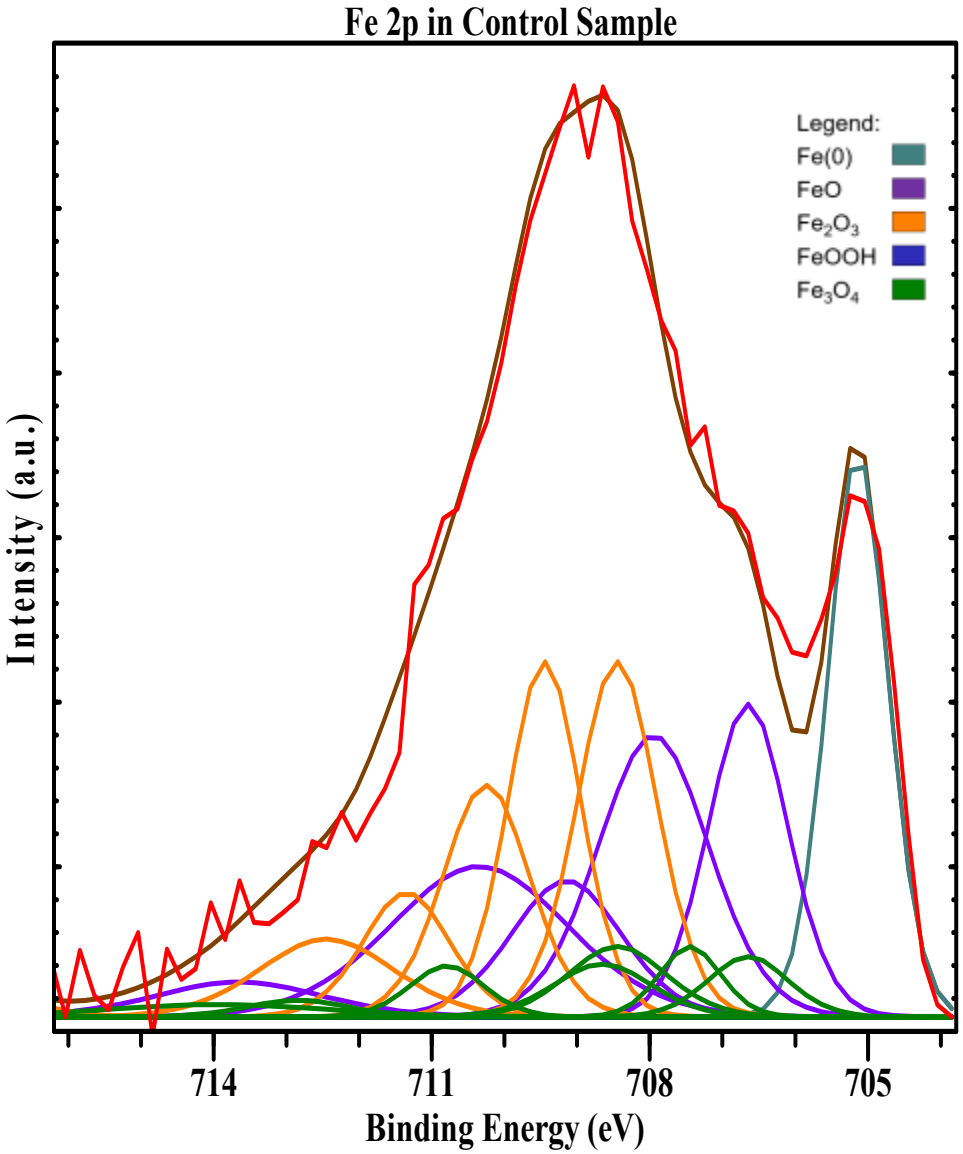

Figure 9: Intensity in Comparison to the Binding Energy detected of Fe 2p Regions in the Control Sample

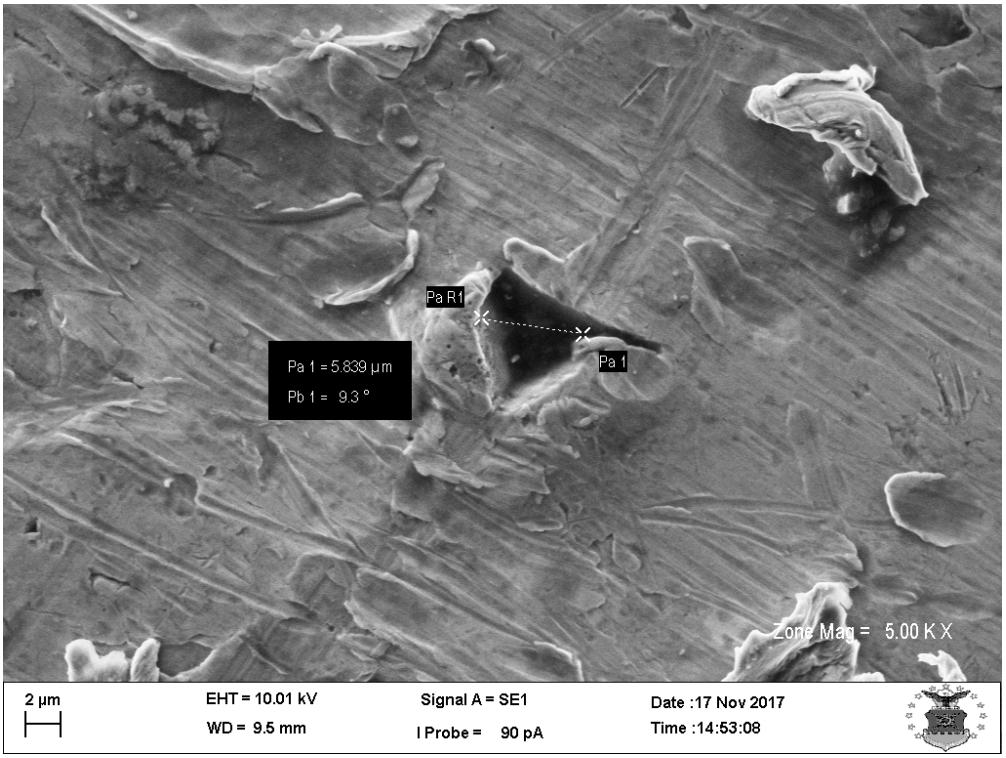

Figure 10: SEM Image of Control Sample

University of Akron Air Exposed 2 Week Sample:

The following is the data and output of the Fe 2p region of the sample from the UA that was exposed to air for two weeks. The percent composition of these components determined from this analysis are; 8.27% Fe(0), 34.89% FeO, 20.75% Fe_2O_3, 24.30% FeOOH, and 11.79% Fe_3O_4. The curve fitting for the iron regions for this sample can be seen in Figure 11. An image of this sample can be seen in Figure 12. This data was collected over 1155 minutes and 33 seconds.

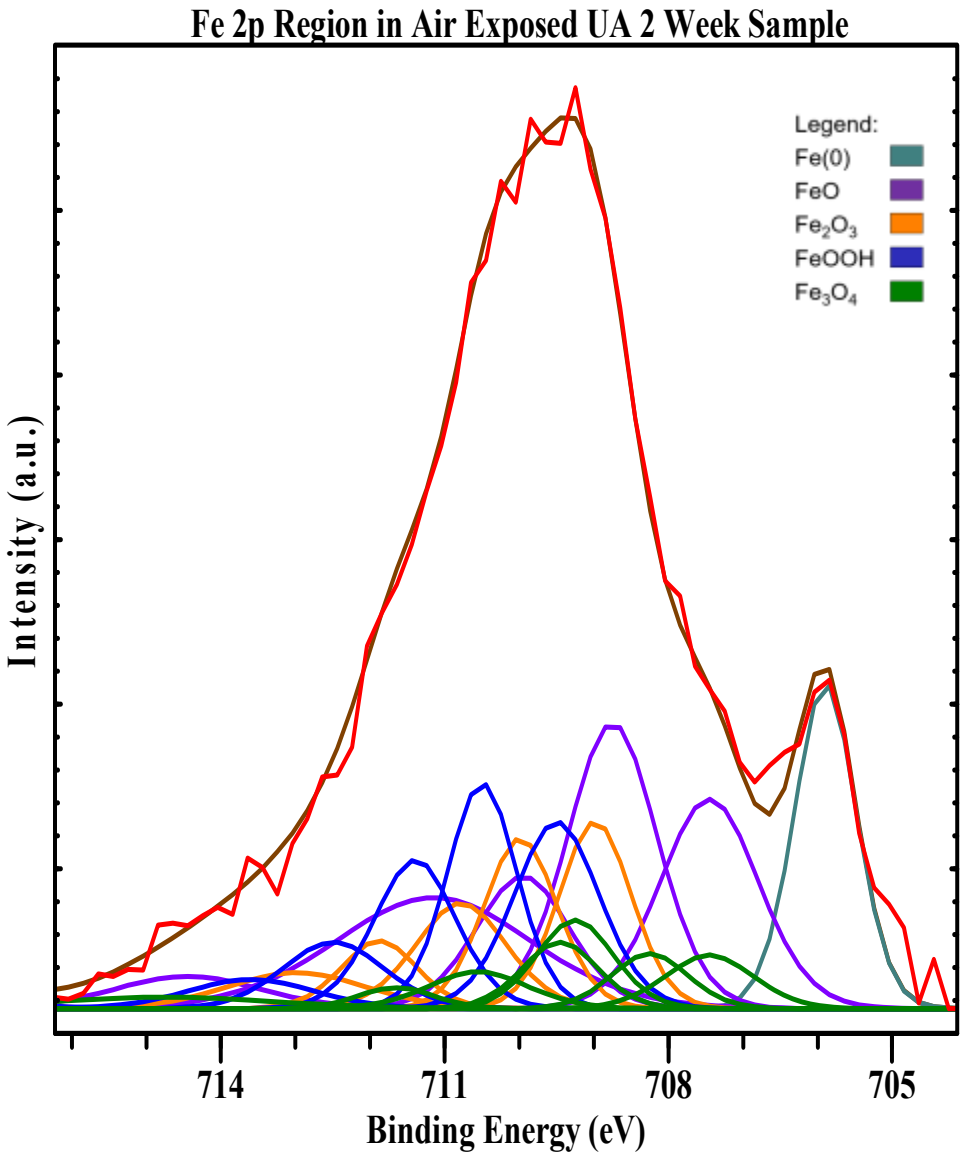

Figure 11: Intensity in Comparison to the Binding Energy detected of Fe 2p Regions in the Air Exposed UA 2 Week Sample

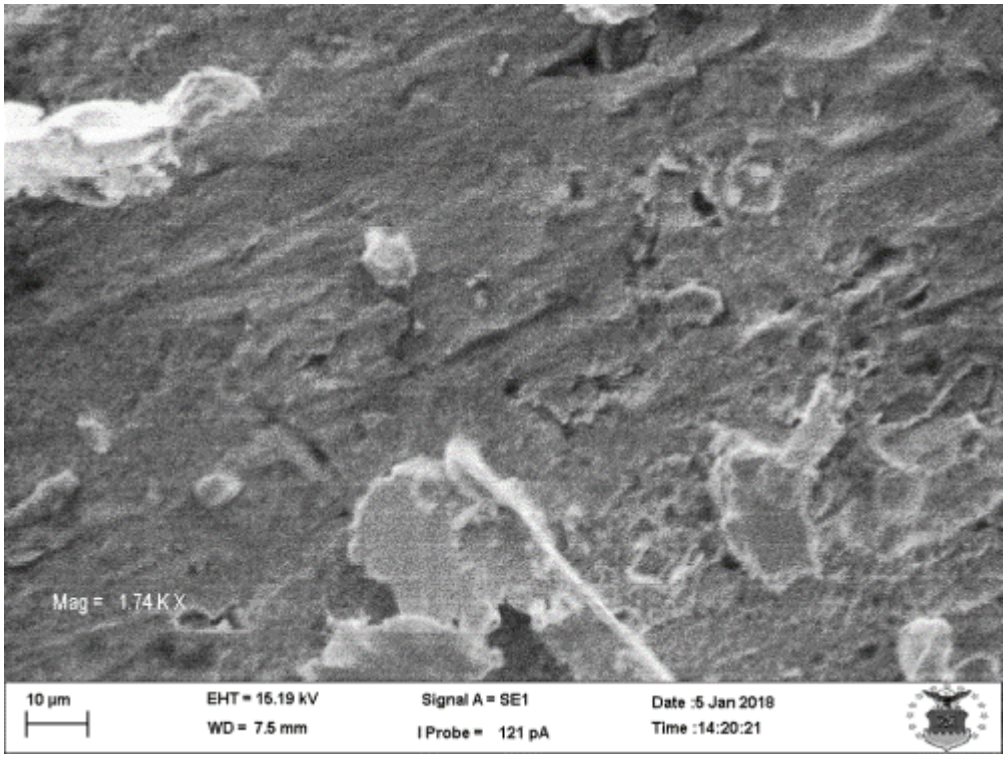

Figure 12: SEM Image of Air Exposed UA 2 Week Sample

University of Akron 2 Week Interface Sample:

The following is the data and outputs of the Fe 2p region of the sample from the UA that was at the interface between the fuel and water substitute for two weeks. The percent composition of the components determined from this analysis are; 5.62 % Fe(0), 19.88% FeO, 10.98% Fe_2O_3, 45.61% FeOOH, and 17.94% Fe_3O_4. The curve fitting for the iron regions for this sample can be seen in Figure 13, an SEM image of this sample can be seen in Figure 14. This data was collected over 1375 minutes and 12 seconds.

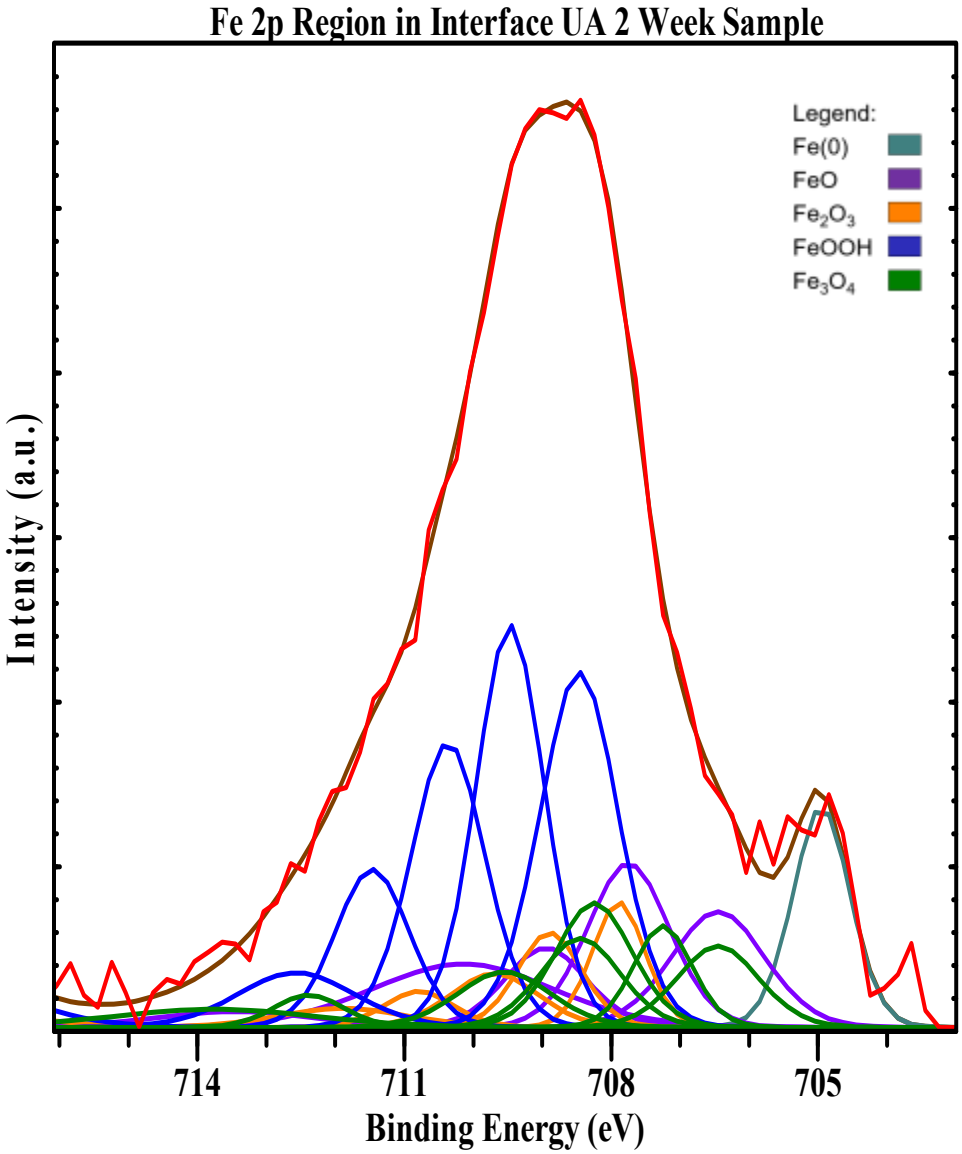

Figure 13: Intensity in Comparison to the Binding Energy detected of Fe 2p Regions in the Interface UA 2 Week Sample

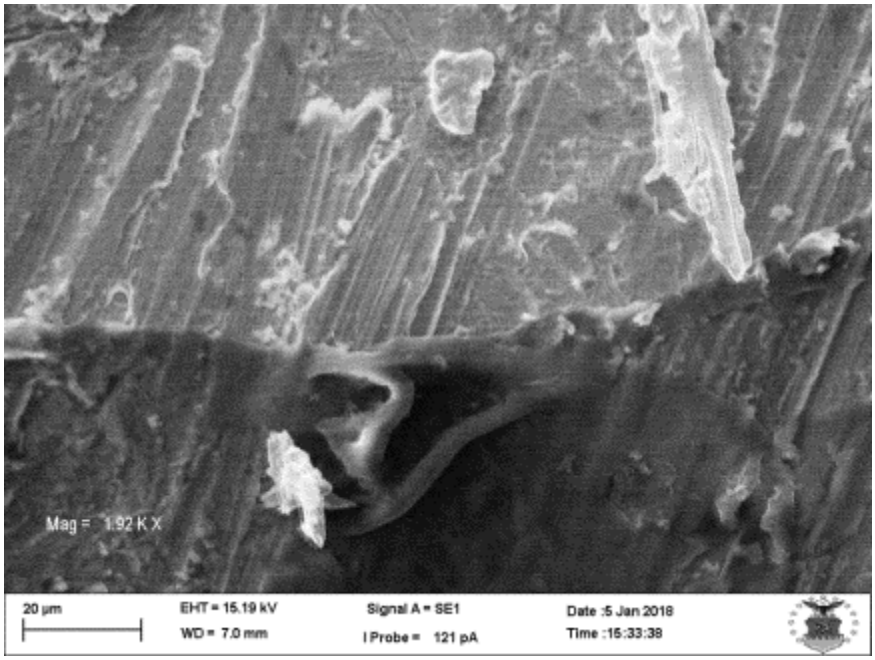

Figure 14: SEM Image of Interface UA 2 Week Sample

University of Akron Water Exposed 2 Week Sample:

The following is the data and outputs of the Fe 2p region of the sample from the UA that was exposed to a water substitute for two weeks. The percent composition of the components determined from this analysis are; 2.92% Fe (0), 60.08% FeO, 0.89% Fe_2O_3, 13.88% FeOOH, and 22.21% Fe_3O_4. The curve fitting for the iron regions for this sample can be seen in Figure 15, an SEM image of this sample can be seen in Figure 16. This data was collected over 636 minutes and 40 seconds.

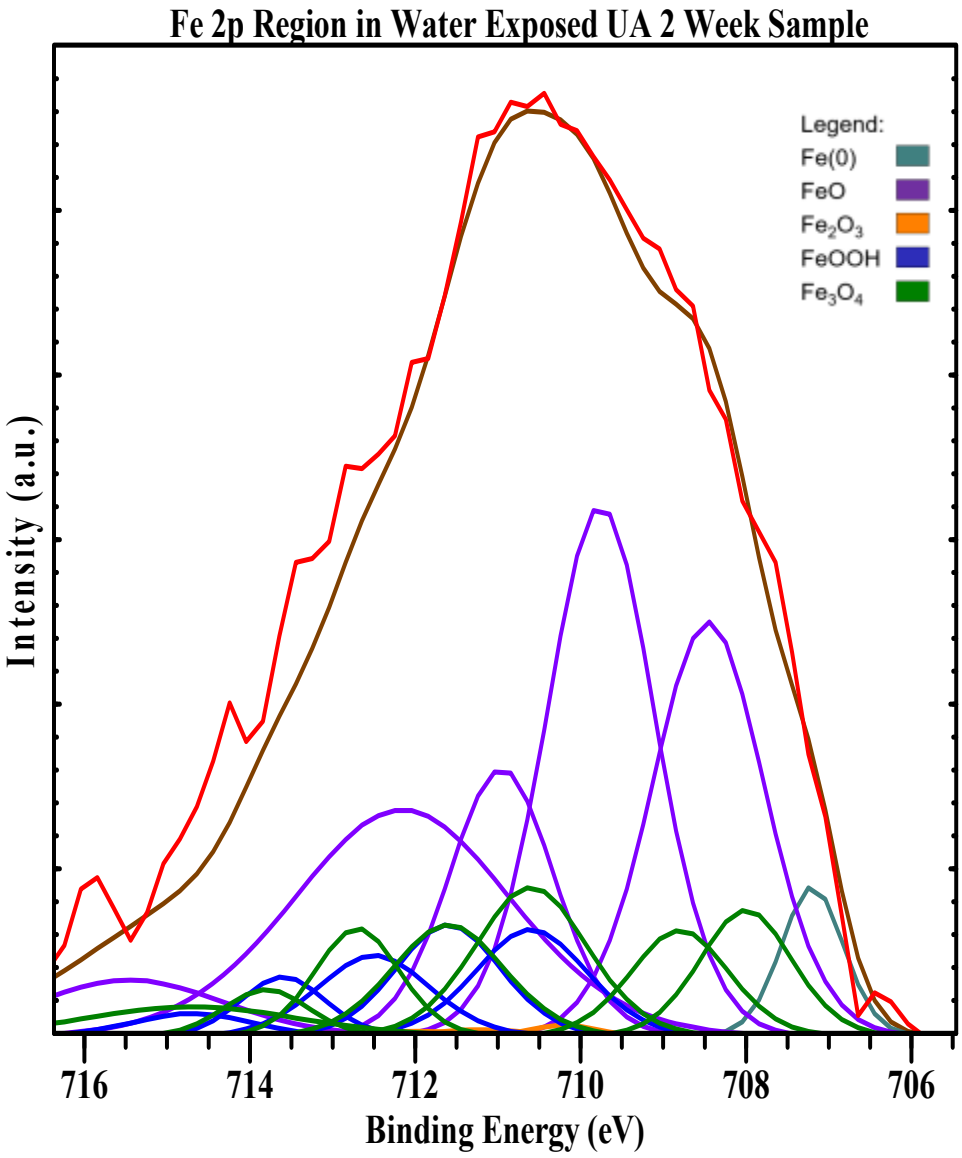

Figure 15: Intensity in Comparison to the Binding Energy detected of Fe 2p Regions in the Water Exposed UA 2 Week Sample

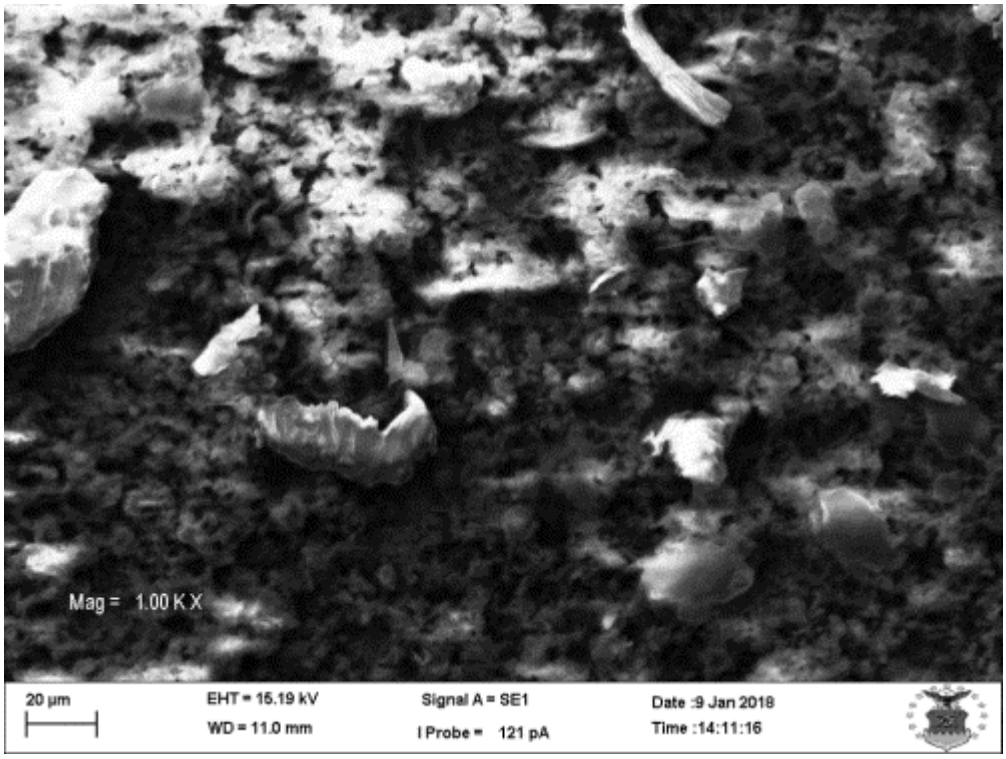

Figure 16: SEM Image of Water Exposed UA 2 Week Sample

University of Akron Air Exposed 4 Week Sample:

The following is the data and outputs of the Fe 2p region of the sample from the UA that was exposed to air for four weeks. The percent composition of the components determined from this analysis are; 1.81% Fe (0), 9.58% FeO, 17.48% Fe_2O_3, 22.01% FeOOH, 22.15% Fe_3O_4, and 26.96% tin (Sn). The curve fitting for the iron regions for this sample can be seen in Figure 17, an SEM image of this sample can be seen in Figure 18. This data was collected over 636 minutes and 40 seconds.

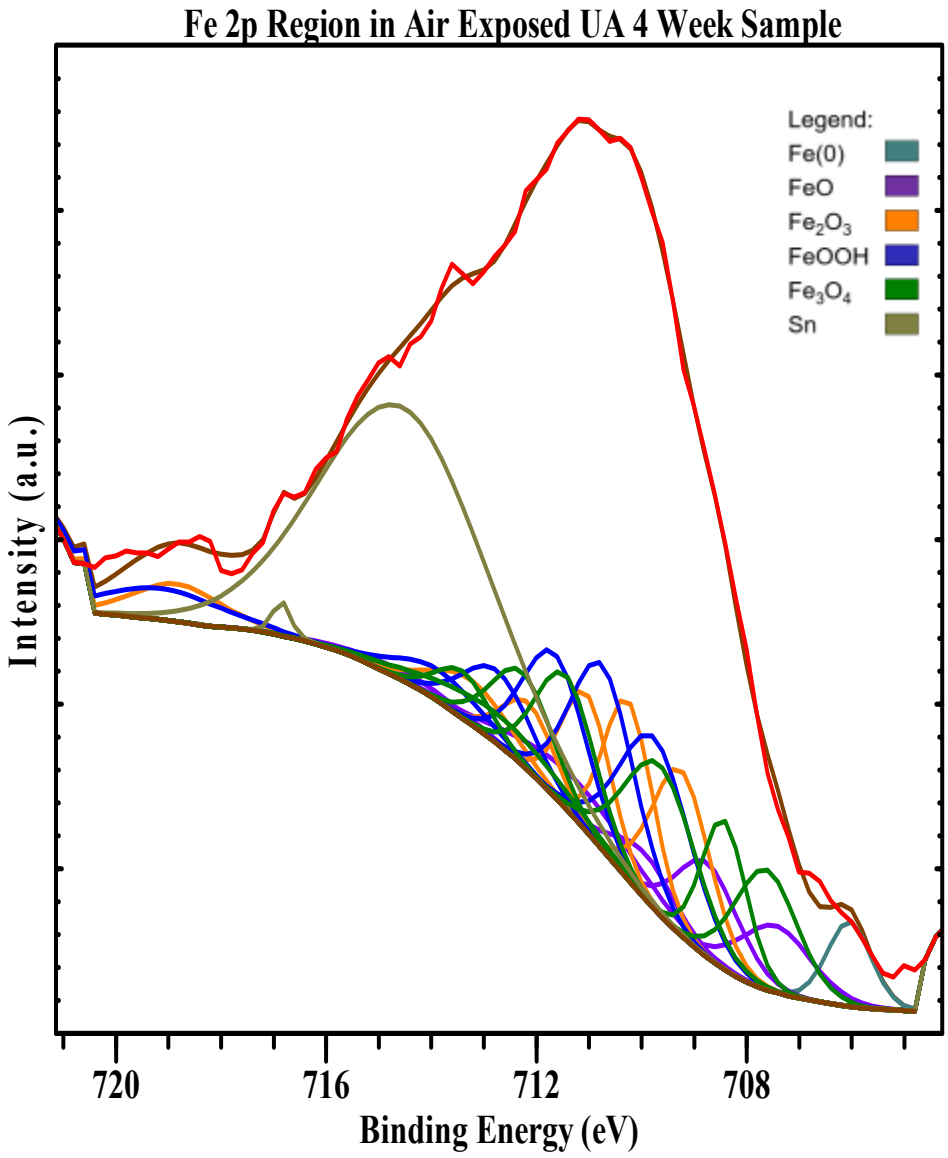

Figure 17: Intensity in Comparison to the Binding Energy detected of Fe 2p Regions in the Air Exposed UA 4 Week Sample

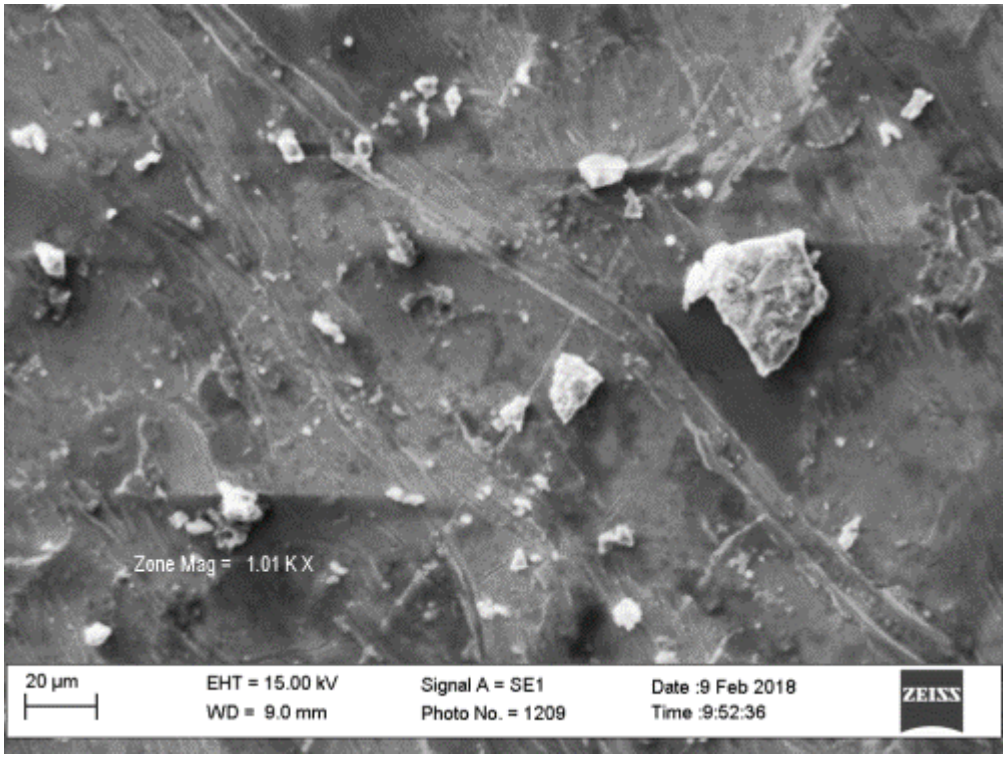

Figure 18: SEM Image of Air Exposed UA 4 Week Sample

University of Akron 4 Week Interface Sample:

The following is the data and outputs of the Fe 2p region of the sample from the UA that was at the interface between the fuel and water substitute for four weeks. The percent composition of the components determined from this analysis are; 3.34% Fe (0), 22.23% FeO, 0.00% Fe_2O_3, 24.69% FeOOH, 2.97% Fe_3O_4, and 46.77% Sn. The curve fitting for the iron regions for this sample can be seen in Figure 19, an SEM image of this sample can be seen in Figure 20. This data was collected over 636 minutes and 40 seconds.

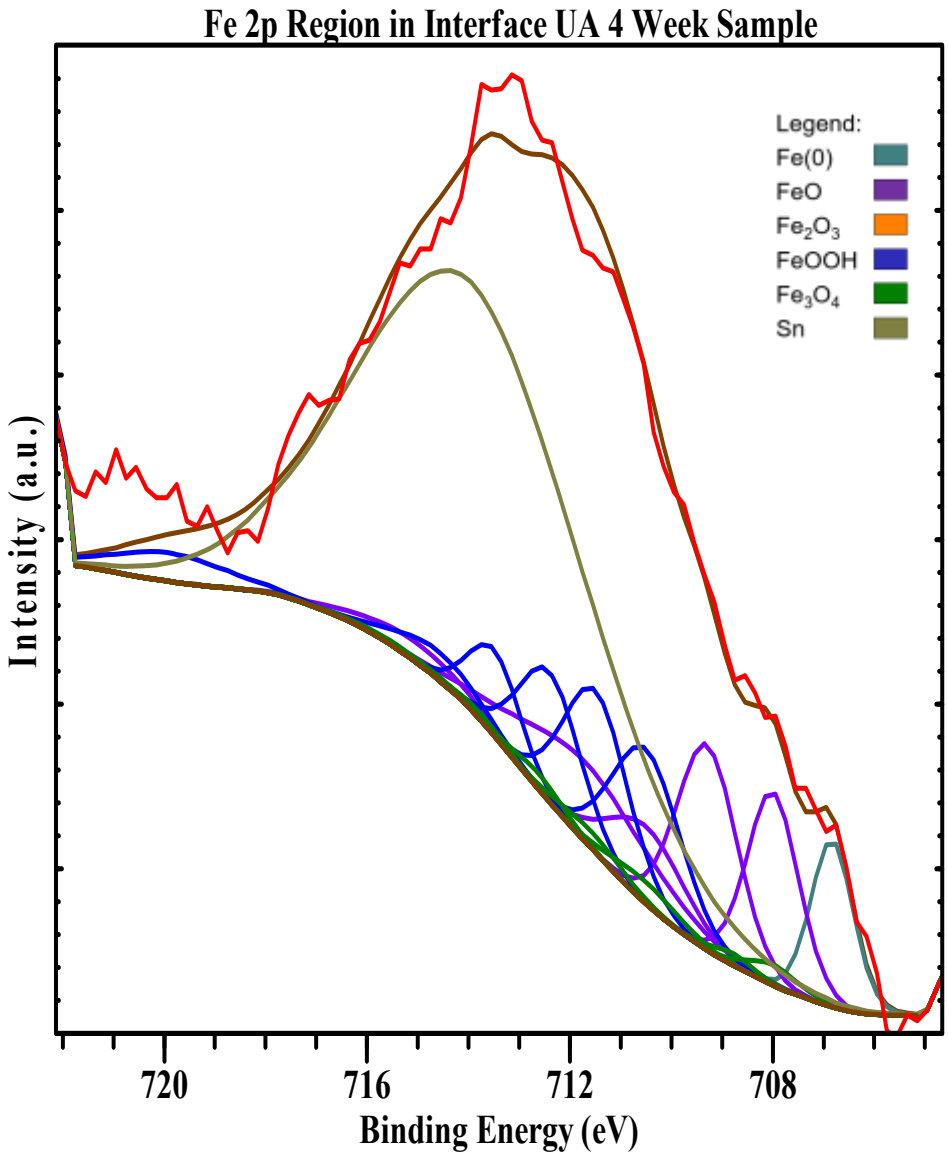

Figure 19: Intensity in Comparison to the Binding Energy detected of Fe 2p Regions in the Interface UA 4 Week Sample

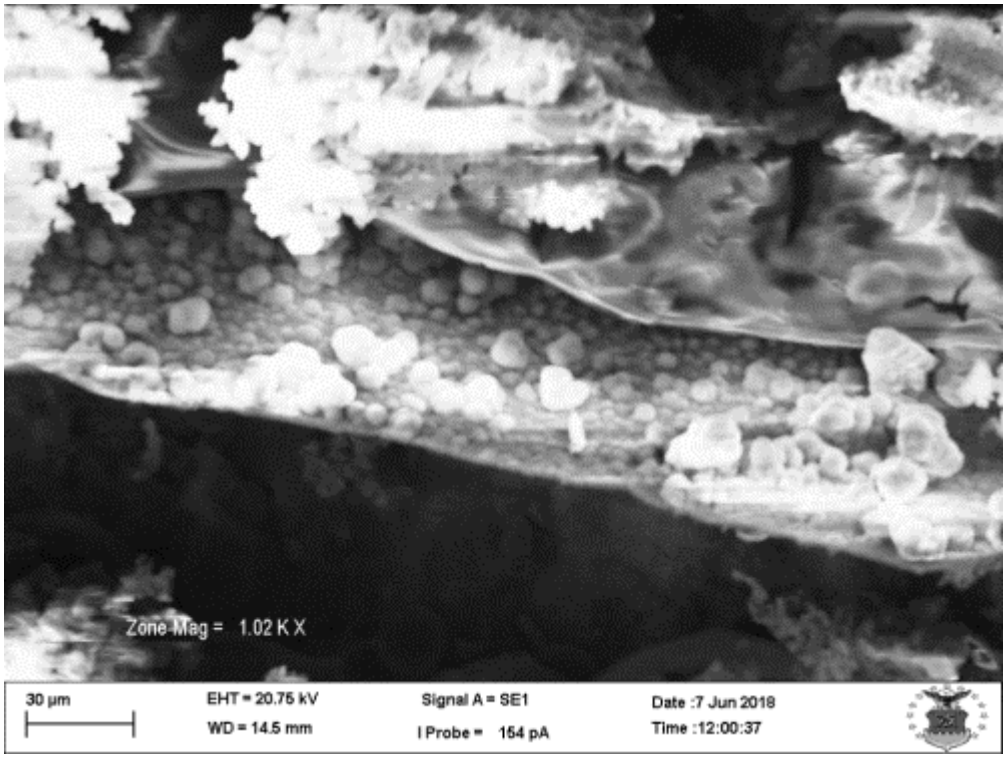

Figure 20: SEM Image of Interface UA 4 Week Sample

University of Akron Water Exposed 4 Week Sample (Dark Area):

The following is the data and outputs of the Fe 2p region of the sample from the UA that was exposed to a water substitute for four weeks. This data represents an area on the sample that was darker than the other portions of the sample. The percent composition of the components determined from this analysis are; 4.55% Fe (0), 11.38% FeO, 3.24% Fe_2O_3, 49.01% FeOOH, and 31.81% Fe_3O_4. The curve fitting for the iron regions for this sample can be seen in Figure 21, an SEM image of this sample can be seen in Figure 22. This data was collected over 636 minutes and 40 seconds.

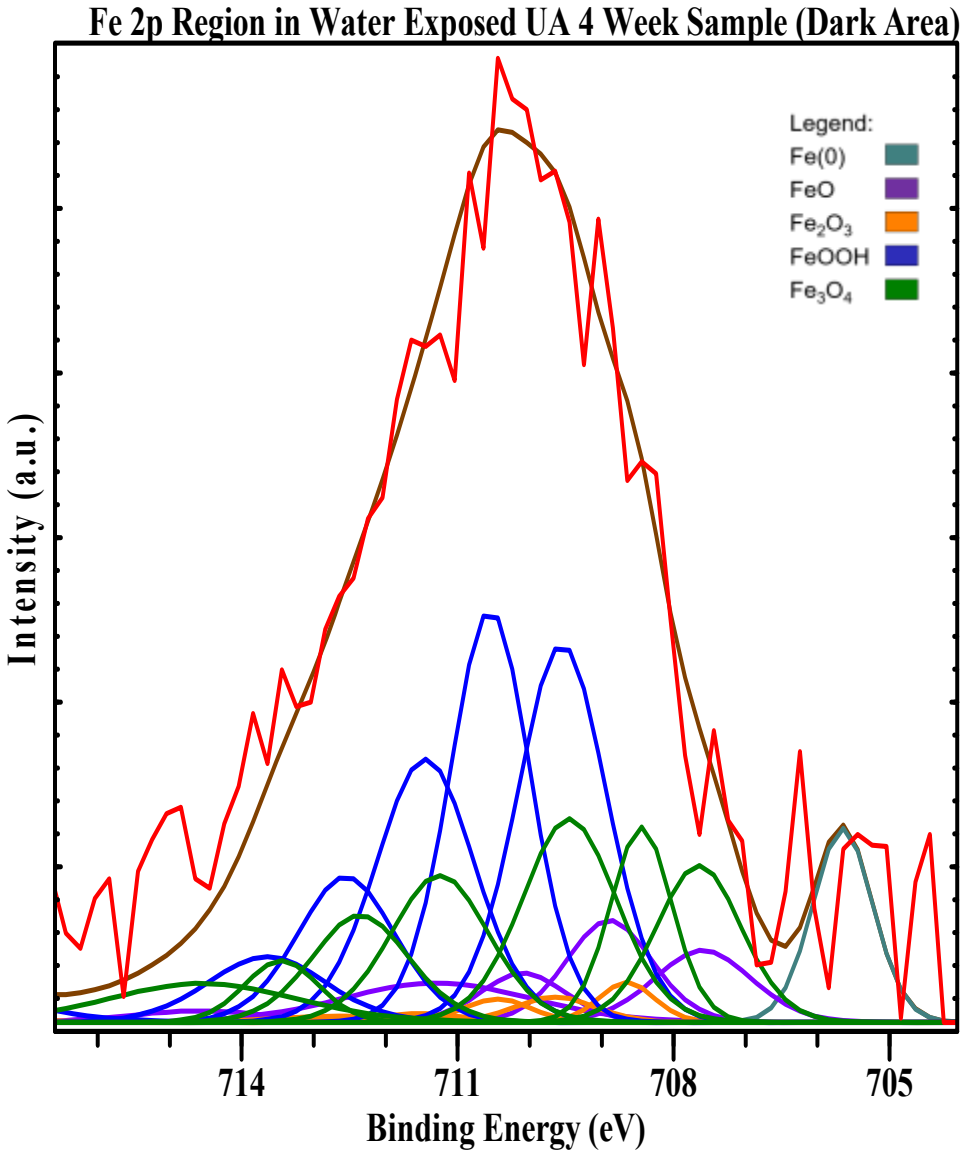

Figure 21: Intensity in Comparison to Binding Energy of Fe 2p Regions in Dark Area of Water Exposed UA 4 Week Sample

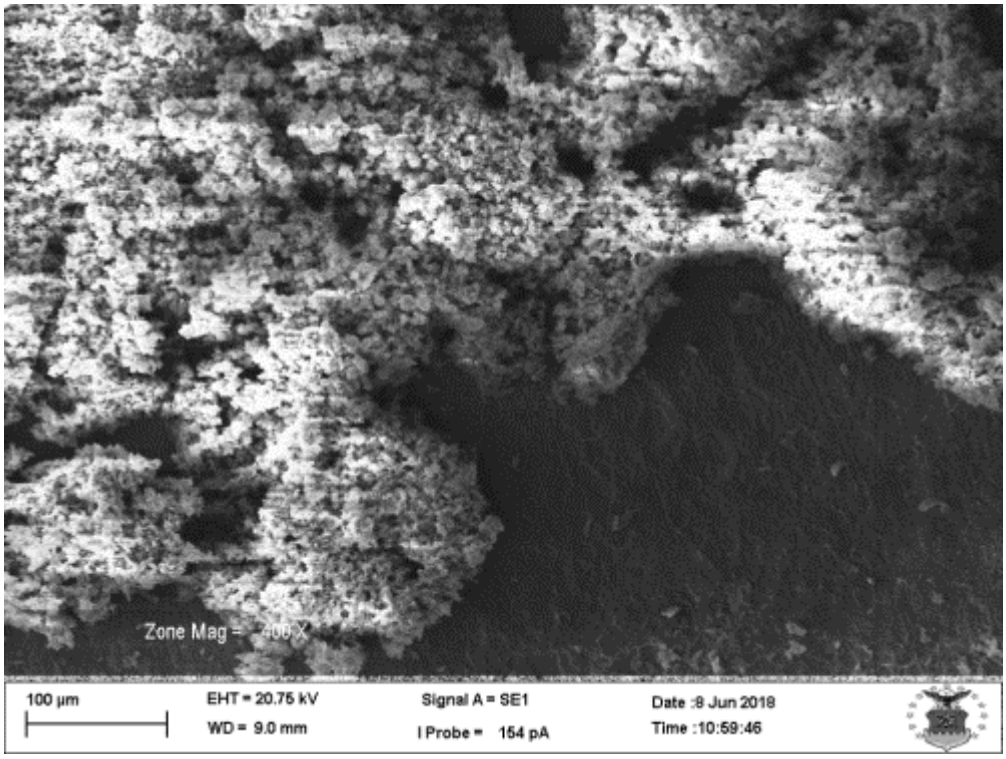

Figure 22: SEM Image of Dark Area of Water Exposed UA 4 Week Sample

University of Akron Water Exposed 4 Week Sample:

The following is the data and outputs of the Fe 2p region of the sample from the UA that was exposed to a water substitute for four weeks. The percent composition of the components determined from this analysis are; 4.27% Fe (0), 56.05% FeO, 23.29% Fe_2O_3, 14.02% FeOOH, and 2.33% Fe_3O_4. The curve fitting for the iron regions for this sample can be seen in Figure 23, an SEM image of this sample can be seen in Figure 24. This data was collected over 636 minutes and 40 seconds.

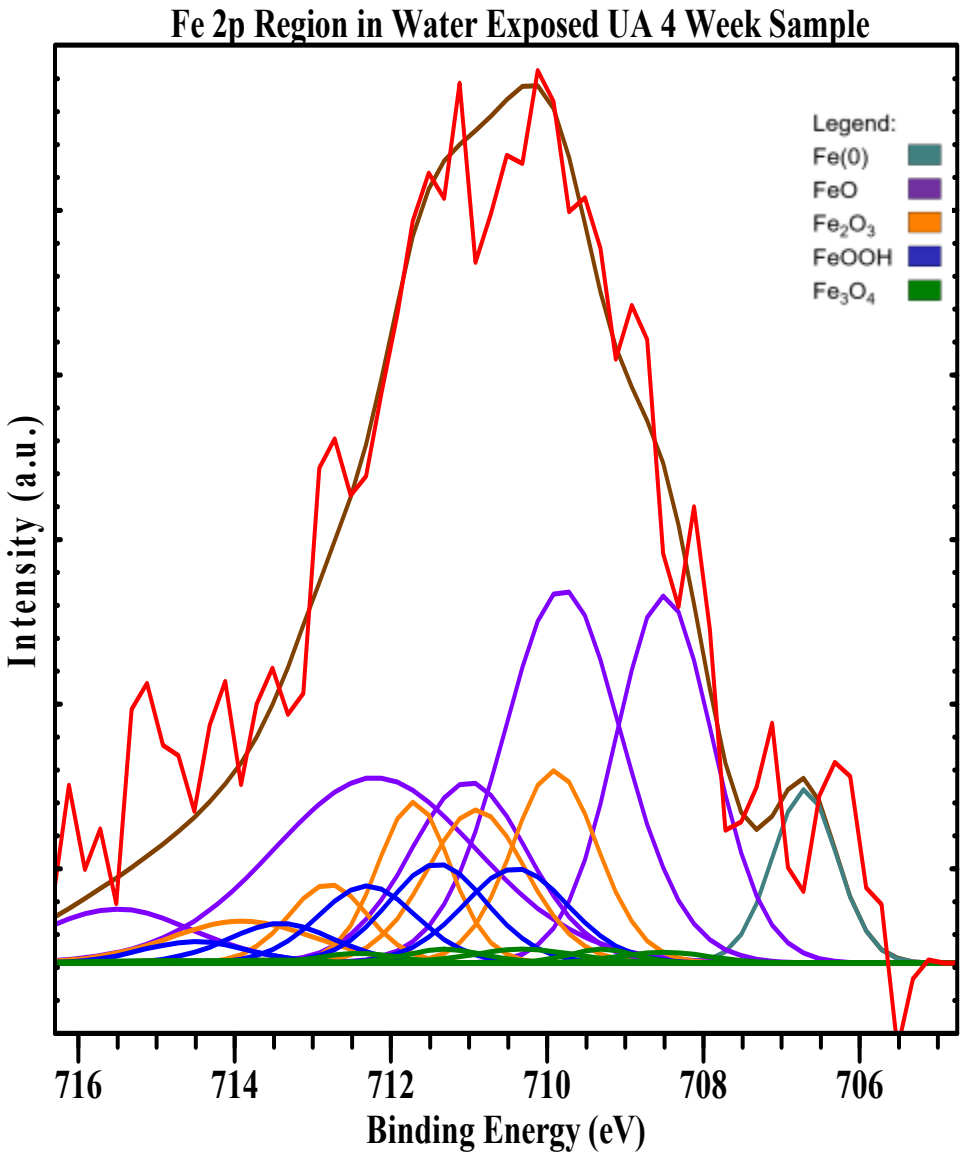

Figure 23: Intensity in Comparison to the Binding Energy detected of Fe 2p Regions in the Water Exposed UA 4 Week Sample

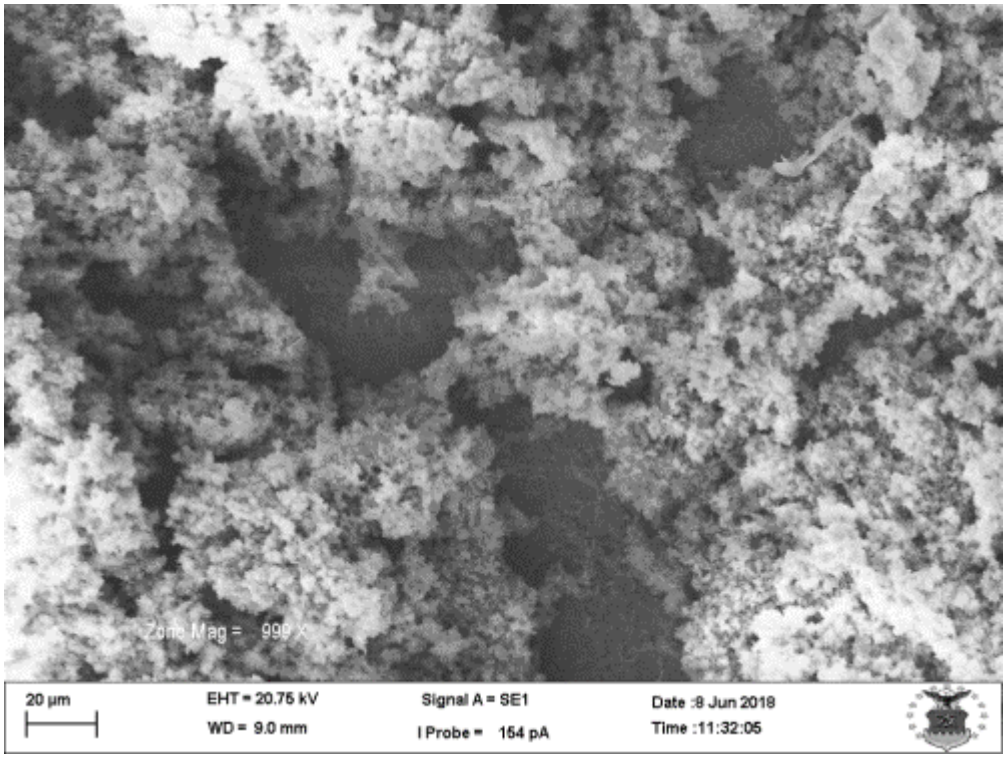

Figure 24: SEM Image of Water Exposed UA 4 Week Sample

University of Akron Sterile Air Exposed 4 Week Sample:

The following is the data and outputs of the Fe 2p region of the sample from the UA that was exposed to air for four weeks, the conical test tube that contained this sample was sterile. The percent composition of the components determined from this analysis are; 2.45% Fe (0), 11.52% FeO, 49.91% Fe_2O_3, 9.06% FeOOH, and 27.03% Fe_3O_4. The curve fitting for the iron regions for this sample can be seen in Figure 25, an SEM image of this sample can be seen in Figure 26. This data was collected over 1442 minutes and 3 seconds.

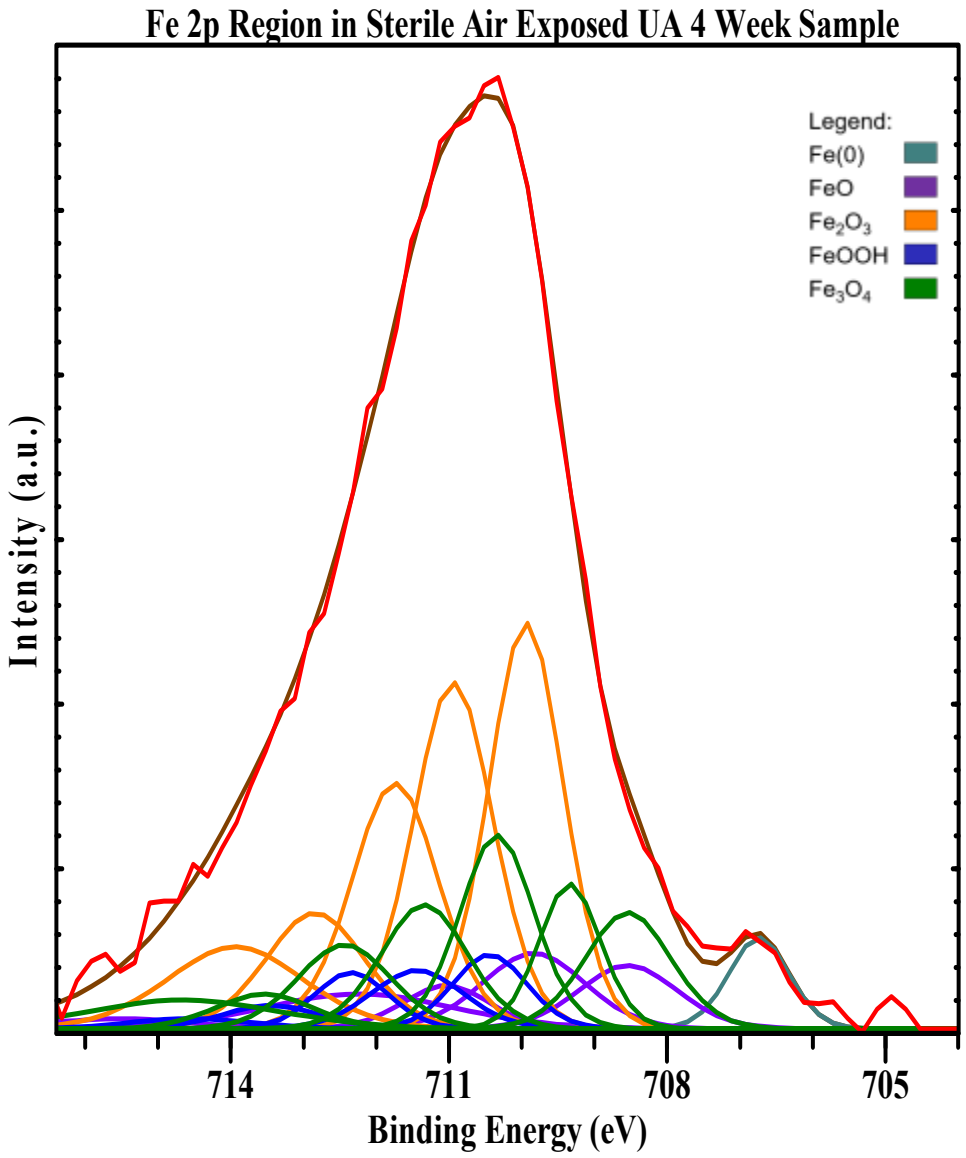

Figure 25: Intensity in Comparison to the Binding Energy detected of Fe 2p Regions in Sterile Air Exposed UA 4 Week Sample

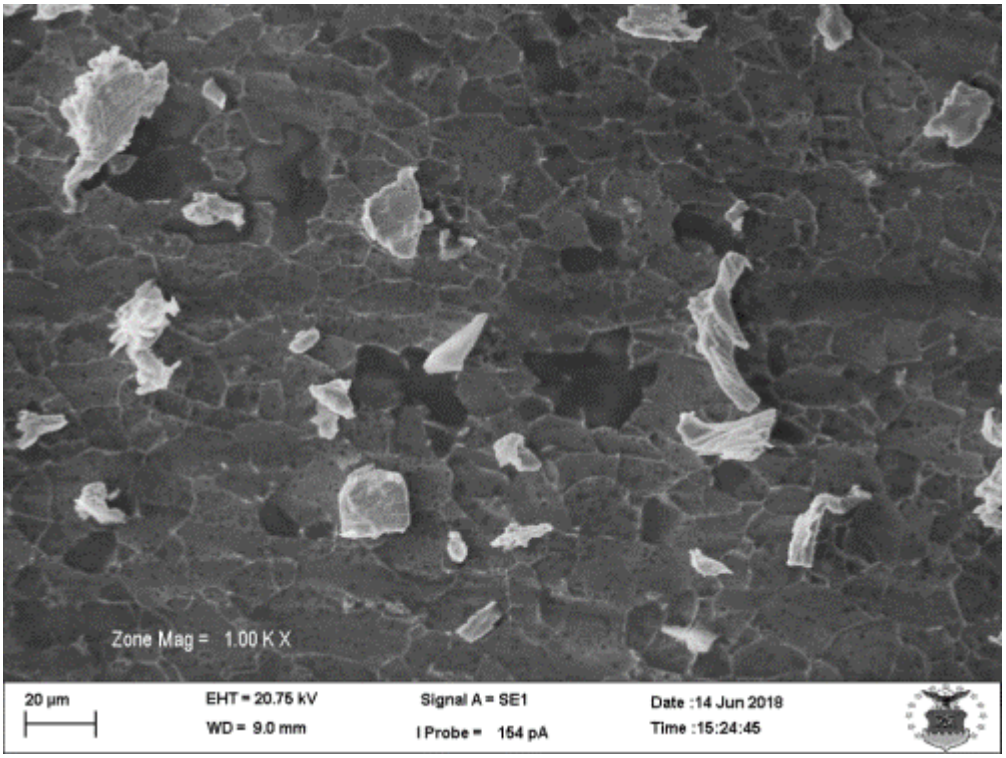

Figure 26: SEM Image of Sterile Air Exposed UA 4 Week Sample

University of Akron Sterile Interface 4 Week Sample:

The following is the data and outputs of the Fe 2p region of the sample from the UA that was at the interface between the fuel and water substitute for four weeks, the conical test tube that contained this sample was sterile. The percent composition of the components determined from this analysis are; 1.71% Fe (0), 3.71% FeO, 9.14% Fe_2O_3, 14.49% FeOOH, 21.07% Fe_3O_4, and 49.90% Sn. The curve fitting for the iron regions for this sample can be seen in Figure 27, an SEM image of this sample can be seen in Figure 28. This data was collected over 2387 minutes and 30 seconds.

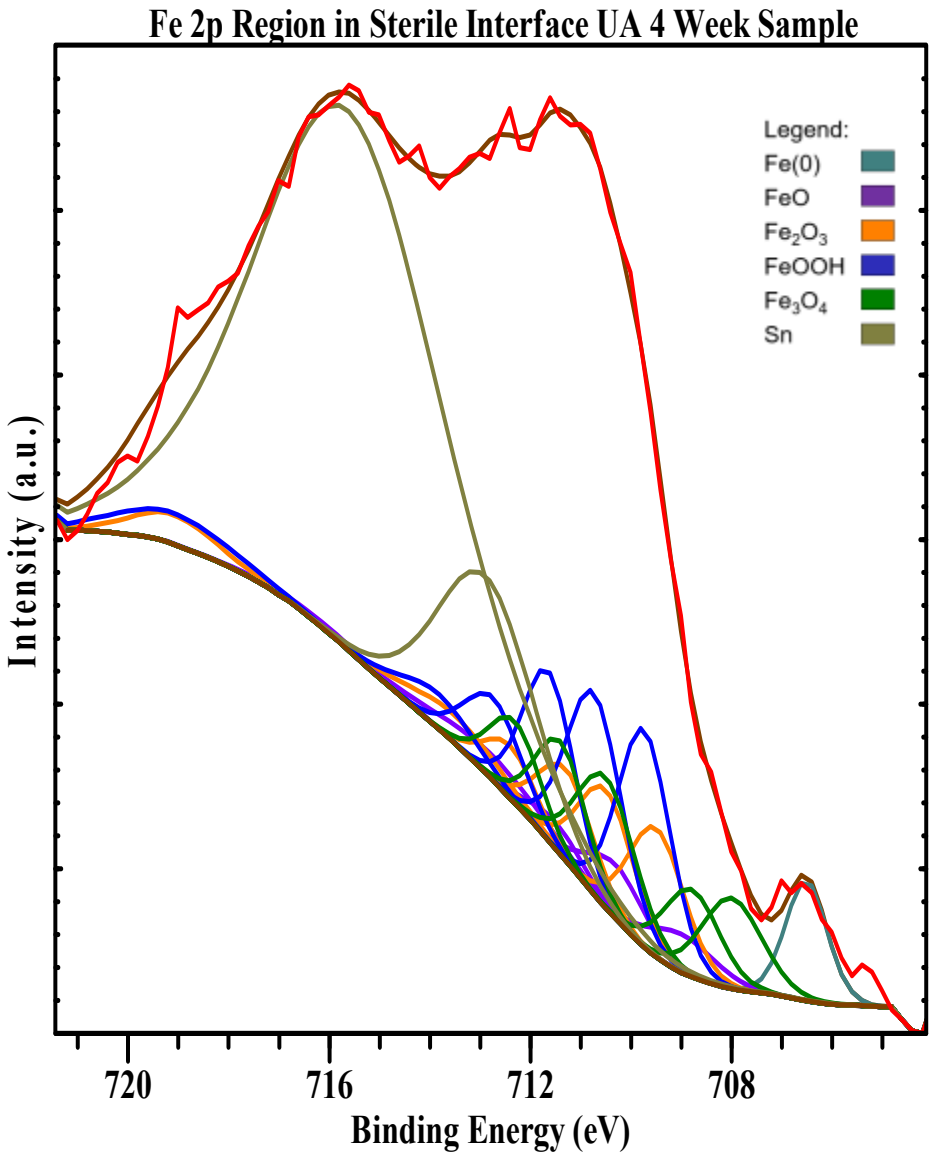

Figure 27: Intensity in Comparison to the Binding Energy detected of Fe 2p Regions in the Sterile Interface UA 4 Week Sample

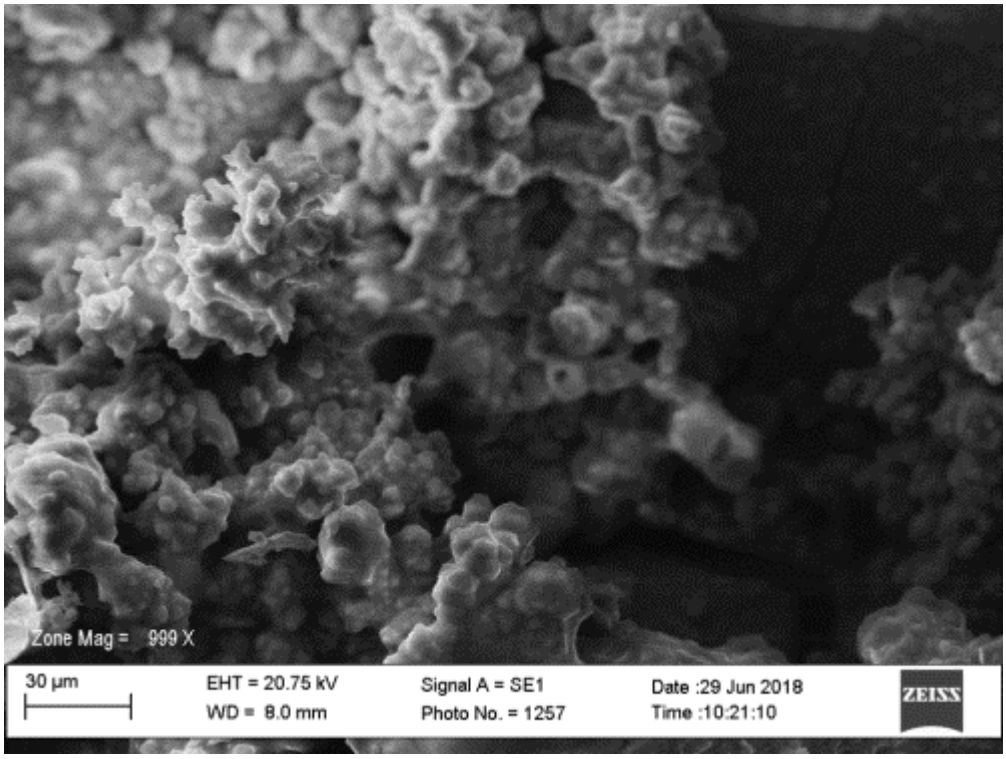

Figure 28: SEM Image of Sterile Interface UA 4 Week Sample

University of Akron Sterile Water Exposed 4 Week Sample:

The following is the data and outputs of the Fe 2p region of the sample from the UA that was exposed to a water substitute for four weeks, the conical test tube that contained this sample was sterile. The percent composition of the components determined from this analysis are; 2.64% Fe (0), 25.48% FeO, 16.13% Fe_2O_3, 21.86% FeOOH, 7.03% Fe_3O_4, and 26.84% Sn. The curve fitting for the iron regions for this sample can be seen in Figure 29, an SEM image of this sample can be seen in Figure 30. This data was collected over 1387 minutes and 56 seconds.

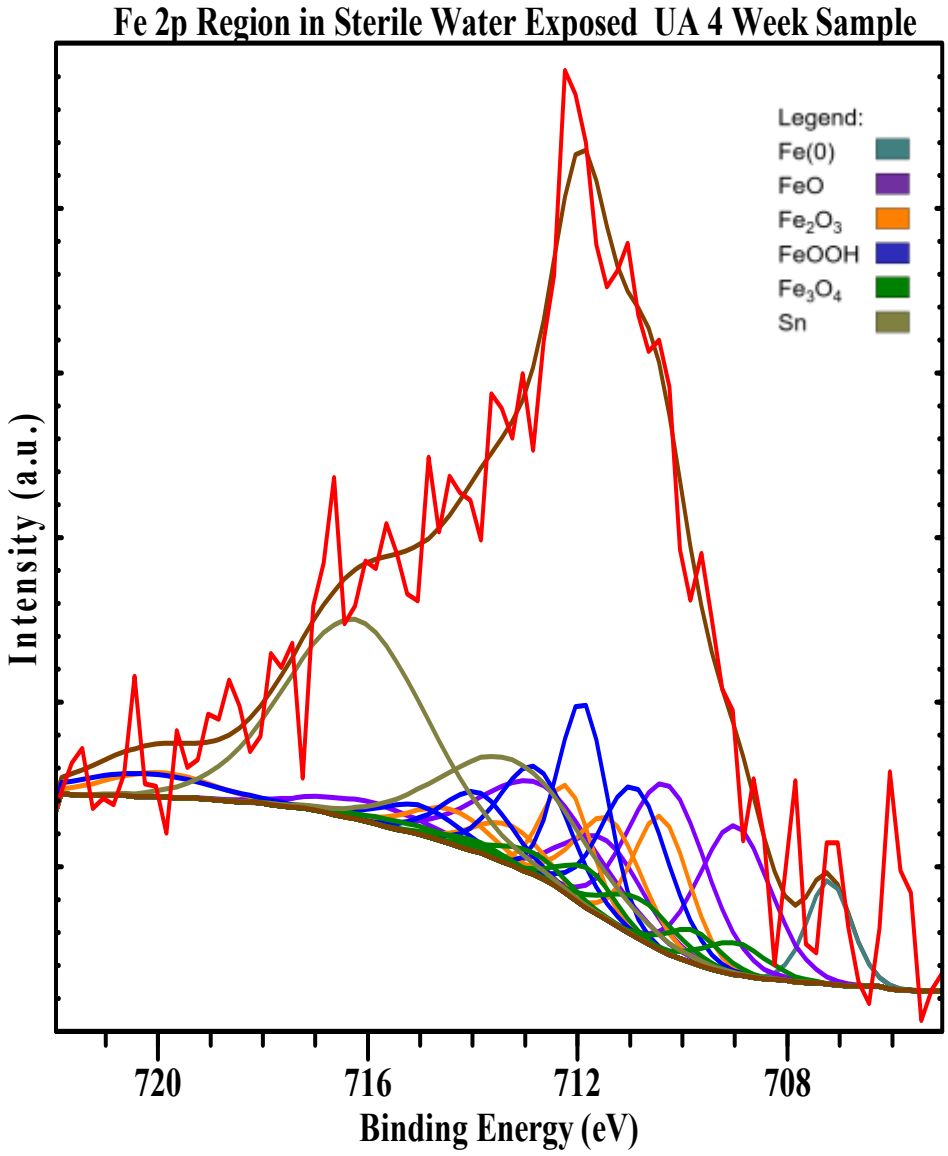

Figure 29: Intensity in Comparison to Binding Energy detected of Fe 2p Regions in Sterile Water Exposed UA 4 Week Sample

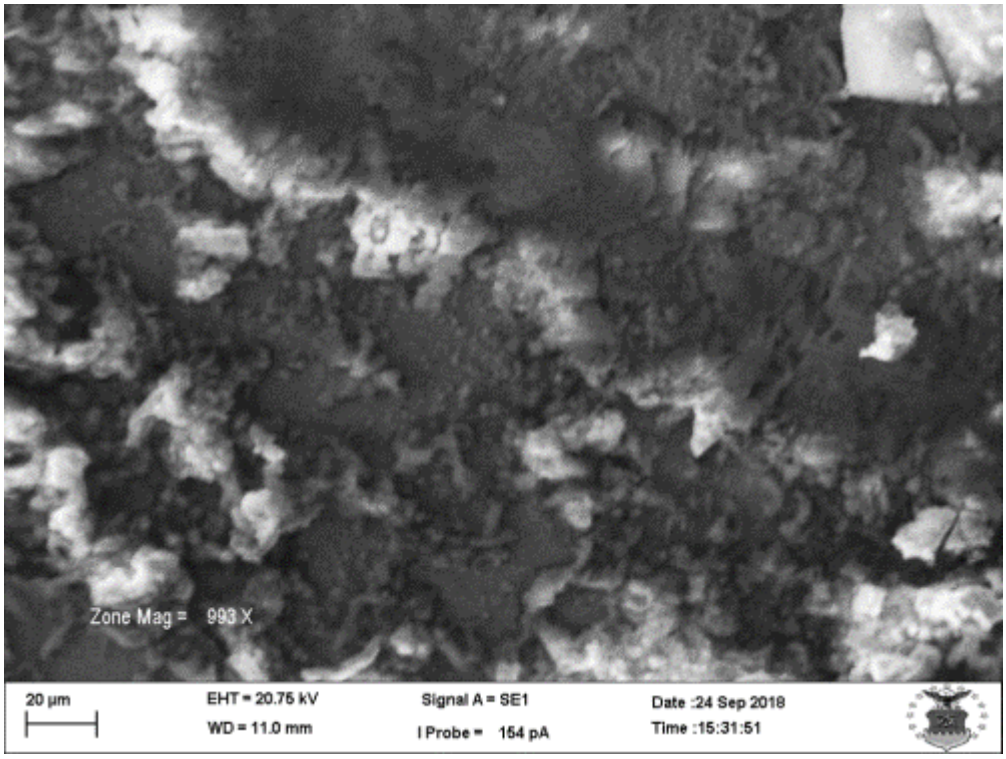

Figure 30: SEM Image of Sterile Water Exposed UA 4 Week Sample

Air Force Research Laboratory Air Exposed 2 Week Sample:

The following is the data and outputs of the Fe 2p region of the sample from the Air Force Research Laboratory that was exposed to air for two weeks. The percent composition of the components determined from this analysis are; 0.59% Fe (0), 50.66% FeO, 39.13% Fe_2O_3, 0.00% FeOOH, and 9.63% Fe_3O_4 . The curve fitting for the iron regions for this sample can be seen in Figure 31, an SEM image of this sample can be seen in Figure 32. This data was collected over 636 minutes and 40 seconds.

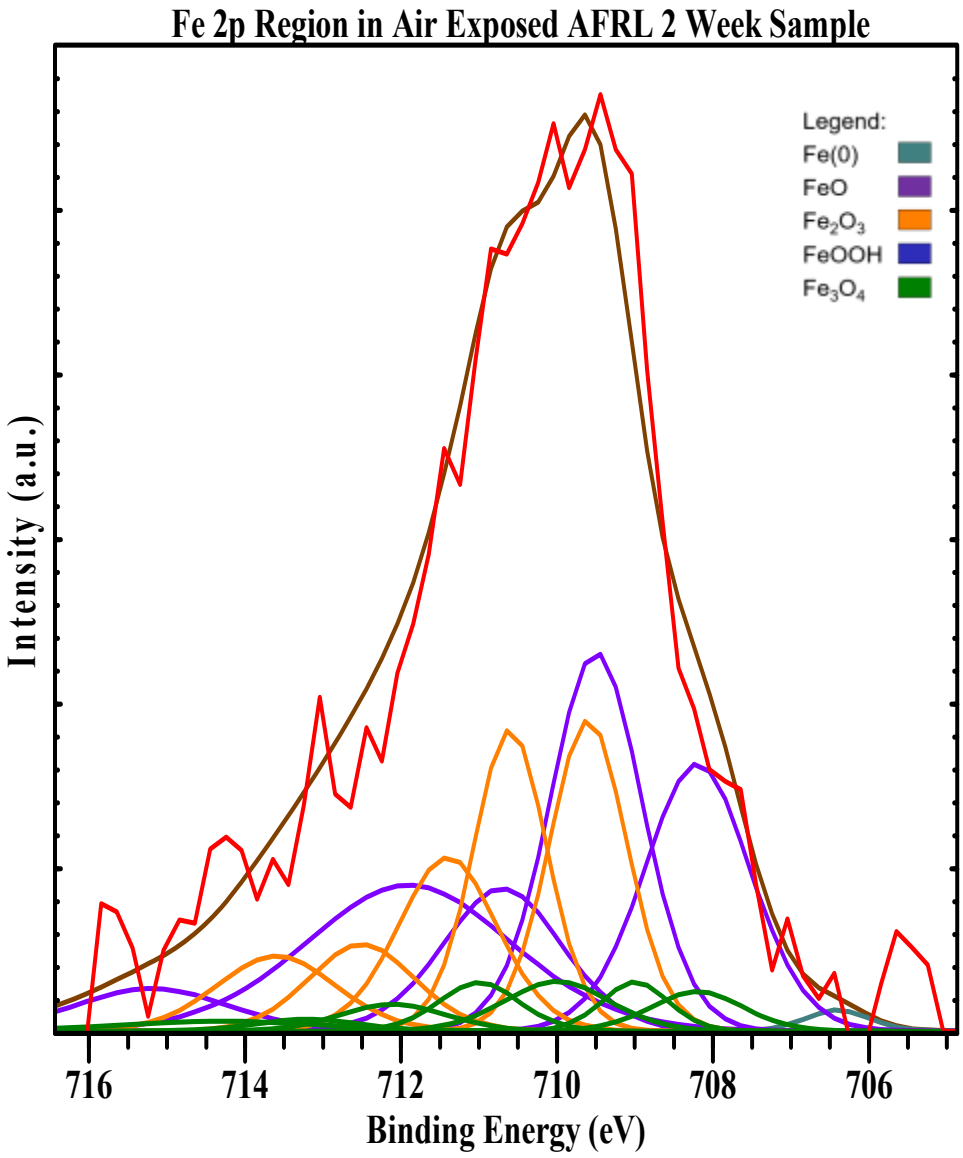

Figure 31: Intensity in Comparison to the Binding Energy detected of Fe 2p Regions in the Air Exposed AFRL 2 Week Sample

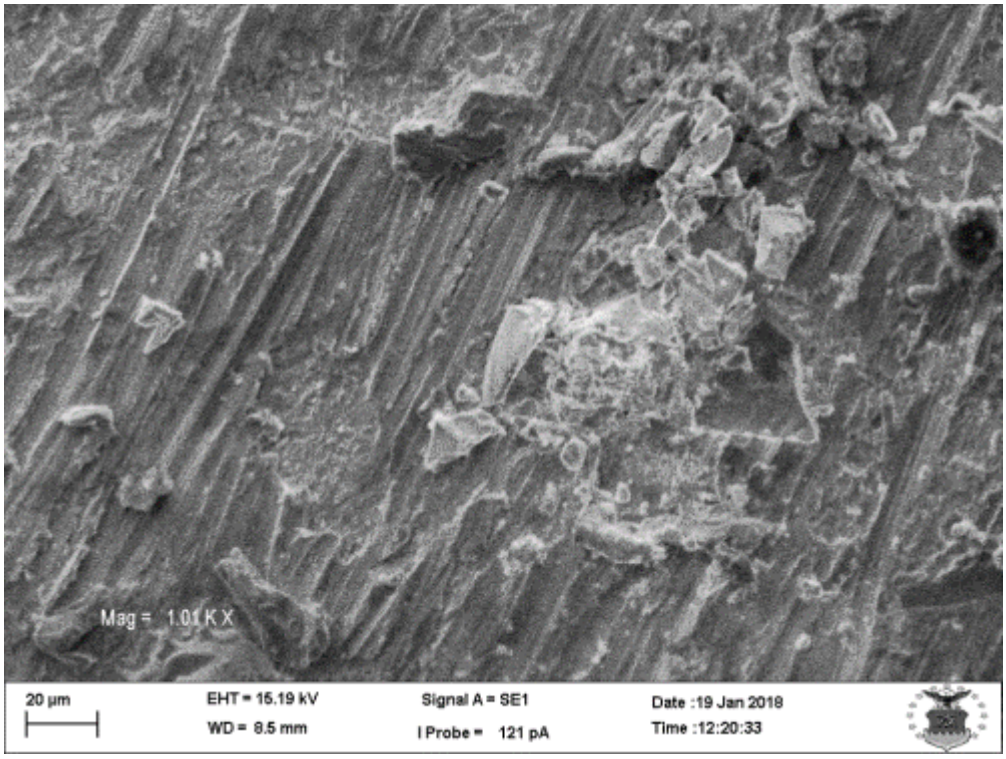

Figure 32: SEM Image of Air Exposed AFRL 2 Week Sample

Air Force Research Laboratory Interface 2 Week Sample:

The following is the data and outputs of the Fe 2p region of the sample from the Air Force Research Laboratory that was at the interface between the fuel and water substitute for two weeks. The percent composition of the components determined from this analysis are; 1.83% Fe (0), 15.68% FeO, 56.58% Fe_2O_3, 0.00% FeOOH, and 25.89% Fe_3O_4. The curve fitting for the iron regions for this sample can be seen in Figure 33, an SEM image of this sample can be seen in Figure 34. This data was collected over 636 minutes and 40 seconds.

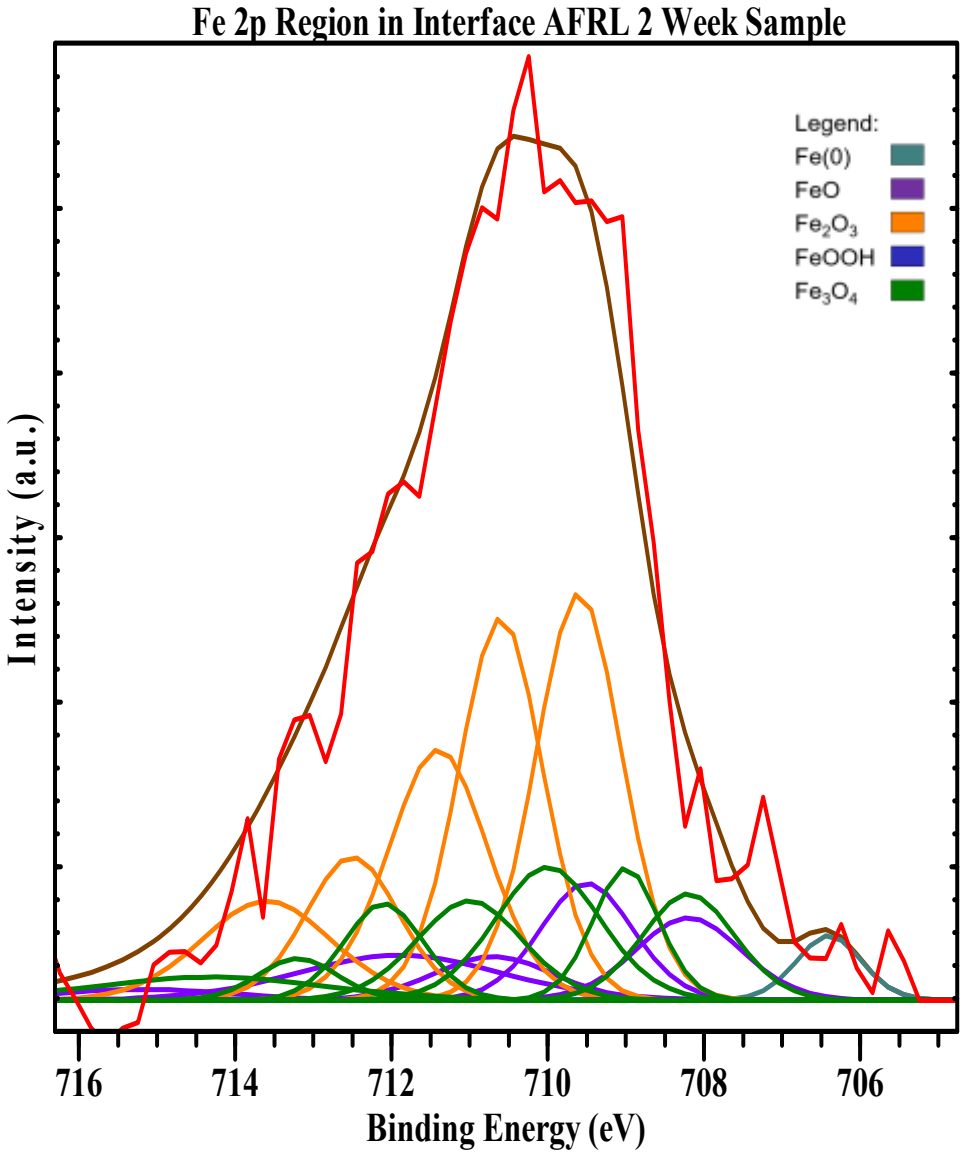

Figure 33: Intensity in Comparison to the Binding Energy detected of Fe 2p Regions in the Interface AFRL 2 Week Sample

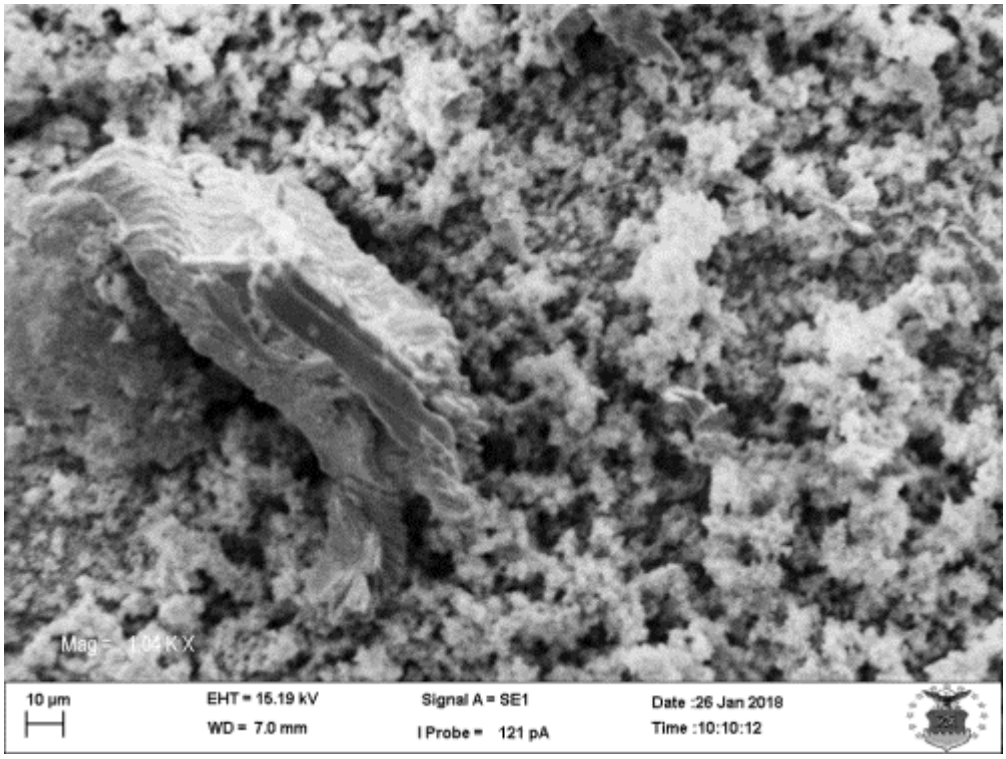

Figure 34: SEM Image of Interface AFRL 2 Week Sample

Air Force Research Laboratory Water Exposed 2 Week Sample:

The following is the data and outputs of the Fe 2p region of the sample from the Air Force Research Laboratory that was exposed to a water substitute for two weeks. The percent composition of the components determined from this analysis are; 1.49% Fe (0), 8.53% FeO, 71.07% Fe_2O_3, 0.19% FeOOH, and 18.73% Fe_3O_4. The curve fitting for the iron regions for this sample can be seen in Figure 35, an SEM image of this sample can be seen in Figure 36. This data was collected over 636 minutes and 40 seconds.

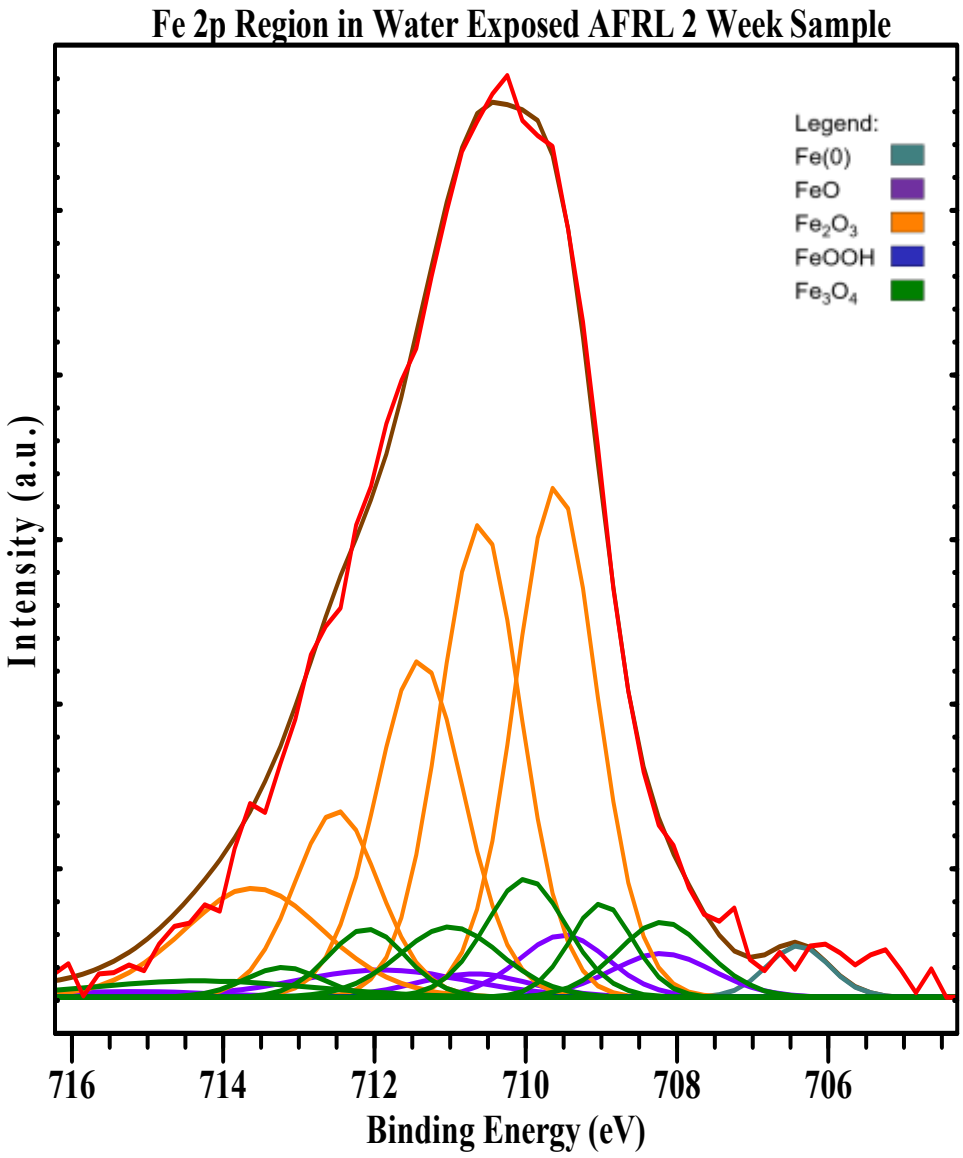

Figure 35: Intensity in Comparison to the Binding Energy detected of Fe 2p Regions in the Water Exposed AFRL 2 Week Sample

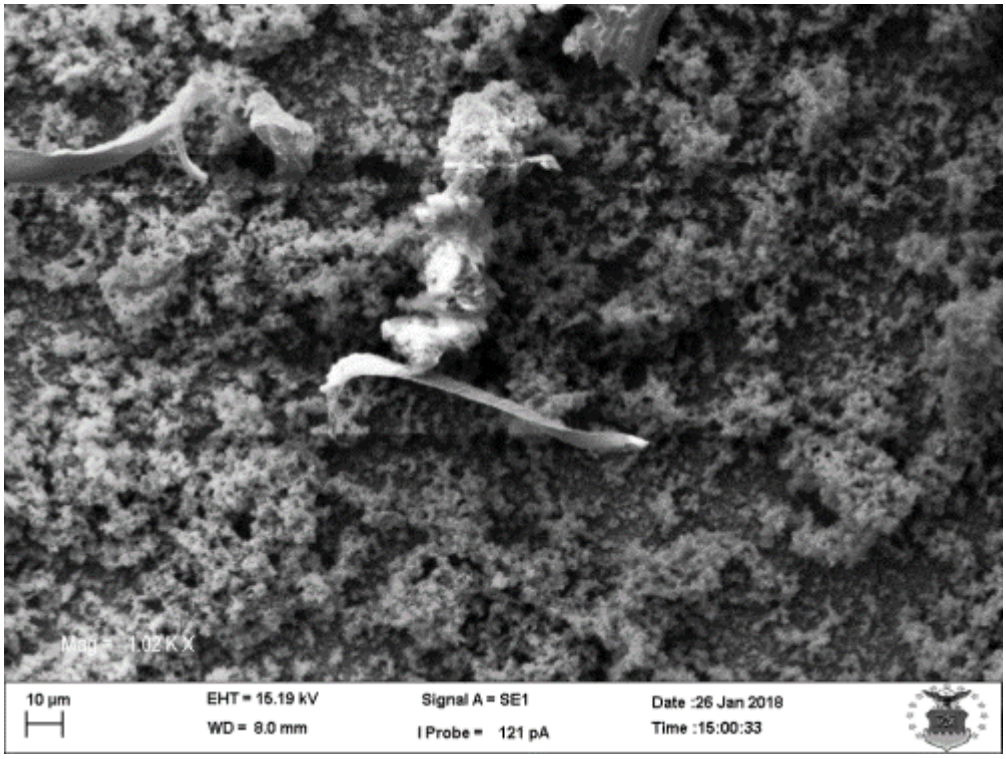

Figure 36: SEM Image of Water Exposed AFRL 2 Week Sample

Discussion

For the purpose of this discussion, the three experiments from the Air Force Research Laboratory (AFRL) will be considered. This is because these samples were kept in the most consistent conditions when compared among the remainder of the samples. Specifically, these samples shared the same environment for the experiment and this experiment occurred at the same location. Furthermore, these samples did not contain any tin, the existence of which is suspected to be a form of contamination. Additionally, the long length of time taken for analysis of the samples indicates that the results obtained from the analysis are reliable and any suspected contamination observed is not a result of instrumental error.

Expected Products of Corrosion:

Each of the three separate environments have different corrosion products that would be expected as a result of those environments. For example, the samples exposed to air would most likely show increased amounts of FeOOH and Fe_2O_3, as these oxides are typical on the surface of steel exposed to air (Mattsson, 2001). If iron reduction MIC was occurring at the interface, greater amounts of FeO would be detected (Ottow et al., 1969) with potentially greater amounts of Fe_3O_4 as the crystal structure of Fe_3O_4 contains both FeO and Fe_2O_3 (Cornell & Schwertmann, 2003). Finally, the surface of typical rust environments consists of FeOOH and Fe_3O_4, therefore the water samples would likely demonstrate a similar surface chemistry (Landolt, 2007).

Observation of the Control and Air Exposed 2 Week AFRL Sample:

When compared with the control sample, the two week AFRL air exposed sample had a significantly lower percent of elemental iron on its surface, which was reduced from 12.51% in the control sample, to 0.59% in the air exposed sample. This significant drop in elemental iron is likely because a large amount of carbon was found on the surface of the sample, this is possibly due to the evaporation of the hydrocarbon-based fuel, which could have been deposited on the surface of the sample. The presence of this carbon would decrease the ability of the instrument to penetrate into the sample which would result in the detection of a lesser percent composition of elemental iron in the air exposed sample, than that of the control sample. However, the percent composition of FeO increased from 37.51% in the control, to 50.66% in the air exposed sample. The amount of Fe_2O_3 within both

samples stayed relatively consistent at 39.70% in the control sample, and 39.13% in the air exposed sample. Finally, the percent composition of Fe_3O_4 was also similar, with the control containing 10.28% and the air exposed samples containing 9.63%. Ultimately, it appears as though the air exposed sample did not differ much from the control sample, and the difference between the chemical composition of oxides is likely related to carbon on the surface of these samples. Figure 37 and Figure 38 are visual representations of the control sample and the 2 week air exposed AFRL sample respectively, both of which were imaged via Scanning Electron Microscope. Both figures display a surface which is not uniform, and both contain various divots and pits, but both images also do not show any major signs of oxidation, nor do they show any significant signs of damage. This observation supports the notion that not much corrosion occurred on the air exposed two week AFRL sample, and the results gathered from the XPS analysis are primarily the result of hydrocarbon deposition on the surface of the sample.

Observation of the Control and the Interface 2 Week AFRL Sample:

At the interface between the two mediums, the percent compositions of iron oxides from the XPS analysis began to differ more. The amount of elemental iron decreased from 12.51% in the control to 1.83% in the interface sample. However, the amount of FeO in the sample dramatically decreased from 37.51% to 15.68% while the percent composition of Fe_2O_3 increased from 39.70% to 56.58%. Furthermore, the percent composition of Fe_3O_4 increased from 10.28% in the control sample to 25.89% in the interface sample.

While uniform rusting of iron is typically associated with Fe_3O_4 and FeOOH (Landolt, 2007), however, because no FeOOH has been observed, it is possible that this sample demonstrates some iron reduction capability of the *Byssochlamys nivea*. This is because MIC involving iron reduction from microbes involves the process of reducing Fe_2O_3 to FeO, not the production of FeOOH (Johnson & McGinness, 1991; Ottow et al., 1969). While this seems counterintuitive at first, as the amount of FeO has decreased rather than increased, the potential for *Byssochlamys nivea* to have caused MIC by iron reduction cannot be ruled out, as Fe_3O_4 is a complex iron oxide that includes both FeO and Fe_2O_3 (Blaney, 2007). Therefore, because the percent volume of Fe_3O_4 has increased, it is possible that iron-reduction occurred, with the FeO product entering into the matrix of Fe_3O_4. However, future research is required to determine this relation.

Figure 39 demonstrates what occurred at the interface between the suspected location of the fungal biofilm and the Bushnell Hass (BH) medium. On the upper left side of the image is the area believed to be previously covered by a biofilm. Interestingly this side does not show as significant of corrosion when compared to the lower right side, which is the side that contains the corrosion which occurred in the BH medium. This observation could indicate that iron reduction MIC did indeed occur on these areas, as these areas do not appear to have the typical porous, friable, reddish-brown surface that is typically associated with normal rusting.

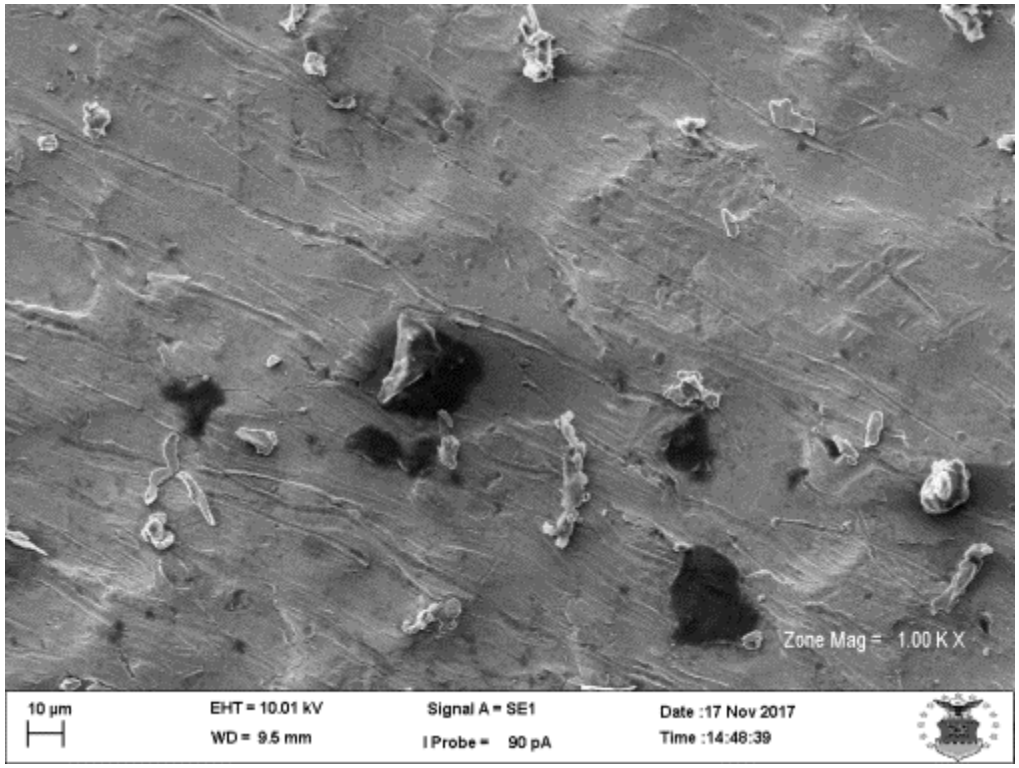

Figure 37: SEM Image of Control Sample

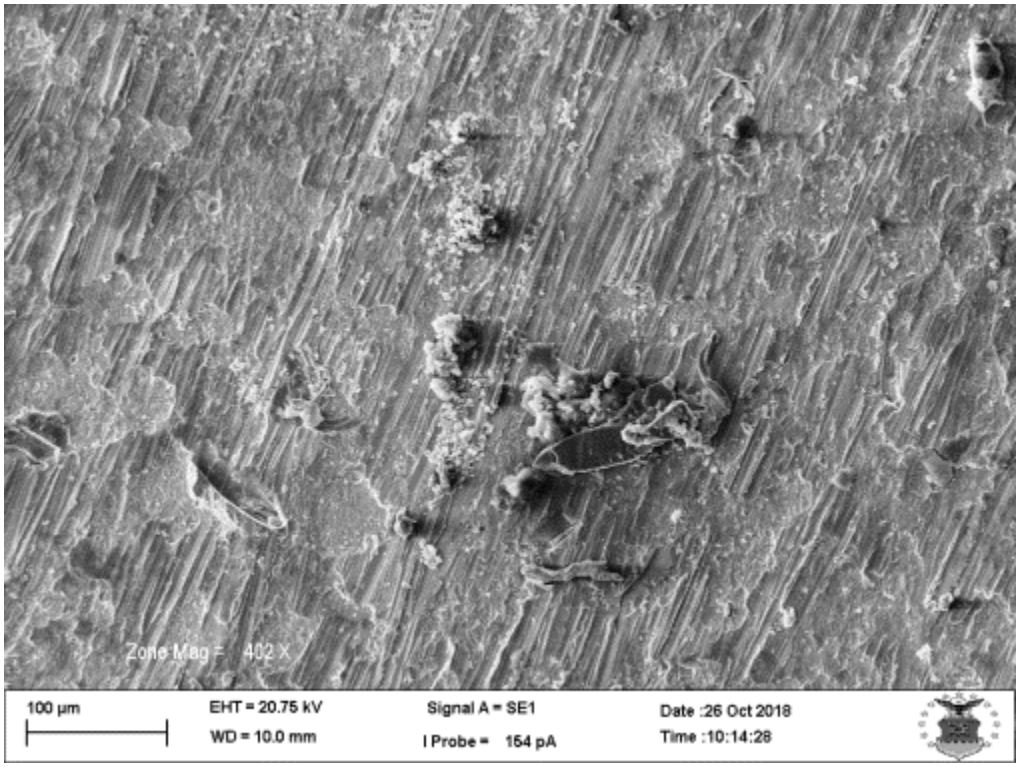

Figure 38: SEM Image of Air Exposed AFRL 2 Week Sample

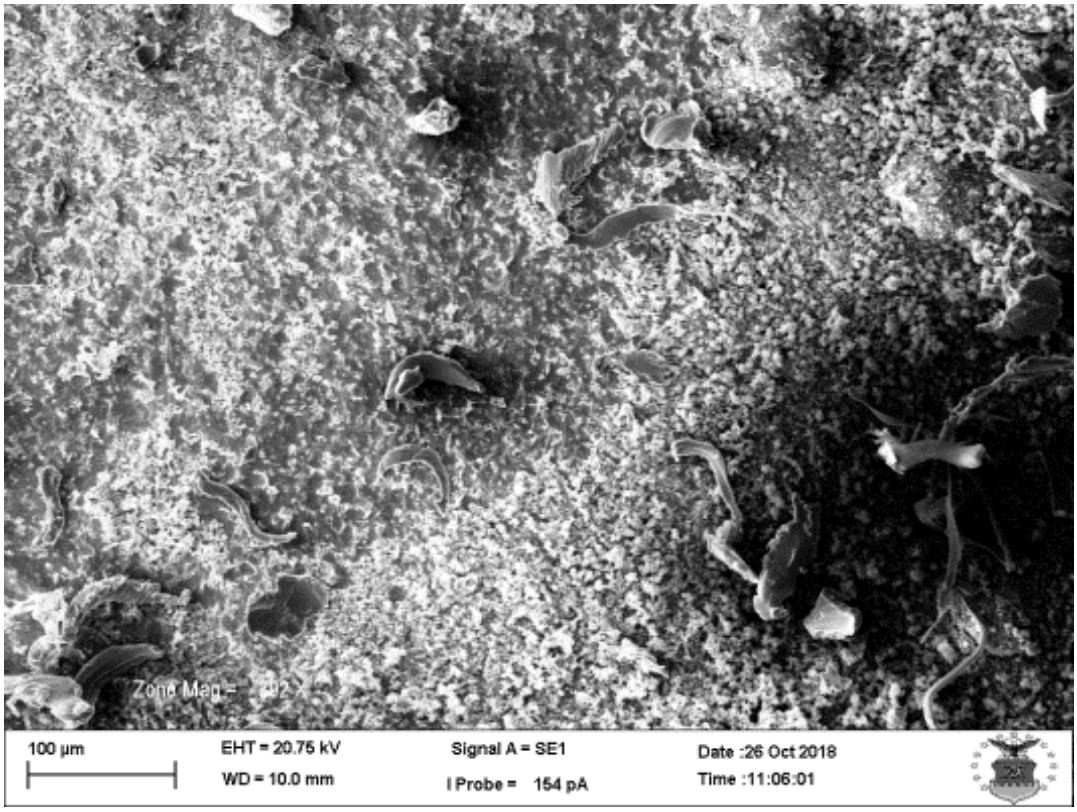

Figure 39: SEM Image of Interface 2 Week AFRL Sample

Observation of the Control and the Water Exposed 2 Week AFRL Sample:

When compared to the control sample, the water exposed sample experienced a significantly greater amount of corrosion, this can be seen in Figure 40: SEM Image of 2 Week Water Exposed AFRL SampleFigure 40. When the amount of elemental iron between the two samples is compared, the water exposed sample follows a similar, and expected, trend of having a much smaller percent composition of elemental iron. From the analysis it was determined that the 12.51% elemental iron of the control sample decreased to 1.49% in the water exposed sample. The FeO in the sample showed a significant decrease in percent composition, being reduced from 37.51% in the control sample, to 8.53%.

Conversely, the amount of Fe_2O_3 increased dramatically, from a percent composition of 39.70% to 71.07%. Likewise, the amount of Fe_3O_4 also increased from 10.28% in the control sample to 18.73% in the water exposed sample. Additionally, the water exposed sample contained trace amounts of FeOOH which totaled approximately 0.19%. This result is fairly inconsistent with what would be expected with normal rusting, as typical rusting includes larger concentrations of FeOOH and Fe_3O_4 (Suzuki, Masuko, & Hisamatsu, 1979). Additionally, these results are inconsistent with iron-reducing MIC, as the amount of Fe_2O_3 has dramatically increased, the opposite of which would be expected during such a reduction reaction (Ottow et al., 1969). It is therefore possible that this is an example of a sample that would have benefited from more stringent preparation, as well if additional locations on the sample were to be analyzed. Or this could be an example of an analysis of a section of iron oxide that has spalled off and revealed the simpler oxides of FeO and Fe_2O_3 underneath the more complex oxides of FeOOH and Fe_3O_4. As can be seen in the SEM image in Figure 40, a substantial amount of corrosion occurred. This sample experienced uniform corrosion across the entire surface which followed a pattern consistent with the large amount of porous oxides seen in Figure 40. This is logically consistent, as this sample was submerged continuously in a Bushnell Hass medium, which resulted in the corrosion seem in the image.

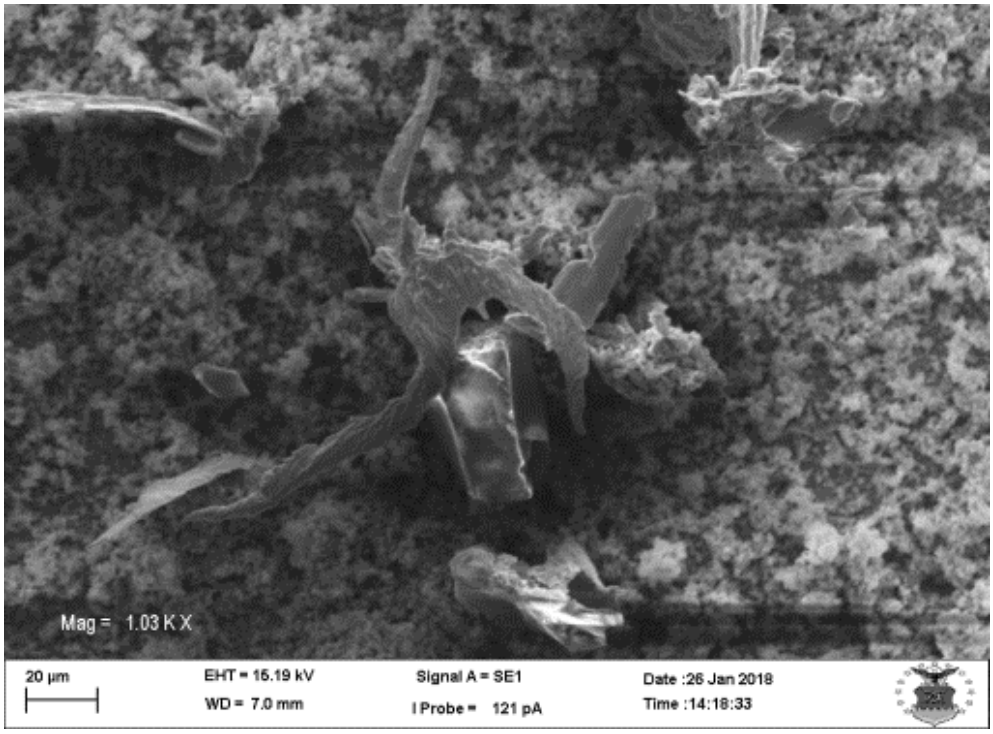

Figure 40: SEM Image of 2 Week Water Exposed AFRL Sample

Summary

This chapter focused on the analysis of the Fe 2p regions of the XPS output from the thirteen analyzed samples. This was done in order to attain the percent composition of the iron oxides associated with the corrosion of iron. These components are; elemental iron, ferrous oxide, ferric oxide, anhydrous iron oxide-hydroxide, and ferrosol-ferric oxide. Additionally, components which match the binding energies associated with tin, 714.6 eV, were found in several samples (Van Attekum & Trooster, 1979). The thirteen samples analyzed via XPS with their component percent compositions are displayed in Table 2. Additional information including the overall spectra, the C 1s region, and the O 1s region, for each sample, as well as the conditions of the XPS during operation can be found in

Appendix A. Additionally, a visual representation of the data for the samples exposed to air can be seen in Figure 41, likewise a visual representation of the data for samples at the interface can be seen in Figure 42, and a visual representation of the data for samples exposed to water can be seen in Figure 43.

Table 2: Percent Composition of All Samples after XPS Analysis

Sample Name	Fe (0)	FeO	Fe_2O_3	FeOOH	Fe_3O_4	Sn
Control	12.51	37.51	39.7	0.00	10.28	0.00
Air Exposed UA 2 Week	8.27	34.89	20.75	24.3	11.79	0.00
Interface UA 2 Week	5.62	19.88	10.98	45.61	17.94	0.00
Water Exposed UA 2 Week	2.92	60.08	0.89	13.88	22.21	0.00
Air Exposed UA 4 Week	1.81	9.58	17.48	22.01	22.15	26.96
Interface UA 4 Week	3.34	22.23	0.00	24.69	2.97	46.77
Water Exposed UA 4 Week (Dark Area)	4.55	11.38	3.24	49.01	31.81	0.00
Water Exposed UA 4 Week	4.27	56.05	23.29	14.02	2.33	0.00
Sterile Air Exposed UA 4 Week	2.45	11.52	49.91	9.06	27.03	0.00
Sterile Interface UA 4 Week	1.71	3.71	9.14	14.49	21.07	49.9
Sterile Water Exposed UA 4 Week	2.64	25.48	16.13	21.86	7.03	26.84
Air Exposed AFRL 2 Week	0.59	50.66	39.13	0.00	9.63	0.00
Interface AFRL 2 Week	1.83	15.68	56.58	0.00	25.89	0.00
Water Exposed AFRL 2 Week	1.49	8.53	71.07	0.19	18.73	0.00

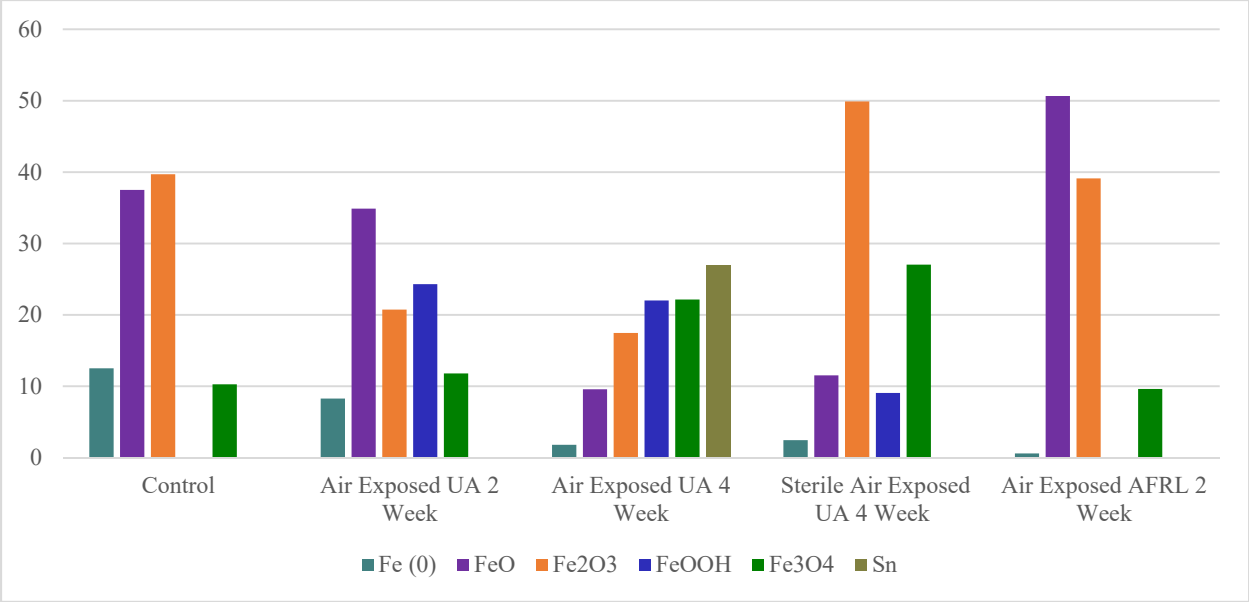

Figure 41: Comparisons of Percent Composition of Air Exposed Samples

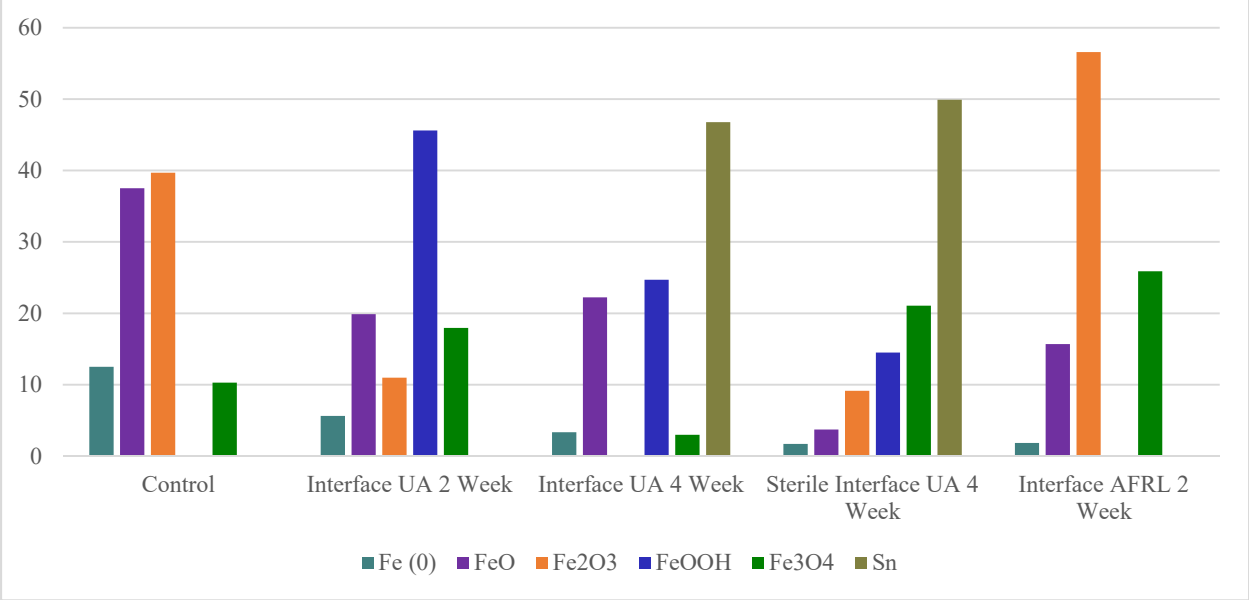

Figure 42: Comparisons of Percent Composition of Interface Samples

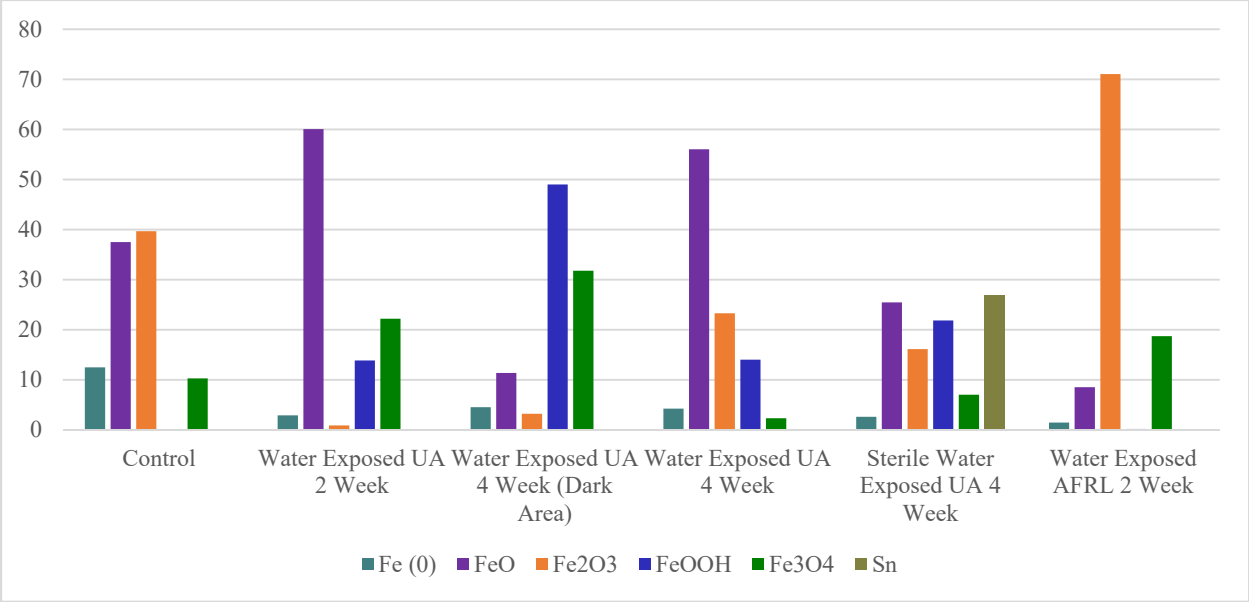

Figure 43: Comparisons of Percent Composition of Water Exposed Samples

V. Conclusions and Recommendations

Chapter Overview

The purpose of this chapter is to discuss the conclusions and recommendations derived from the results attained and identified in Chapter 4 in the form of analytical data from X-ray Photoelectric Spectroscopy (XPS), and qualitative information in the form of Scanning Electron Microscope (SEM) images. Furthermore, this chapter will discuss the recommended future of this research, primarily in the form of developing a new experiment.

Recommendations for Future Research

Due to the inconsistencies in both the results of the analysis, as well as the method of sample preparation, it is highly recommended that this experiment be repeated with the intent of obtaining more consistent information. In order to do so, the following methodology for sample preparation should be considered in order to keep as many variables within the experiment as consistent as possible.

The proposal for the next experiment continues the use of the analytical foundations of the experiment, namely the use of XPS and SEM to show what effect, if any, the introduction of *Byssochlamys nivea* has on mild steel submerged in an environment that replicates modern day fuel tanks. Specifically, the environment in fuel tanks contains an interface of water and hydrocarbon based fuel where the submerged steel comes into contact with water, fuel, and microorganisms. Therefore, the next experiment should include the same types of samples including; a sample only exposed to the air above the hydrocarbon, a sample containing the hydrocarbon, fungus, and water interface, and a

sample only exposed to water. In order to determine how this environment affects the mild steel over time, one group of samples should be removed from this environment on a weekly basis, leaving other samples in the environment to experience further corrosion. For example, if the experiment is run for four weeks, a total of four samples should be placed in the environment, with one sample being removed per week. Furthermore, in order to better clarify the effect of MIC, a control environment should be created under the same conditions as the experiment, with the only difference being the lack of fungus within the control environment. In the experiment conducted for this thesis, the experimental environment was created a total of four times, each within separate conical tubes. However, in the interest of reducing variability, a method of containing all samples within the two environments should be developed from an inert material that will not have any effect on the XPS analysis. If all steel samples were able to be kept in a single container, the variability of this experiment would be reduced, as all the corrosion would occur in the same environment, rather than in several separate environments. However, before this could be determined to be a viable option, there are two considerations to take into account. The first is that it is vital that the container be sterile prior to the creation of this environment, any researcher attempting this experiment would have to ensure that it would be possible to not only guarantee that the container was sterile prior to use, but also that no action taken by them would render the container contaminated. Secondly, the method of removing samples would need to be determined to not be harmful towards the results of the experiment, likely through a method of blocking off samples through insertion of hollow rectangular prisms that will allow the removal of individual samples without disturbing others. Due to the extreme sensitivity of the instrument, it is essential to ensure

that the samples are prepared without accidently modifying the surface of the samples (Briggs & Grant, 2003). It is for this reason that it is not acceptable to simply remove the samples from the environment, as this would result in samples passing through mediums they were not intended to be exposed to. Doing so would dramatically affect the results of the analysis and could result in inconsistent data. As such, the mediums should instead be removed via pipette, the first to be removed should be the fuel medium, followed by a removal of the fungus via a sterile cotton swab, which would then be proceeded by removing the BH. Likewise, the control environment should follow this methodology as well. At this point the samples could then be extracted without fear of contamination. Additionally, the use of samples that do not require removal from a coupon via Dremel tool would be ideal, as the action of cutting out samples from a coupon could accidently affect the surface chemistry of the sample, which could be detected by the XPS and provide an inaccurate analysis. Due to the complexity revolving this experimental set up, it may not be feasible to create a single container that can reliably allow for the samples to be removed without contamination. If this is the conclusion of any future researcher, while not ideal, it is likely that the use of several individual environments would still be a viable option.

In the interest of consistency, the environment should consist of BH produced from the same source, fungal spores grown from the same source, and B20 Biofuel produced from the same source. This is because slight inconsistencies within these mediums could likewise result in inconsistent data; therefore it is best to keep all variables as constant as possible. Similarly, the mild steel should be sanded uniformly, potentially via bead blasting, in order to ensure that as much prior oxidation has been removed as possible. This

also ensures that all samples start the experiment under approximately the same conditions. Additionally, during the experiment conducted in this thesis the samples were placed within a shaking incubator after the environments had been created. The use of a shaking incubator is beneficial for the growth of fungus, but it can disturb the mediums of BH and fuel which can cause the samples to not corrode in a realistic manner as this creates an environment that does not replicate the interior of a fuel tank very well. Most importantly however, this can prevent a clear interface where the fungus is growing and corroding a surface. This then makes it difficult to observe the effect that the microbes are having on the steel both visually with the SEM and analytically with the XPS. Therefore, it is recommended that future research not use a shaking incubator, and instead use a typical incubator that still supports the growth of fungus, but does not have the potential to disturb the results of the experiment.

Furthermore, another key component of ensuring the success of this experiment is to time the experiment in such a way that once it has been concluded, it is removed and placed within the XPS instrument as soon as possible. As mentioned previously, the process of analyzing a sample via XPS is exceptionally sensitive, as a result, if the samples are not placed into the XPS as soon as possible, the risk of contamination occurring from an outside source begin to dramatically increase, as does the risk of oxidation occurring from non-experimental sources. Additionally, this increases the risk of any biological products being degraded or lost over time, the existence of which could be very helpful in determining the type of corrosion occurring. A source of difficulty for the experiment done in this thesis is that the samples were not able to be analyzed until several months after they had been removed from their environments. This could be a likely explanation towards

the inconsistencies found in the data, as this could have allowed for significant changes to the surface chemistry of the samples to have occurred. Additionally, considering that the resolution of the XPS is considerably small, it could prove beneficial to run the XPS on multiple areas of interest in order to gain a greater understanding of the chemical composition of the entire sample. Lastly, during the analysis, the spectrum of iron sulfide should be included, as it is a potential product of corrosion (Xu, Li, & Gu, 2016).

Summary

In conclusion, while other research has determined that the existence of microorganisms have an effect on corrosion (Hamilton, 2003), this effect cannot be verified in this experiment. Though visual inspection of the samples developed during this experiment, and XPS analysis of those samples, could potentially point to signs of MIC by the fungus *Byssochlamys nivea*, the lack of a consistent and reliable control makes it impossible to make any claim that MIC has occurred. The two pieces of potential evidence first points to the image of the interface sample from AFRL as seen in Figure 39 which shows a difference between where the fungus was speculated to grow and where the BH medium was. The second potential piece of evidence is the XPS data gathered from the large quantity of Fe_3O_4 that exists on the interface sample, which could potentially indicate iron-reduction MIC due to the complex nature of Fe_3O_4 (Blaney, 2007). As a result of the complexities experienced during this research, the ultimate recommendation is that further research in the form of a more controlled experiment is recommended. A more consistent environment for the experiment, in conjunction with greater care towards the produced samples will likely lead to greater success for future research on this subject.

Appendix A

Overall Spectra of Experimental Samples

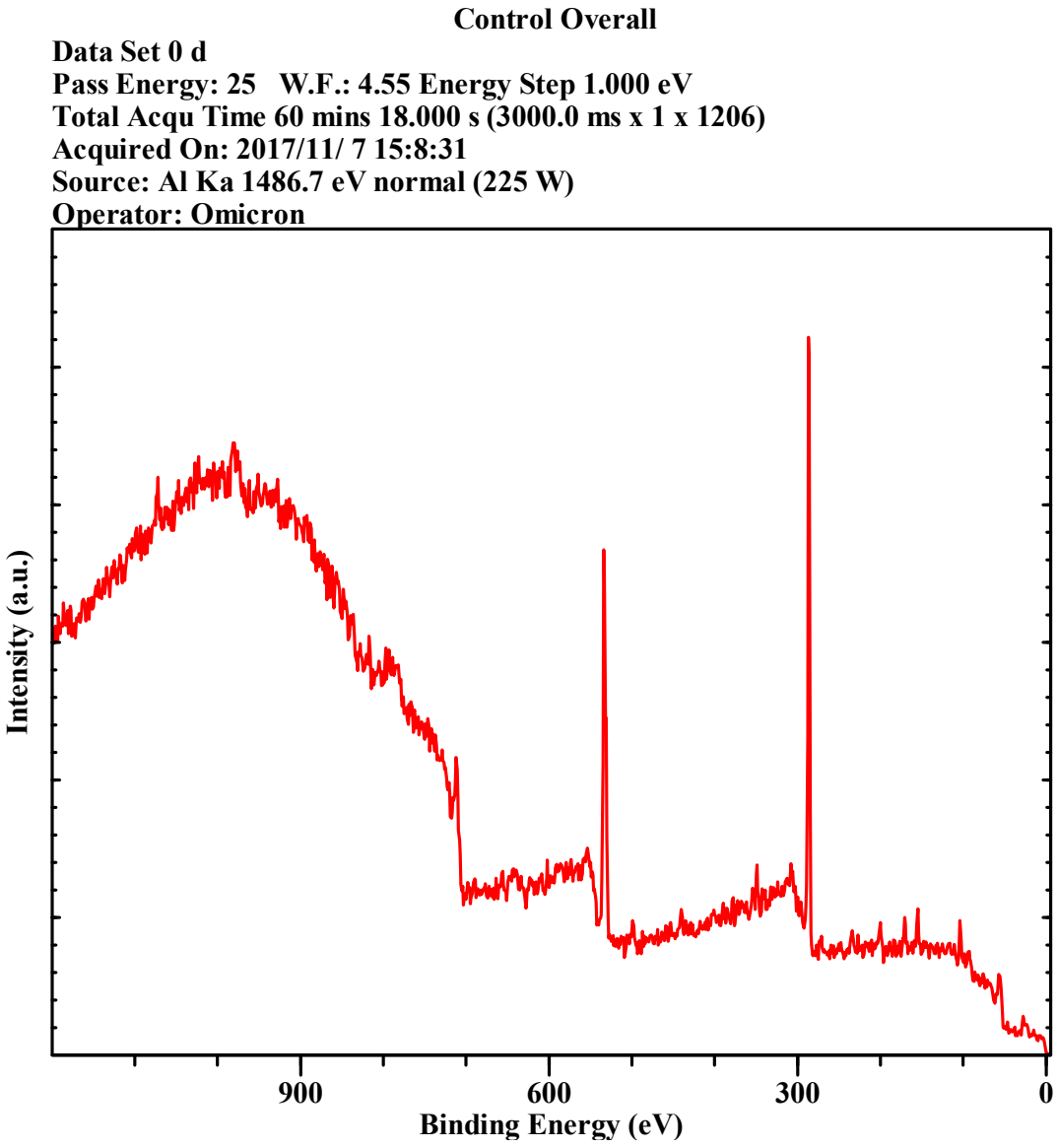

Air Exposed UA 2 Week

Data Set 3 d
Pass Energy: 25 W.F.: 4.55 Energy Step 1.000 eV
Total Acqu Time 18 mins 5.400 s (900.0 ms x 1 x 1206)
Acquired On: 2018/ 3/15 13:53:40
Source: Al Ka 1486.7 eV mono (225 W)
Operator: Omicron

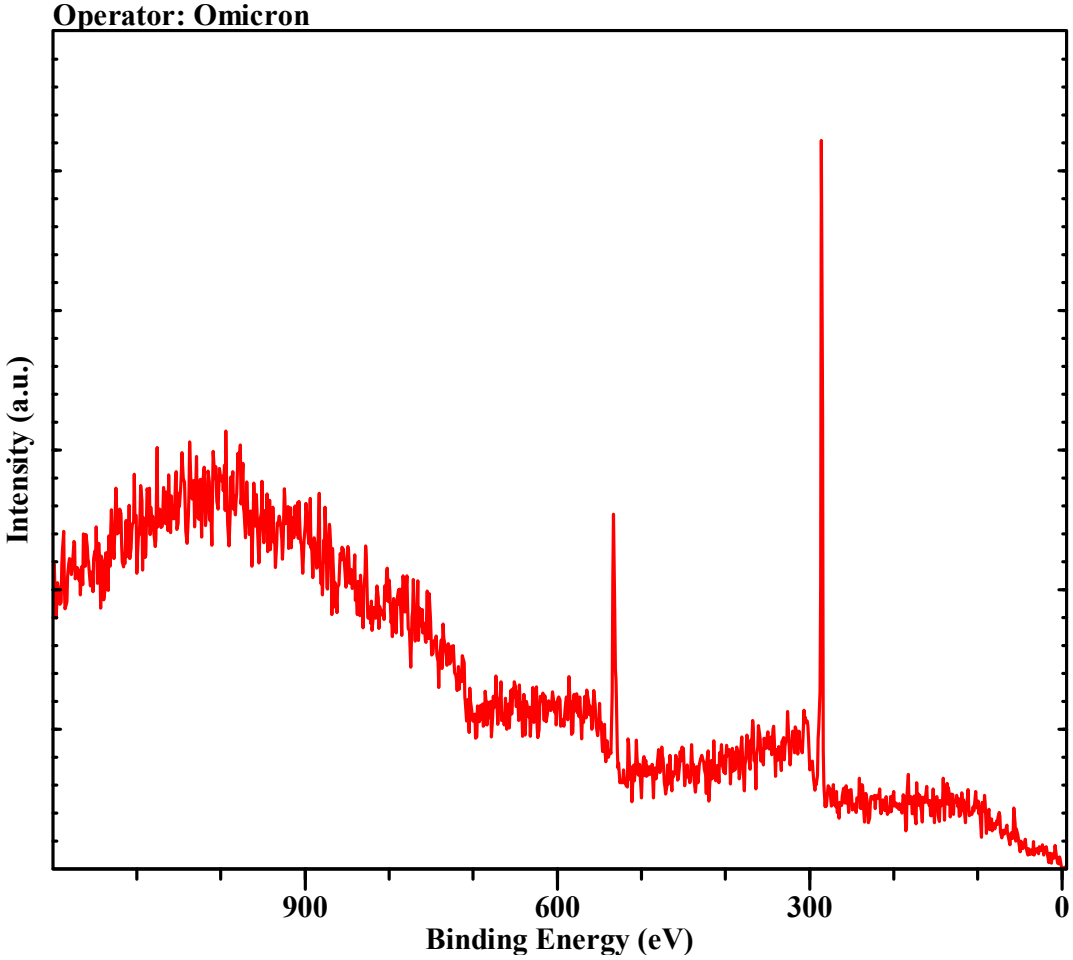

Interface UA 2 Week

Data Set 2 d
Pass Energy: 25 W.F.: 4.55 Energy Step 1.000 eV
Total Acqu Time 18 mins 5.400 s (900.0 ms x 1 x 1206)
Acquired On: 2018/ 3/ 9 12:41:27
Source: Al Ka 1486.7 eV mono (225 W)
Operator: Omicron

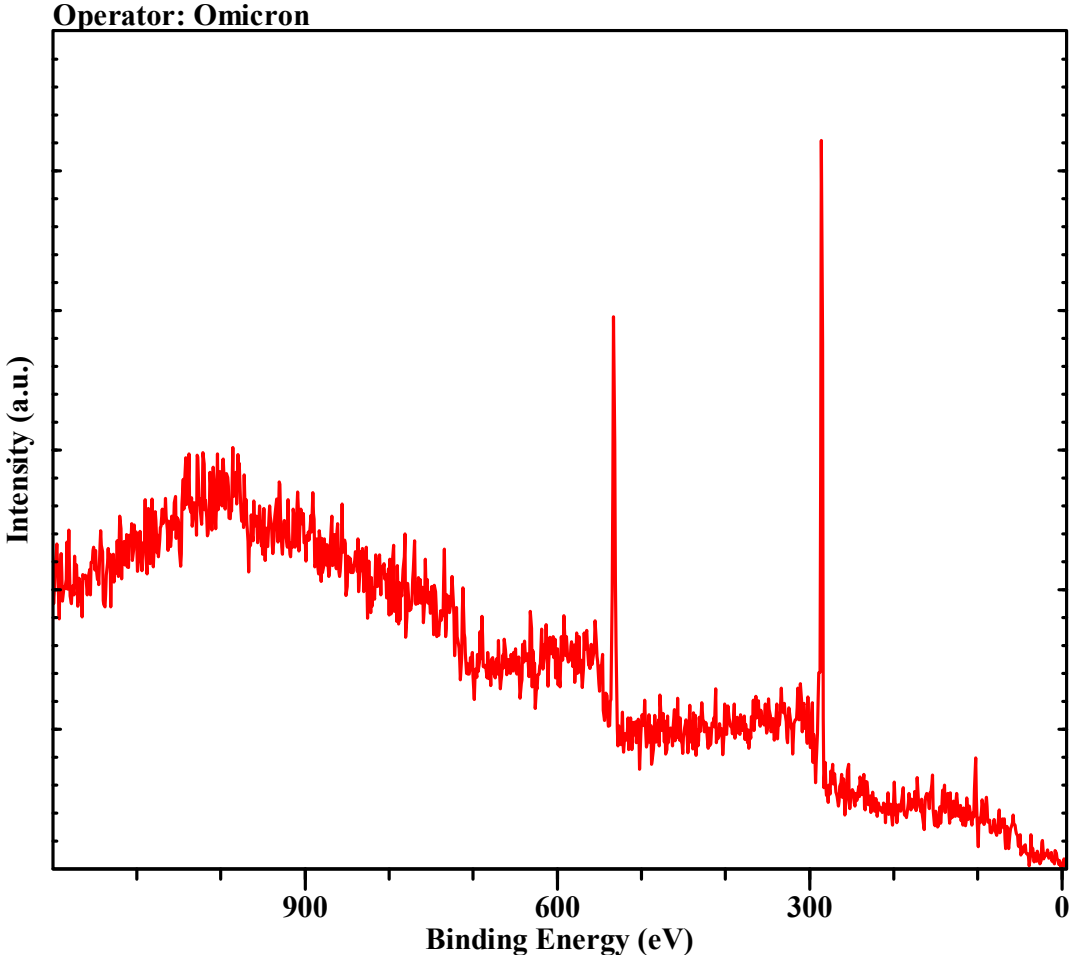

Water Exposed UA 2 Week

Data Set 1 d
Pass Energy: 25 W.F.: 4.55 Energy Step 1.000 eV
Total Acqu Time 60 mins 18.000 s (3000.0 ms x 1 x 1206)
Acquired On: 2018/ 1/10 13:47:10
Source: Al Ka 1486.7 eV normal (225 W)
Operator: Omicron

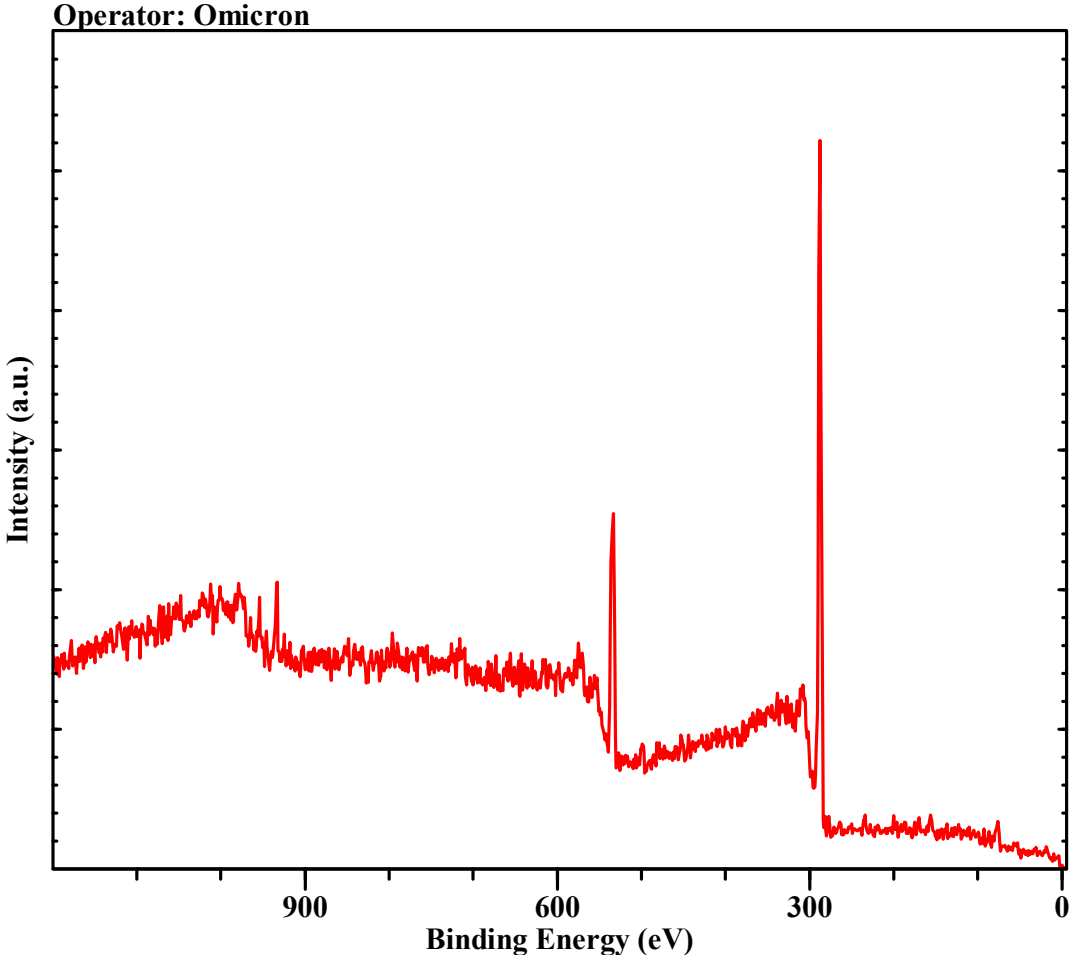

Air Exposed UA 4 Week

Data Set 10 d
Pass Energy: 25 W.F.: 4.55 Energy Step 1.000 eV
Total Acqu Time 60 mins 18.000 s (3000.0 ms x 1 x 1206)
Acquired On: 2018/ 1/24 13:3:17
Source: Al Ka 1486.7 eV normal (225 W)
Operator: Omicron

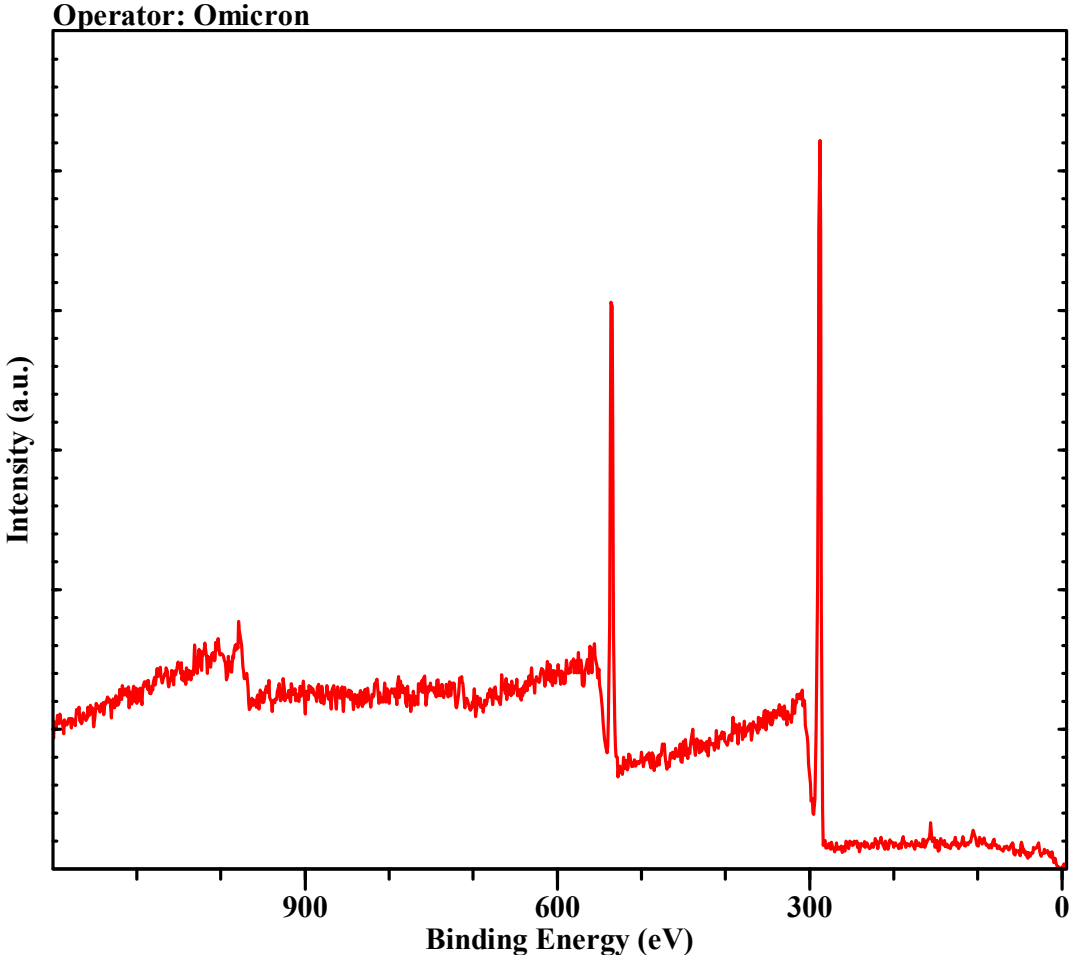

Interface UA 4 Week

Data Set 6 d
Pass Energy: 25 W.F.: 4.55 Energy Step 1.000 eV
Total Acqu Time 60 mins 18.000 s (3000.0 ms x 1 x 1206)
Acquired On: 2018/ 1/28 9:51:54
Source: Al Ka 1486.7 eV normal (225 W)
Operator: Omicron

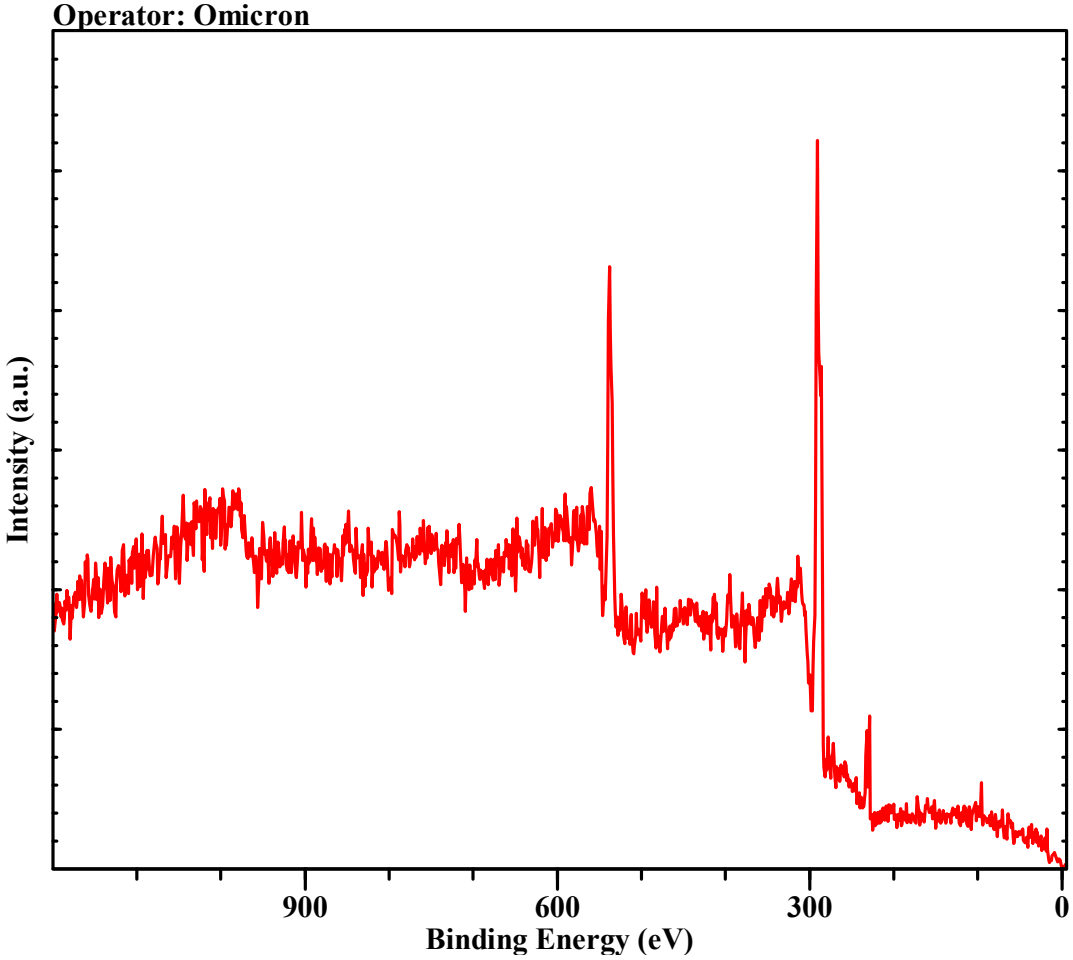

Water Exposed UA 4 Week (Dark Area)

Data Set 4 d
Pass Energy: 25 W.F.: 4.55 Energy Step 1.000 eV
Total Acqu Time 60 mins 18.000 s (3000.0 ms x 1 x 1206)
Acquired On: 2018/ 1/26 9:22:16
Source: Al Ka 1486.7 eV normal (225 W)
Operator: Omicron

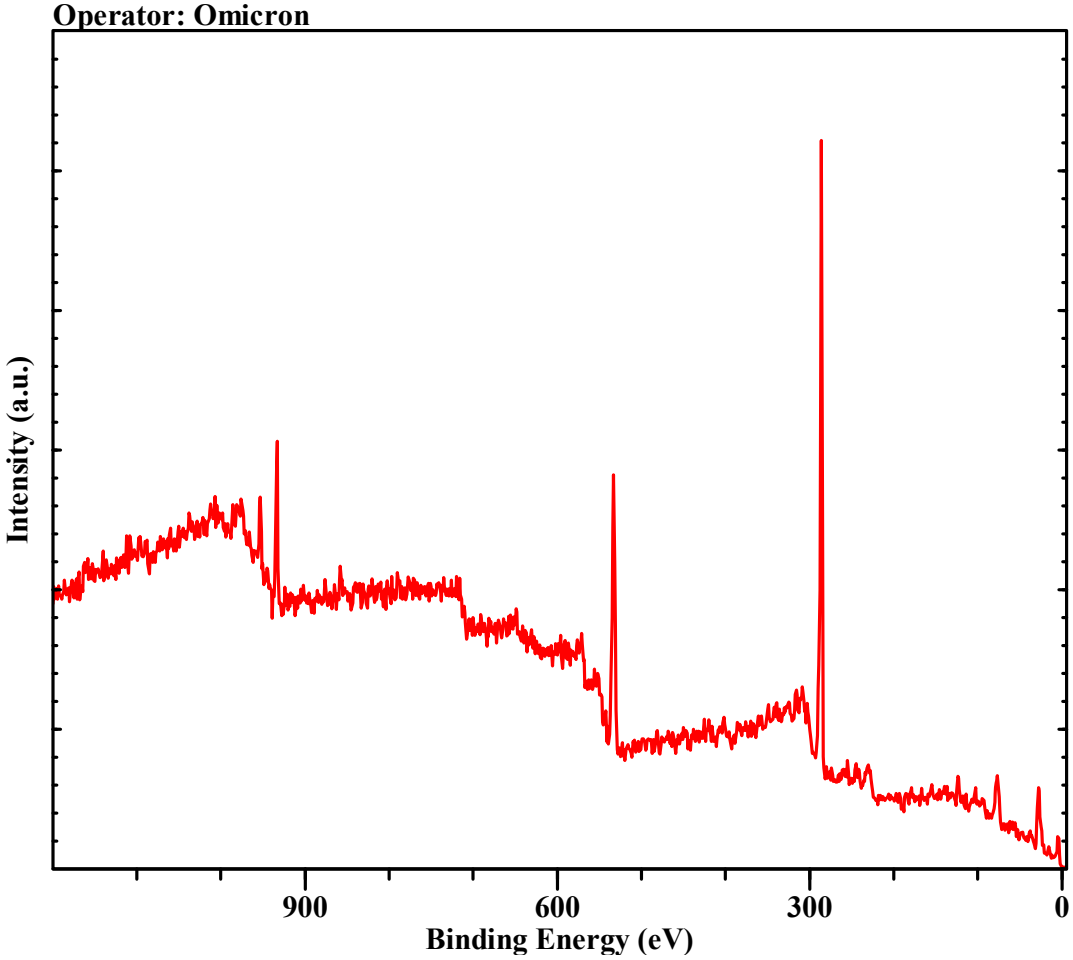

Water Exposed UA 4 Week

Data Set 5 d
Pass Energy: 25 W.F.: 4.55 Energy Step 1.000 eV
Total Acqu Time 60 mins 18.000 s (3000.0 ms x 1 x 1206)
Acquired On: 2018/ 1/25 10:20:53
Source: Al Ka 1486.7 eV normal (225 W)
Operator: Omicron

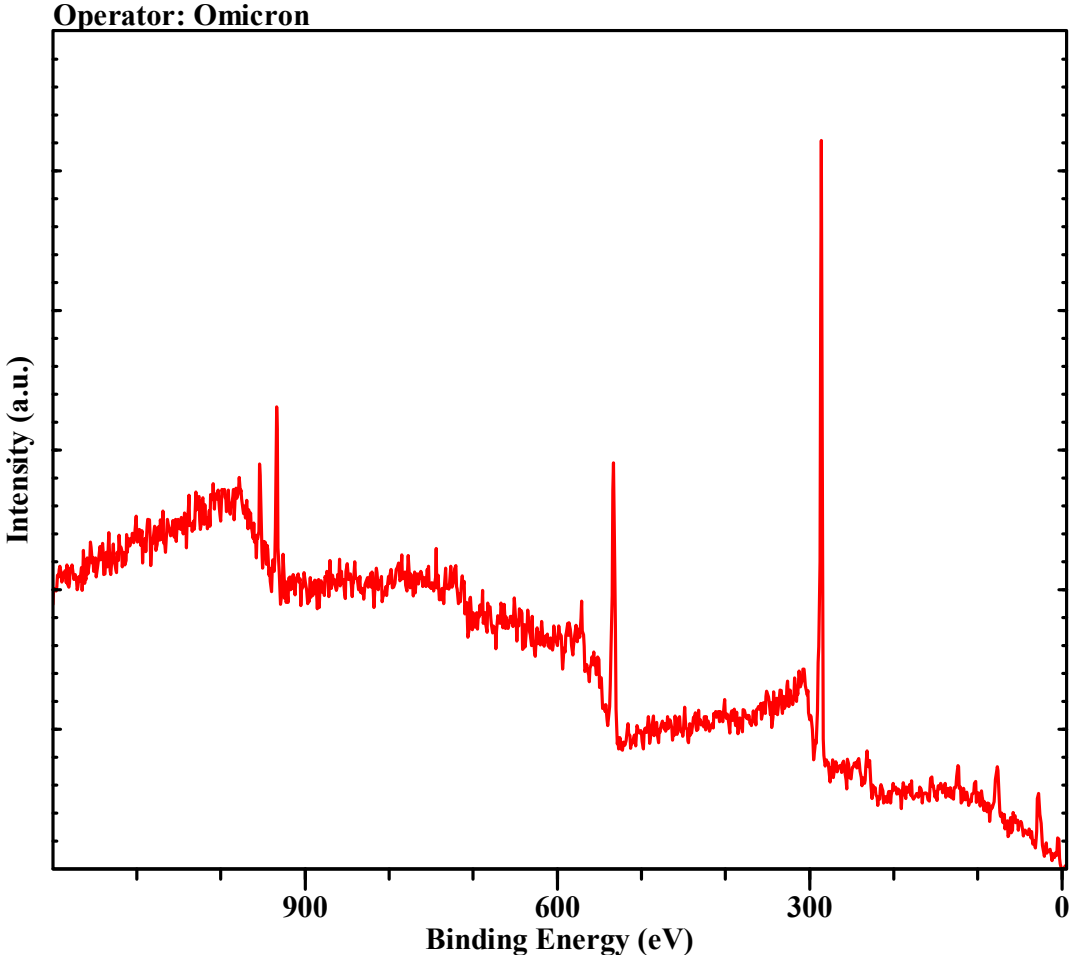

Sterile Air Exposed UA 4 Week

Data Set 9 d
Pass Energy: 25 W.F.: 4.55 Energy Step 1.000 eV
Total Acqu Time 18 mins 5.400 s (900.0 ms x 1 x 1206)
Acquired On: 2018/ 3/10 15:28:54
Source: Al Ka 1486.7 eV mono (225 W)
Operator: Omicron

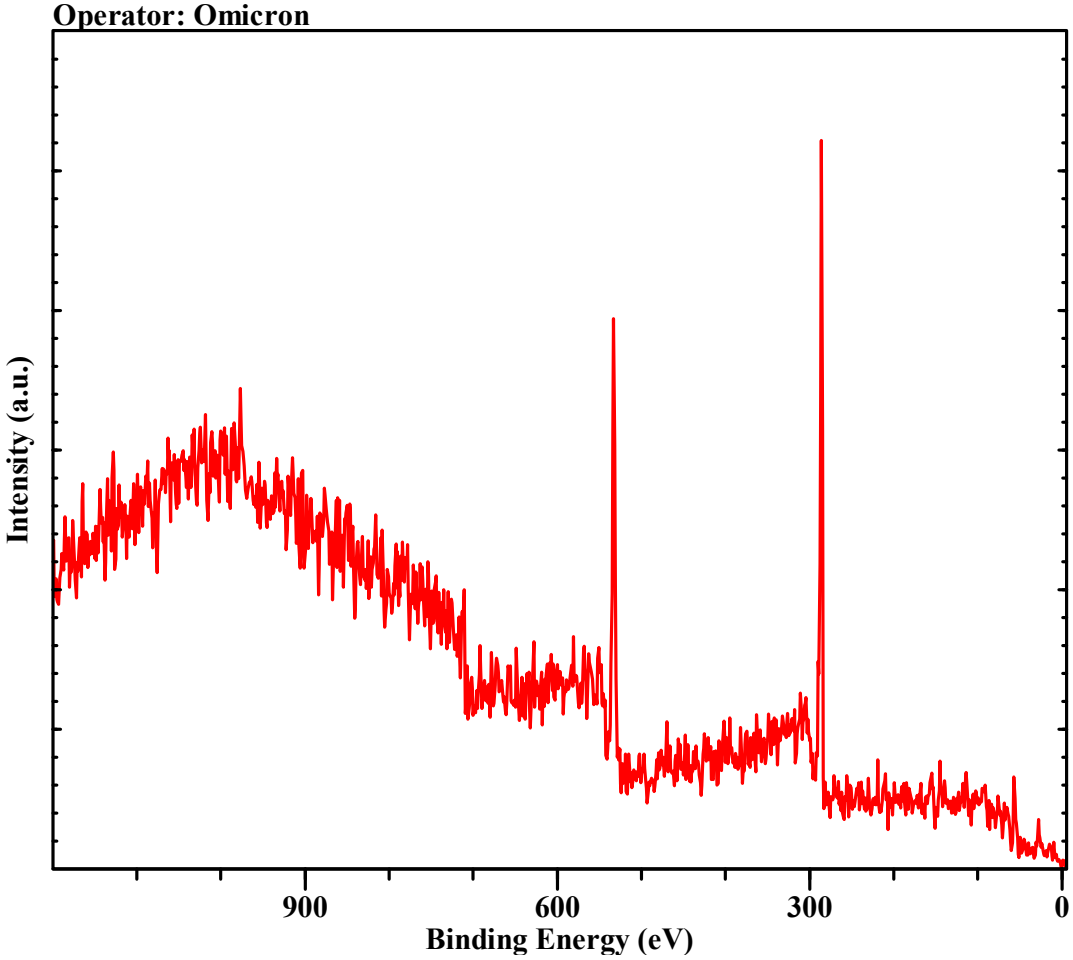

Sterile Interface UA 4 Week

Data Set 8 d
Pass Energy: 25 W.F.: 4.55 Energy Step 1.000 eV
Total Acqu Time 60 mins 18.000 s (3000.0 ms x 1 x 1206)
Acquired On: 2018/ 2/ 4 15:58:48
Source: Al Ka 1486.7 eV normal (225 W)
Operator: Omicron

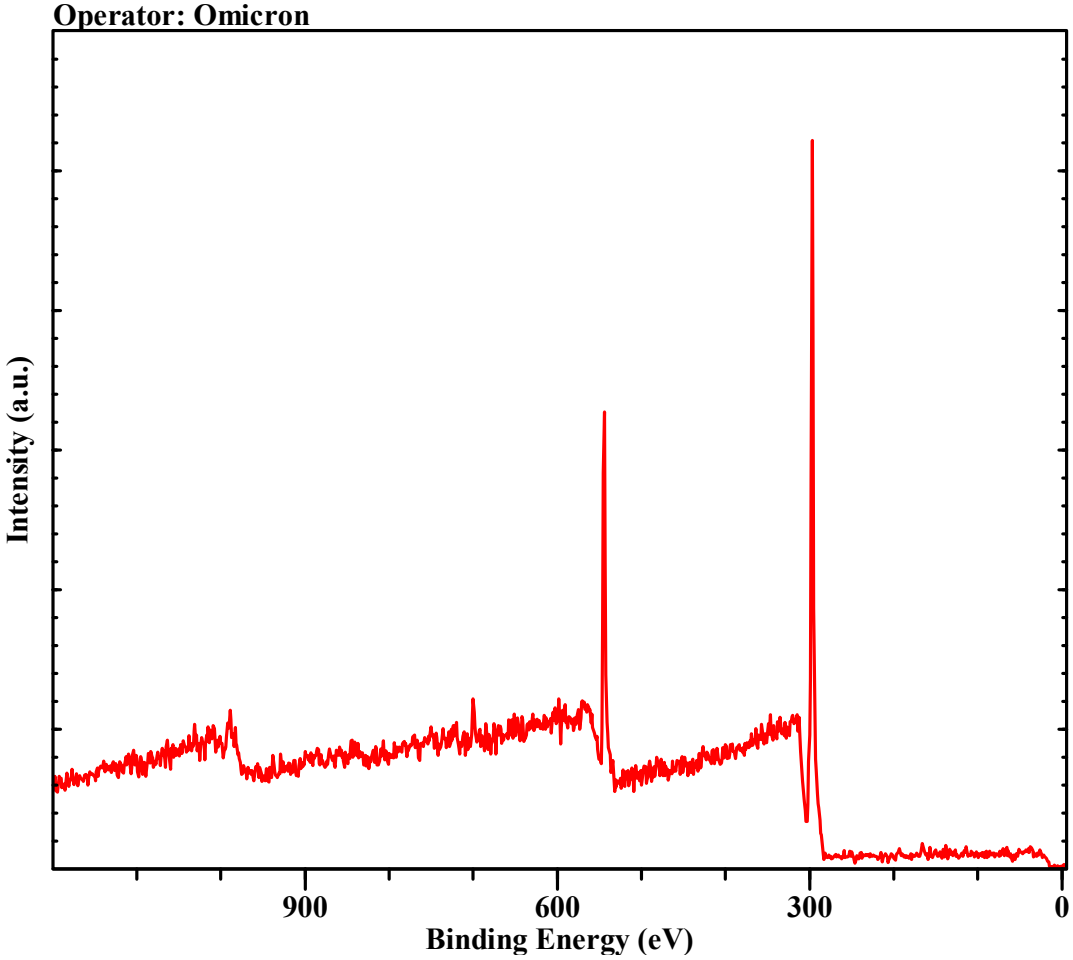

Sterile Water Exposed UA 4 Week

Data Set 7 d
Pass Energy: 25 W.F.: 4.55 Energy Step 1.000 eV
Total Acqu Time 60 mins 18.000 s (3000.0 ms x 1 x 1206)
Acquired On: 2018/ 3/ 4 10:56:18
Source: Al Ka 1486.7 eV normal (225 W)
Operator: Omicron

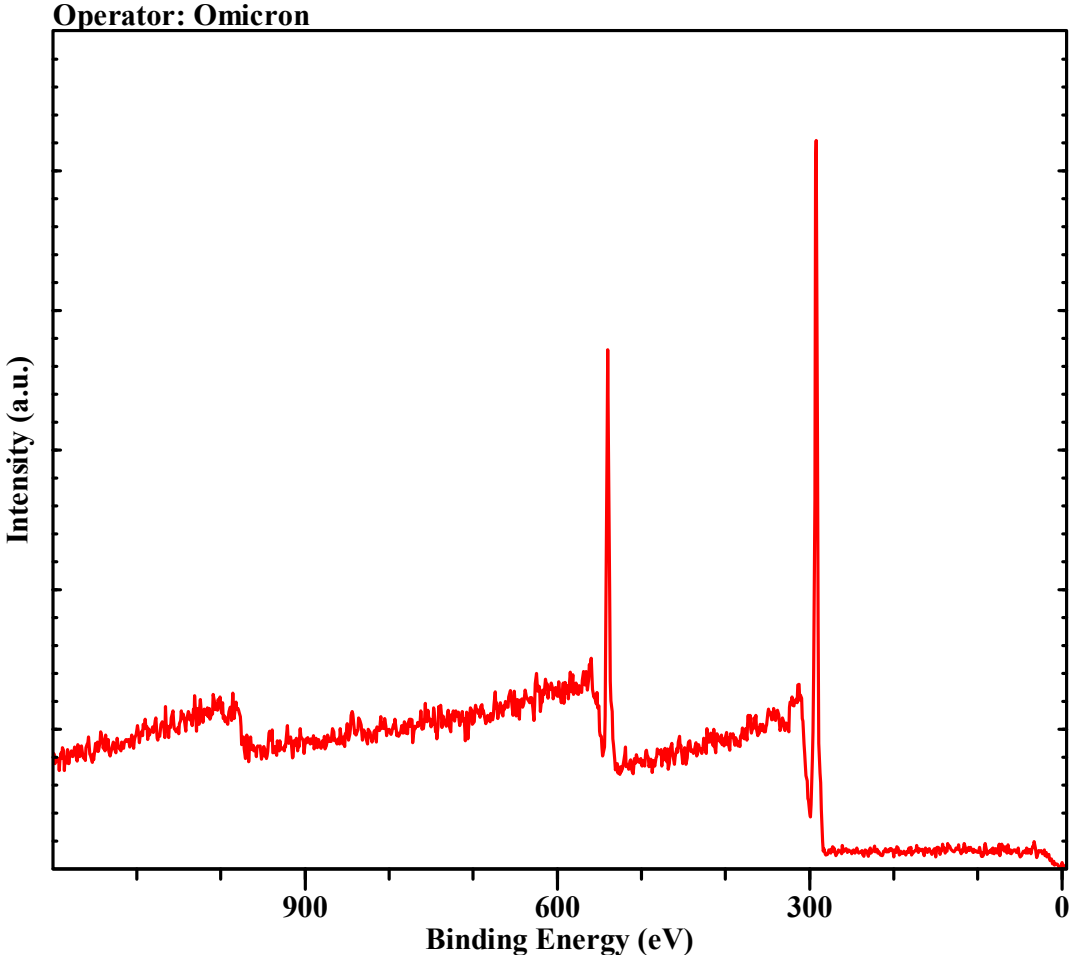

Air Exposed AFRL 2 Week

Data Set 13 d
Pass Energy: 25 W.F.: 4.55 Energy Step 1.000 eV
Total Acqu Time 60 mins 18.000 s (3000.0 ms x 1 x 1206)
Acquired On: 2018/ 1/13 9:20:52
Source: Al Ka 1486.7 eV normal (225 W)
Operator: Omicron

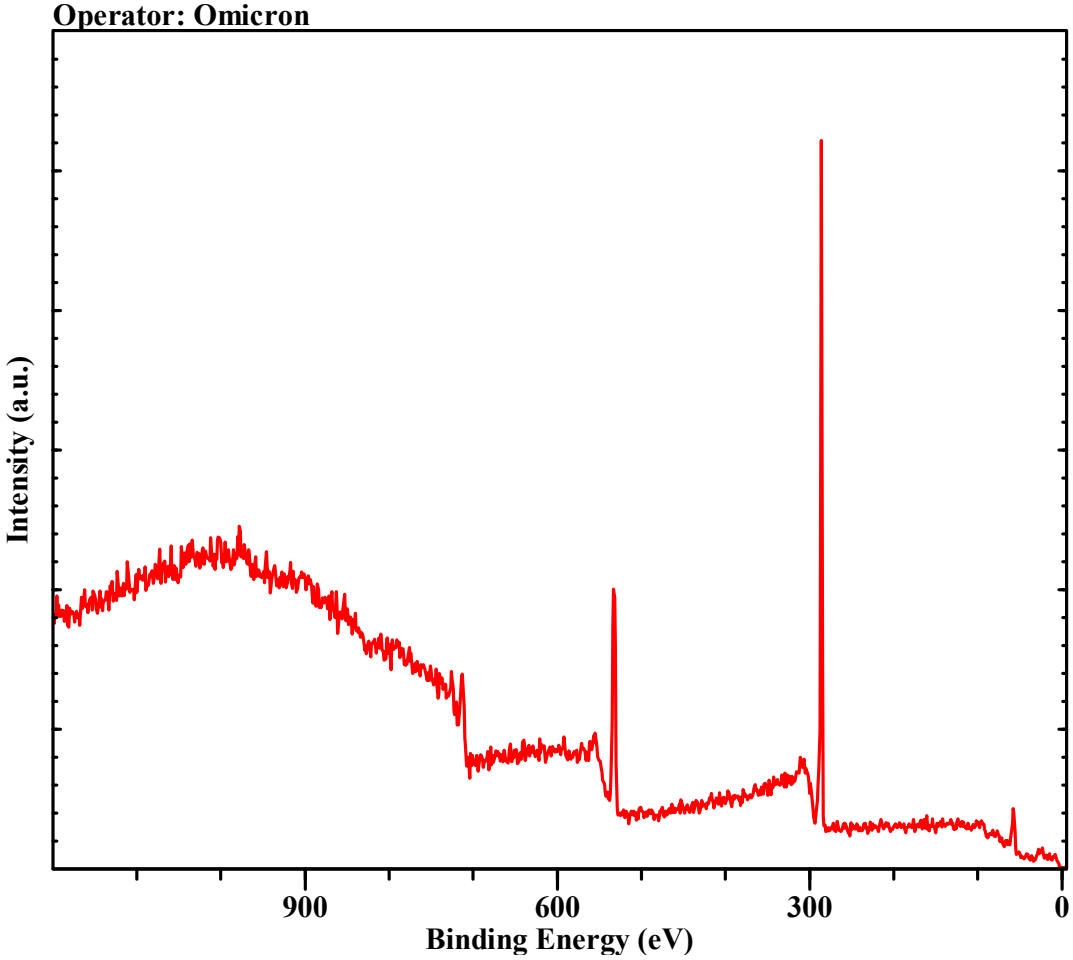

Interface AFRL 2 Week

Data Set 12 d
Pass Energy: 25 W.F.: 4.55 Energy Step 1.000 eV
Total Acqu Time 60 mins 18.000 s (3000.0 ms x 1 x 1206)
Acquired On: 2018/ 1/14 13:55:27
Source: Al Ka 1486.7 eV normal (225 W)
Operator: Omicron

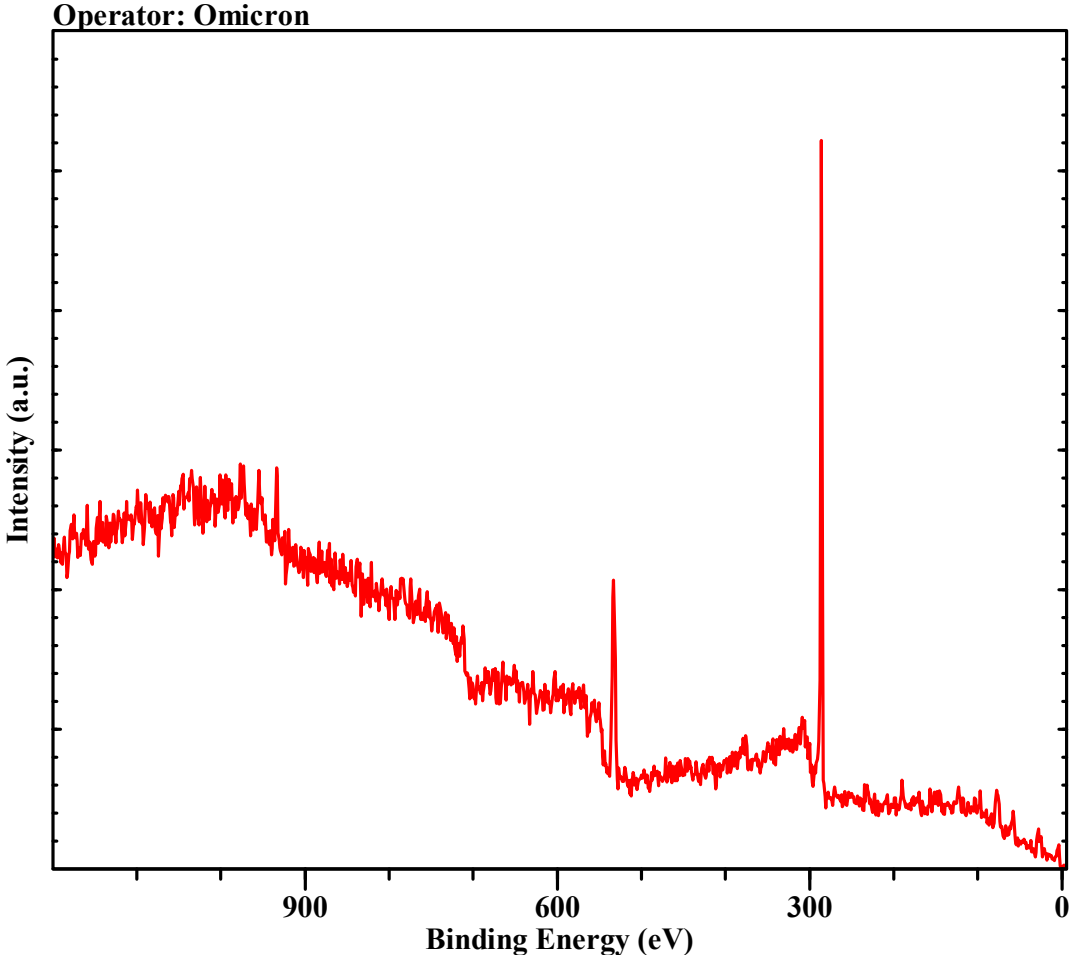

Water Exposed AFRL 2 Week

Data Set 11 d
Pass Energy: 25 W.F.: 4.55 Energy Step 1.000 eV
Total Acqu Time 60 mins 18.000 s (3000.0 ms x 1 x 1206)
Acquired On: 2018/ 1/16 8:7:21
Source: Al Ka 1486.7 eV normal (225 W)
Operator: Omicron

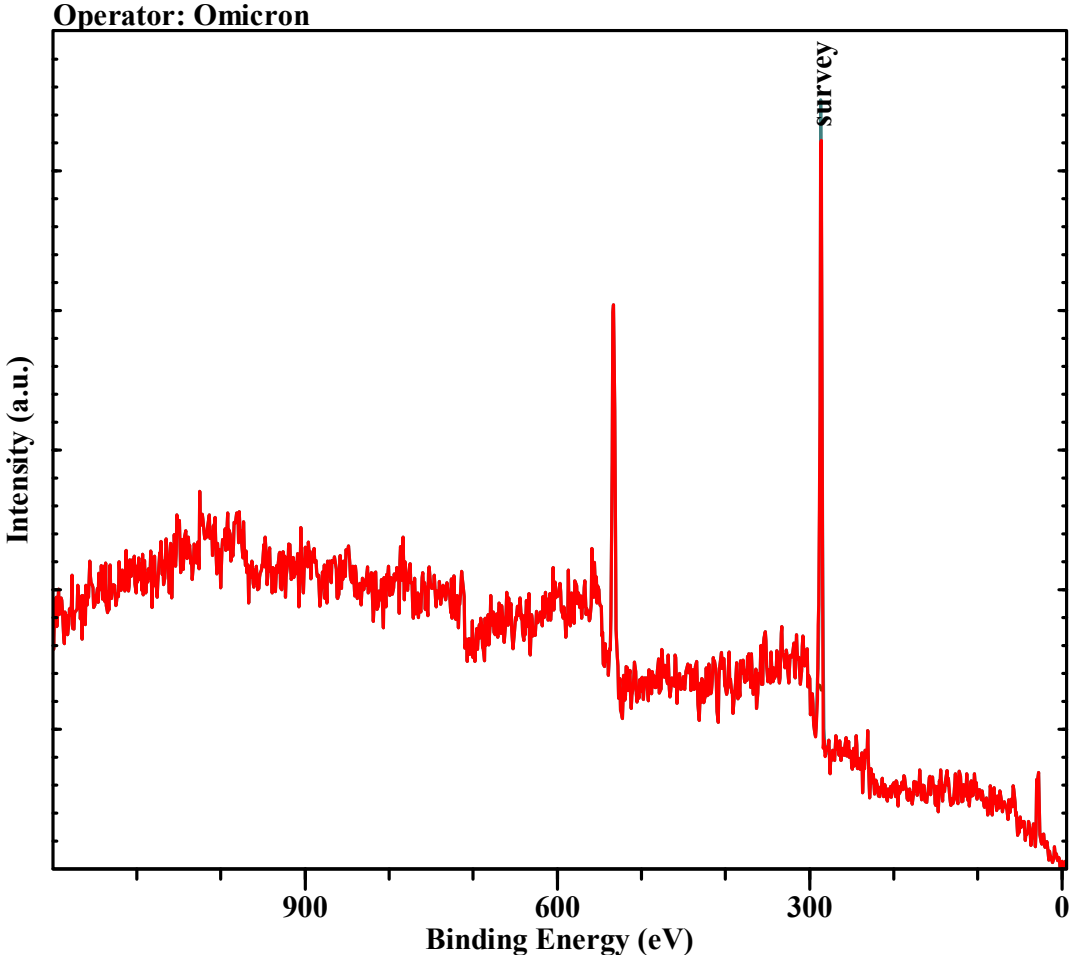

Fe 2p Regions of Experiment Samples

Fe 2p

Data Set 1 d
Pass Energy: 10 W.F.: 4.55 Energy Step 0.200 eV
Total Acqu Time 54 mins 0.000 s (40000.0 ms x 1 x 81)
Acquired On: 2017/11/ 7 15:8:31
Source: Al Ka 1486.7 eV normal (225 W)
Operator: Omicron

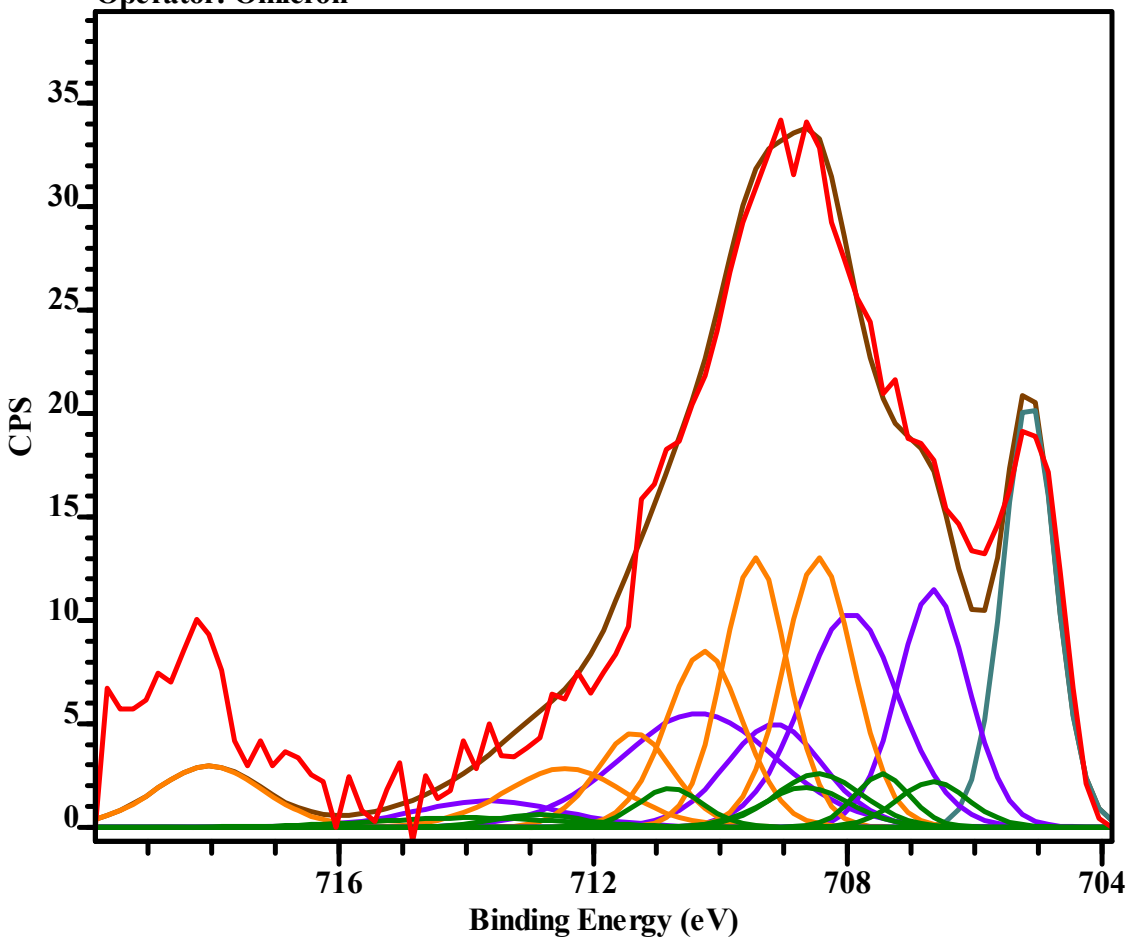

Fe 2p Region in Air Exposed UA 2 Week Sample

Data Set 3 d

Pass Energy: 10 W.F.: 4.55 Energy Step 0.200 eV

Total Acqu Time 1155 mins 33.000 s (363000.0 ms x 1 x 191)

Acquired On: 2018/ 3/15 13:53:41

Source: Al Ka 1486.7 eV mono (225 W)

Operator: Omicron

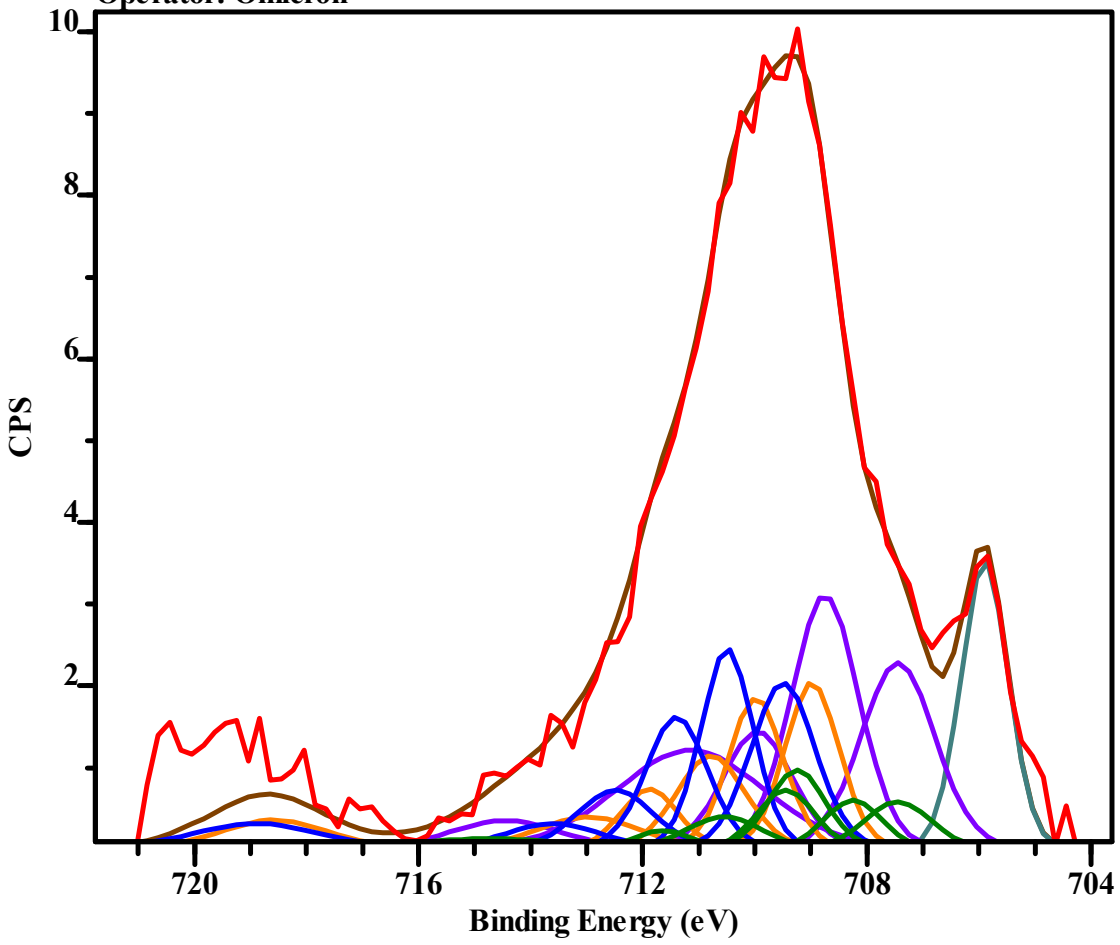

Fe 2p Region in Interface UA 2 Week Sample
Data Set 8 d
Pass Energy: 10 W.F.: 4.55 Energy Step 0.200 eV
Total Acqu Time 1375 mins 12.000 s (432000.0 ms x 1 x 191)
Acquired On: 2018/ 3/ 9 12:41:28
Source: Al Ka 1486.7 eV mono (225 W)
Operator: Omicron

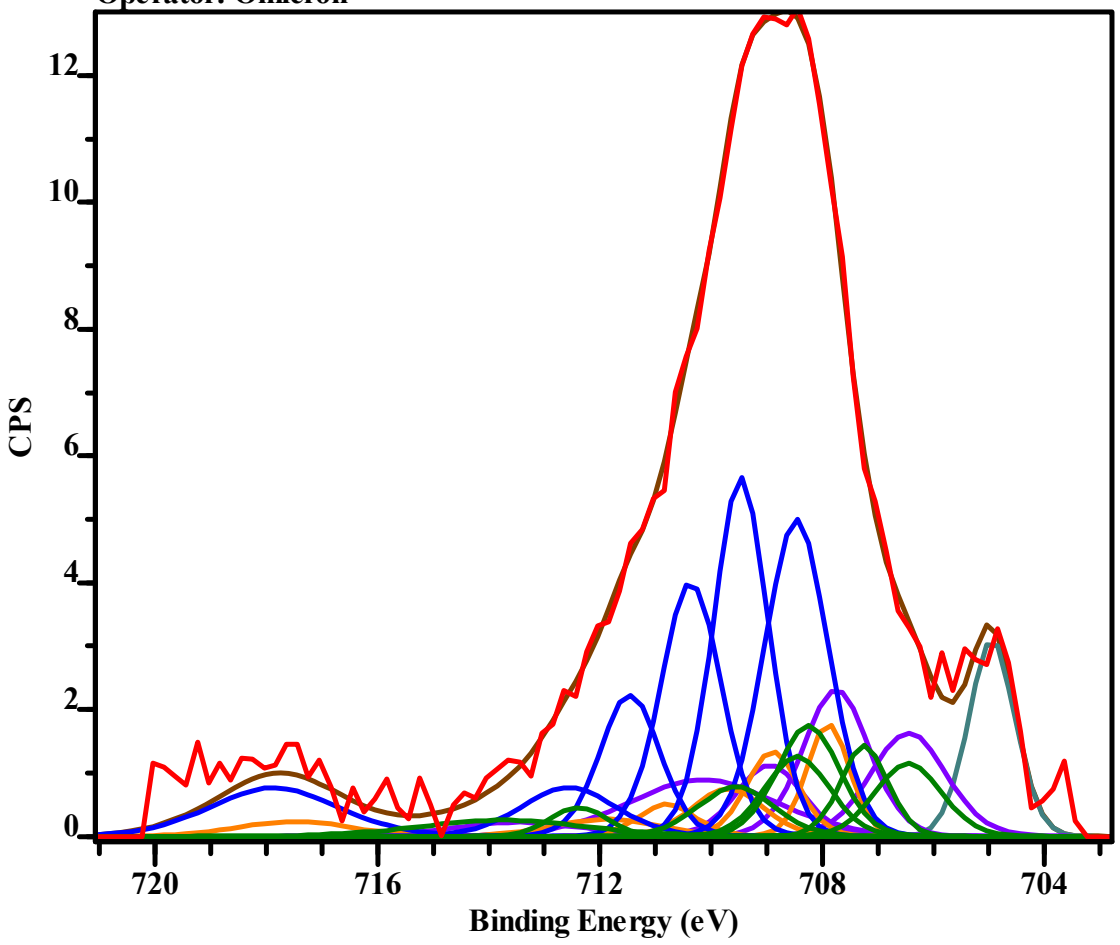

Fe 2p Region in Water Exposed UA 2 Week Sample

Data Set 11 d

Pass Energy: 10 W.F.: 4.55 Energy Step 0.200 eV

Total Acqu Time 636 mins 40.000 s (200000.0 ms x 1 x 191)

Acquired On: 2018/ 1/10 13:47:10

Source: Al Ka 1486.7 eV normal (225 W)

Operator: Omicron

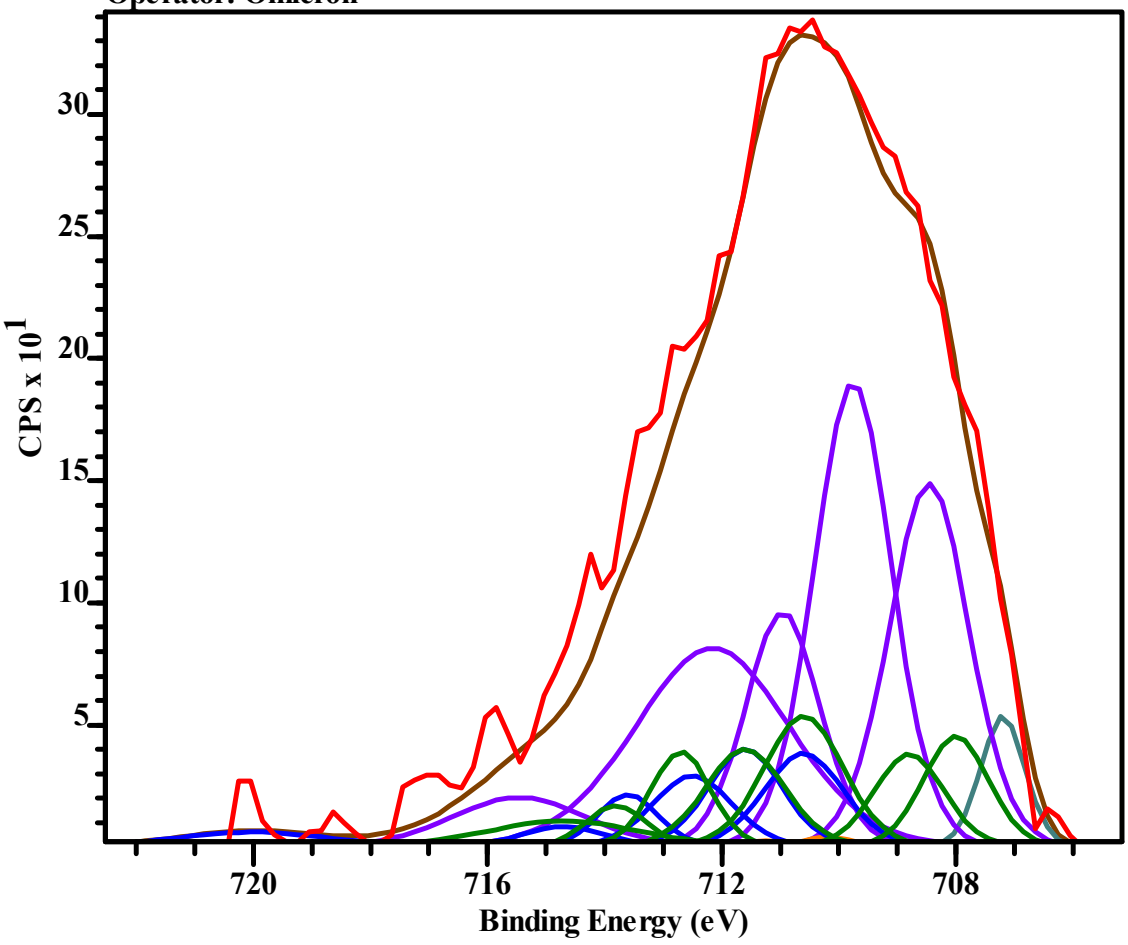

Fe 2p Region in Air Exposed UA 4 Week Sample

Data Set 13 d

Pass Energy: 10 W.F.: 4.55 Energy Step 0.200 eV

Total Acqu Time 636 mins 40.000 s (200000.0 ms x 1 x 191)

Acquired On: 2018/ 1/24 13:3:19

Source: Al Ka 1486.7 eV normal (225 W)

Operator: Omicron

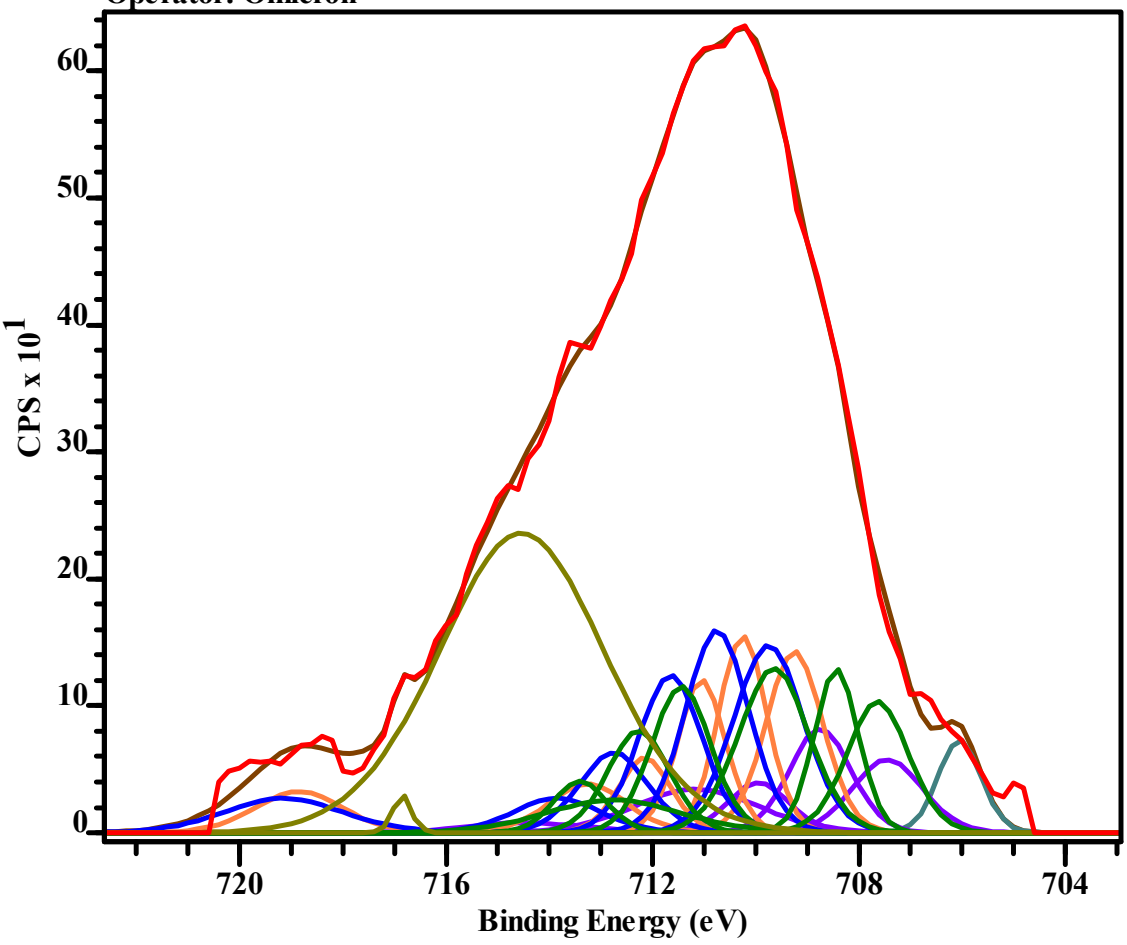

Fe 2p Region in Interface UA 4 Week Sample
Data Set 16 d
Pass Energy: 10 W.F.: 4.55 Energy Step 0.200 eV
Total Acqu Time 636 mins 40.000 s (200000.0 ms x 1 x 191)
Acquired On: 2018/ 1/28 9:51:55
Source: Al Ka 1486.7 eV normal (225 W)
Operator: Omicron

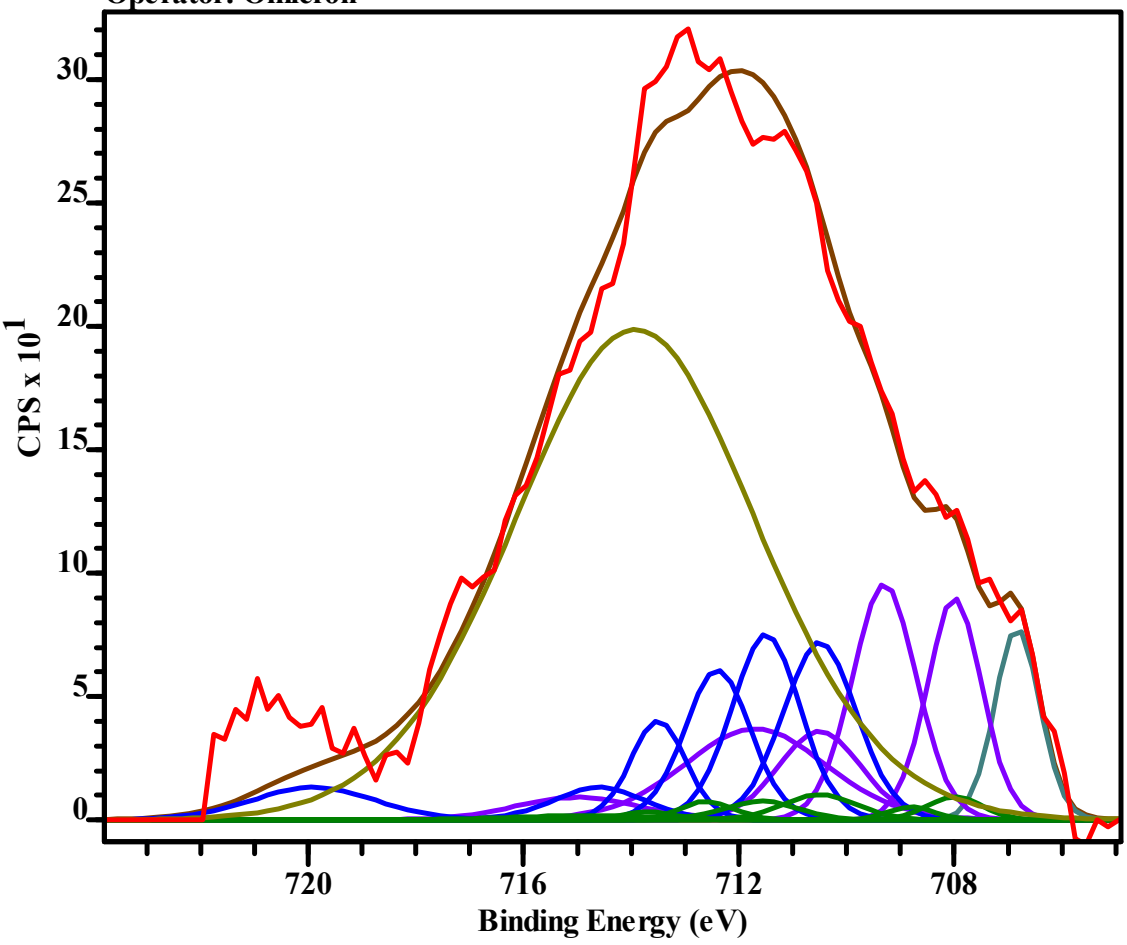

Fe 2p Region in Water Exposed UA 4 Week Sample (Dark Area)
Data Set 18 d
Pass Energy: 10 W.F.: 4.55 Energy Step 0.200 eV
Total Acqu Time 636 mins 40.000 s (200000.0 ms x 1 x 191)
Acquired On: 2018/ 1/26 9:22:17
Source: Al Ka 1486.7 eV normal (225 W)
Operator: Omicron

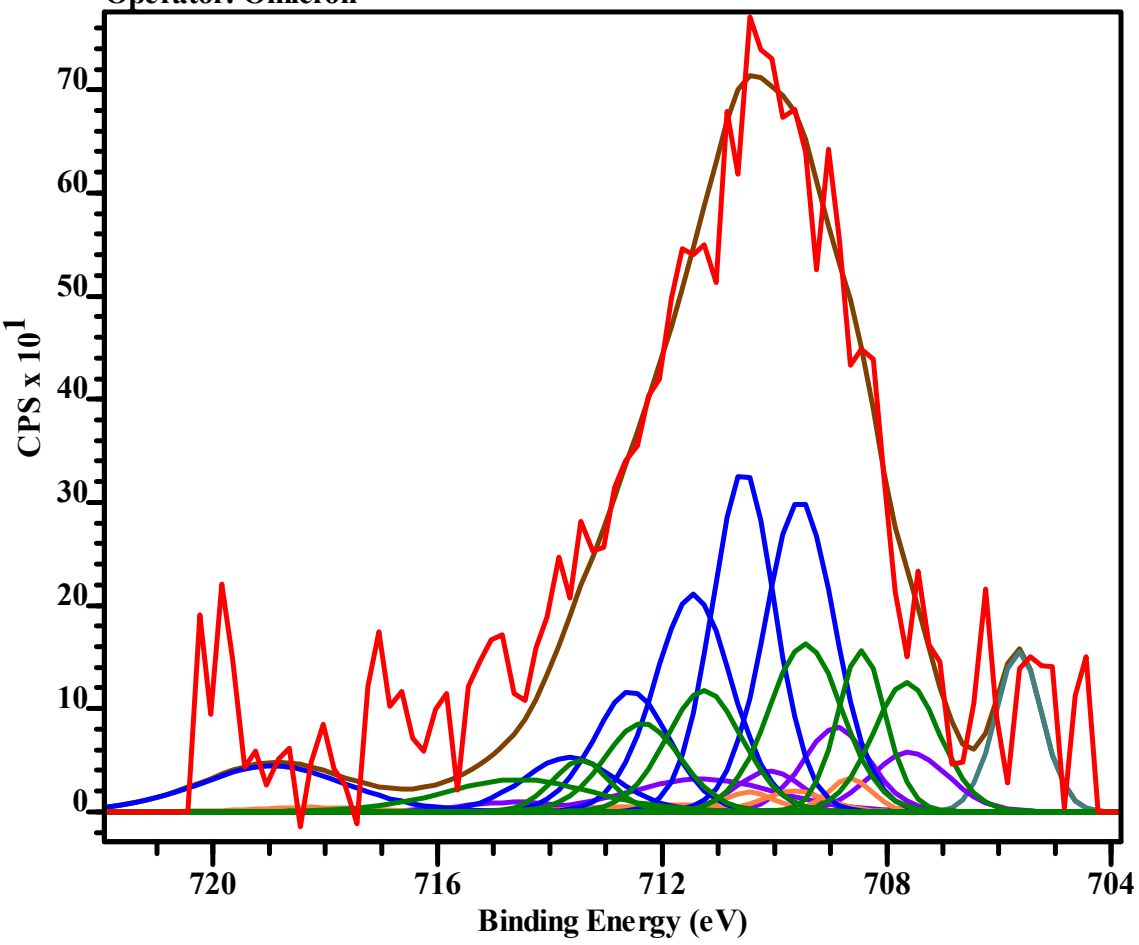

Fe 2p in Water Exposed UA 4 Week Sample
Data Set 20 d
Pass Energy: 10 W.F.: 4.55 Energy Step 0.200 eV
Total Acqu Time 636 mins 40.000 s (200000.0 ms x 1 x 191)
Acquired On: 2018/ 1/25 10:20:52
Source: Al Ka 1486.7 eV normal (225 W)
Operator: Omicron

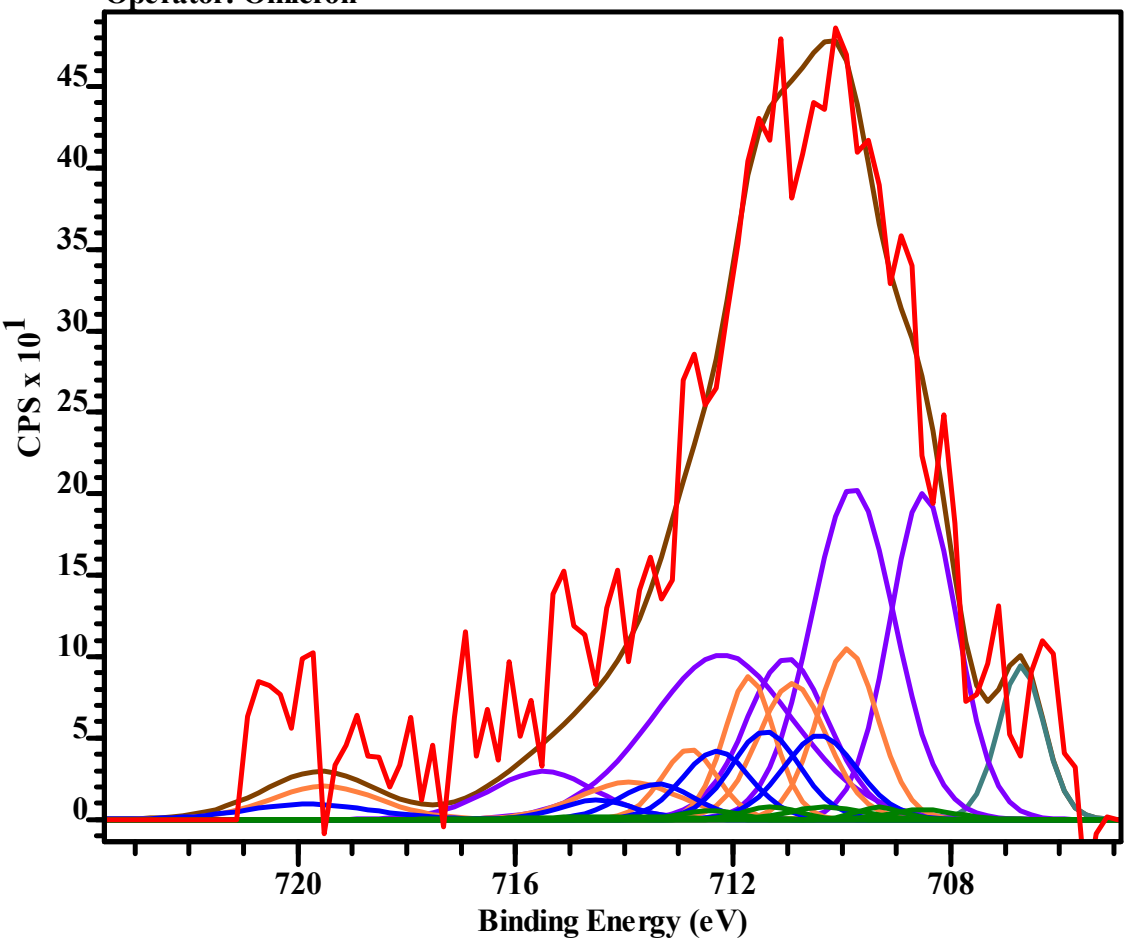

Fe 2p Region in Sterile Air Exposed UA 4 Week Sample
Data Set 23 d
Pass Energy: 10 W.F.: 4.55 Energy Step 0.200 eV
Total Acqu Time 1442 mins 3.000 s (453000.0 ms x 1 x 191)
Acquired On: 2018/ 3/10 15:28:55
Source: Al Ka 1486.7 eV mono (225 W)
Operator: Omicron

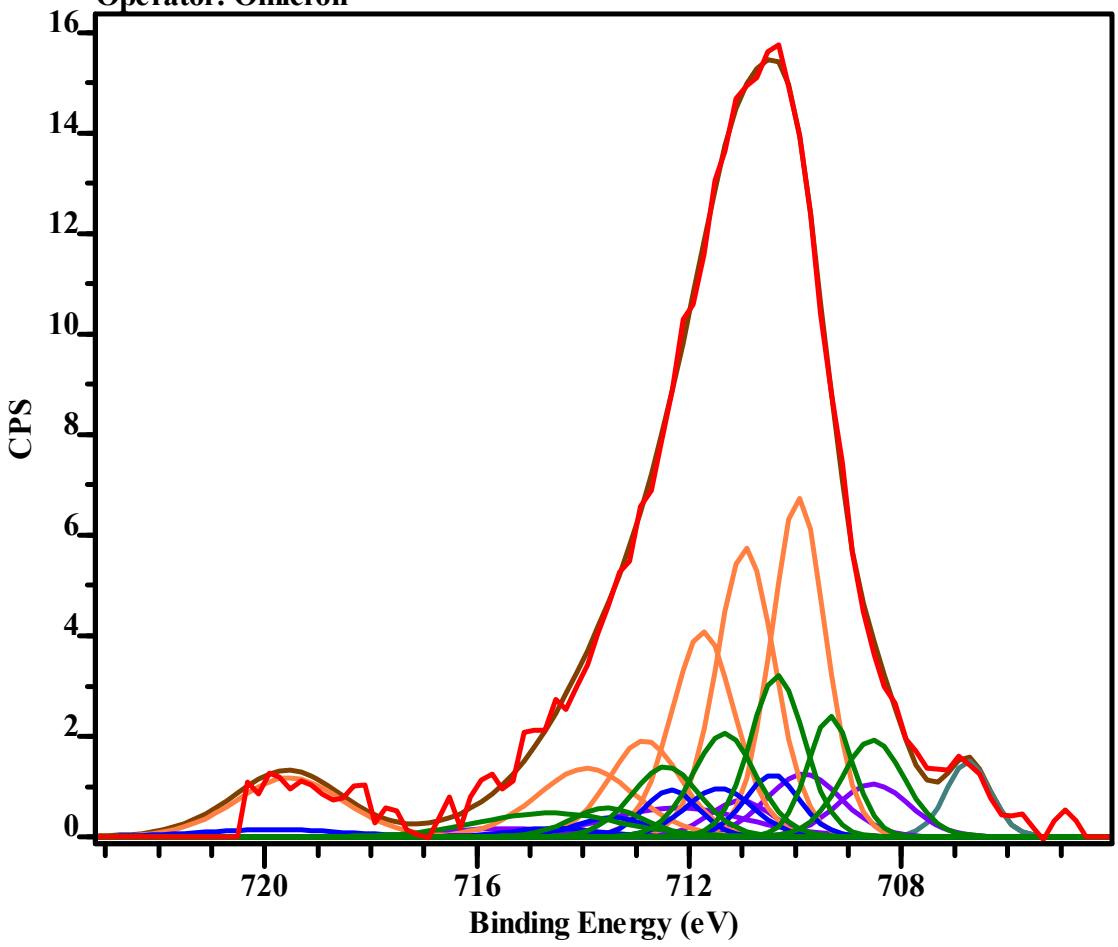

Fe 2p Region in Sterile Interface UA 4 Week Sample
Data Set 27 d
Pass Energy: 10 W.F.: 4.55 Energy Step 0.200 eV
Total Acqu Time 2387 mins 30.000 s (750000.0 ms x 1 x 191)
Acquired On: 2018/ 3/ 7 9:30:50
Source: Al Ka 1486.7 eV mono (225 W)
Operator: Omicron

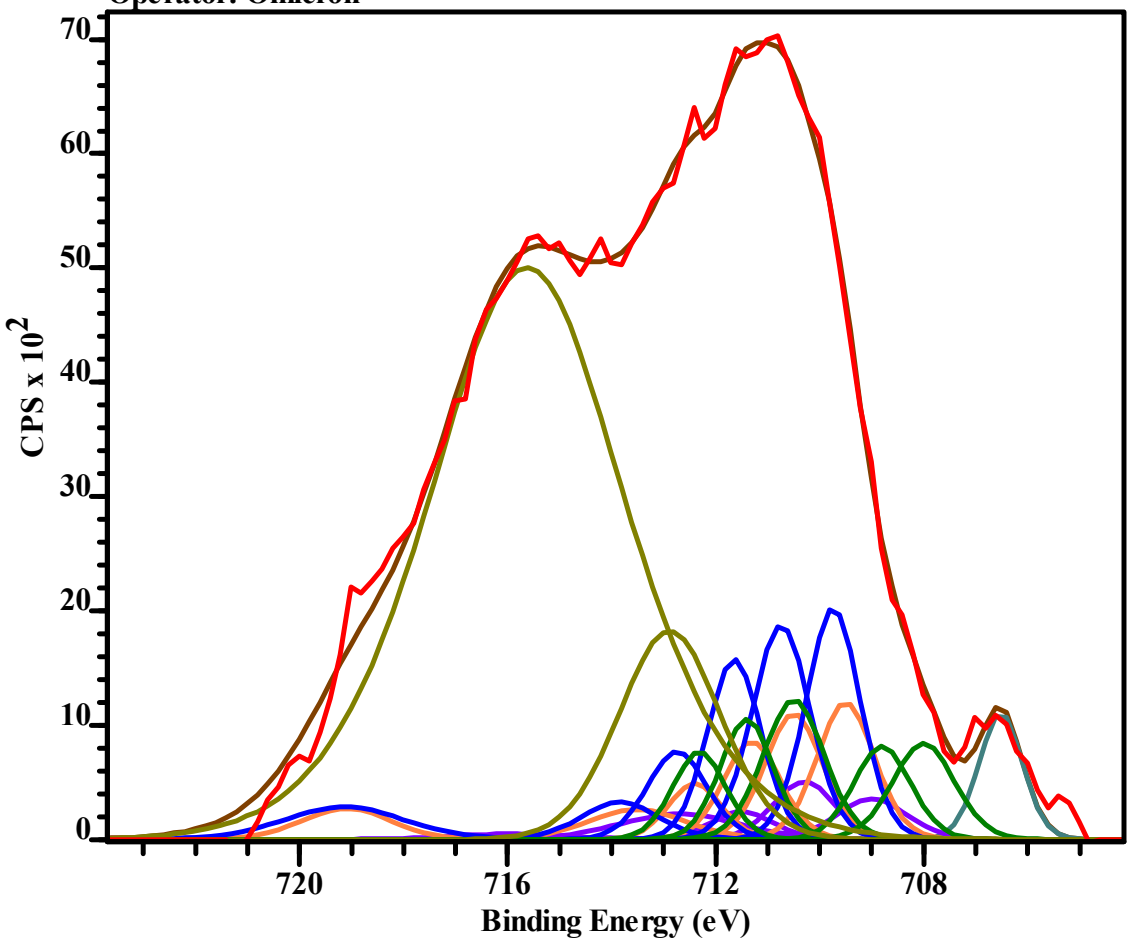

Fe 2p Region in Sterile Water Exposed UA 4 Week Sample
Data Set 30 d
Pass Energy: 10 W.F.: 4.55 Energy Step 0.200 eV
Total Acqu Time 1387 mins 56.000 s (436000.0 ms x 1 x 191)
Acquired On: 2018/ 3/ 4 10:56:20
Source: Al Ka 1486.7 eV normal (225 W)
Operator: Omicron

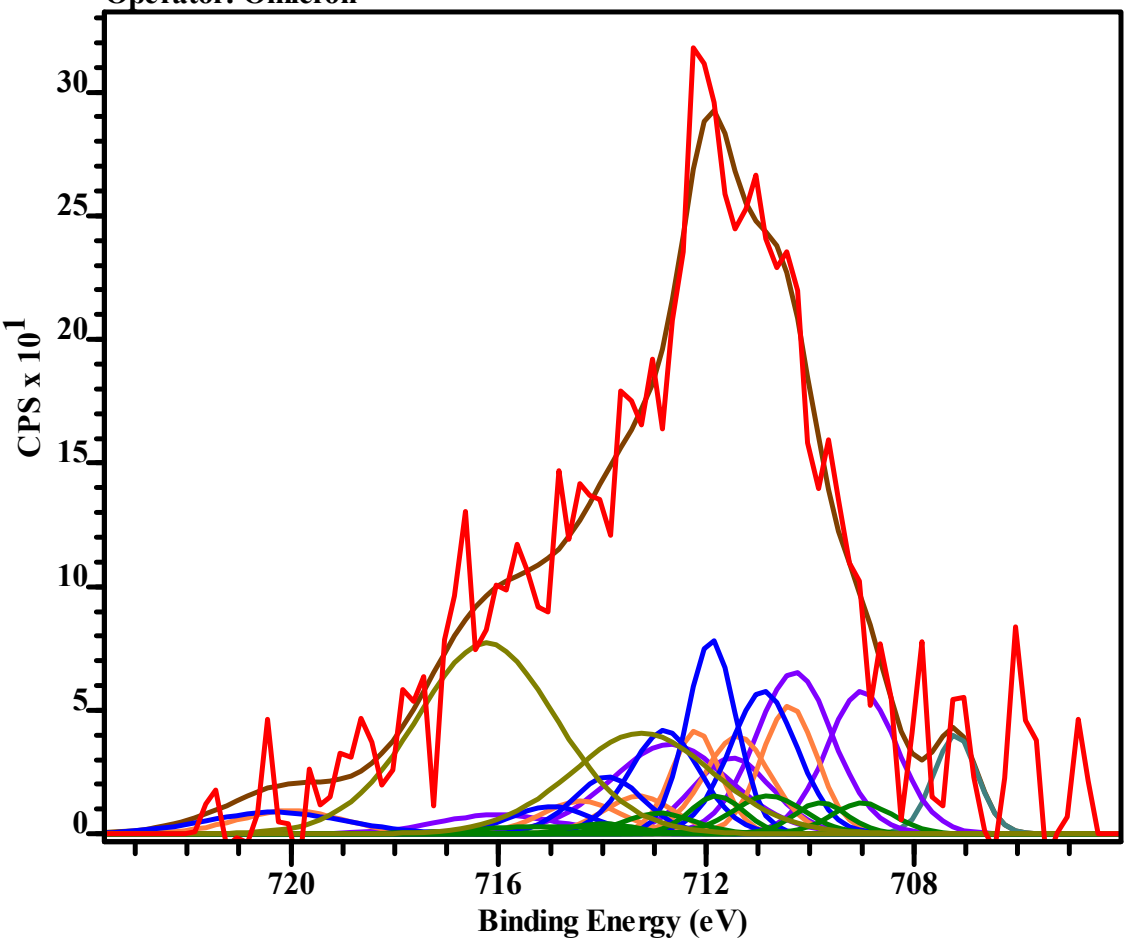

Fe 2p Region in Air Exposed AFRL 2 Week Sample

Data Set 32 d

Pass Energy: 10 W.F.: 4.55 Energy Step 0.200 eV

Total Acqu Time 636 mins 40.000 s (200000.0 ms x 1 x 191)

Acquired On: 2018/ 1/17 8:35:3

Source: Al Ka 1486.7 eV normal (225 W)

Operator: Omicron

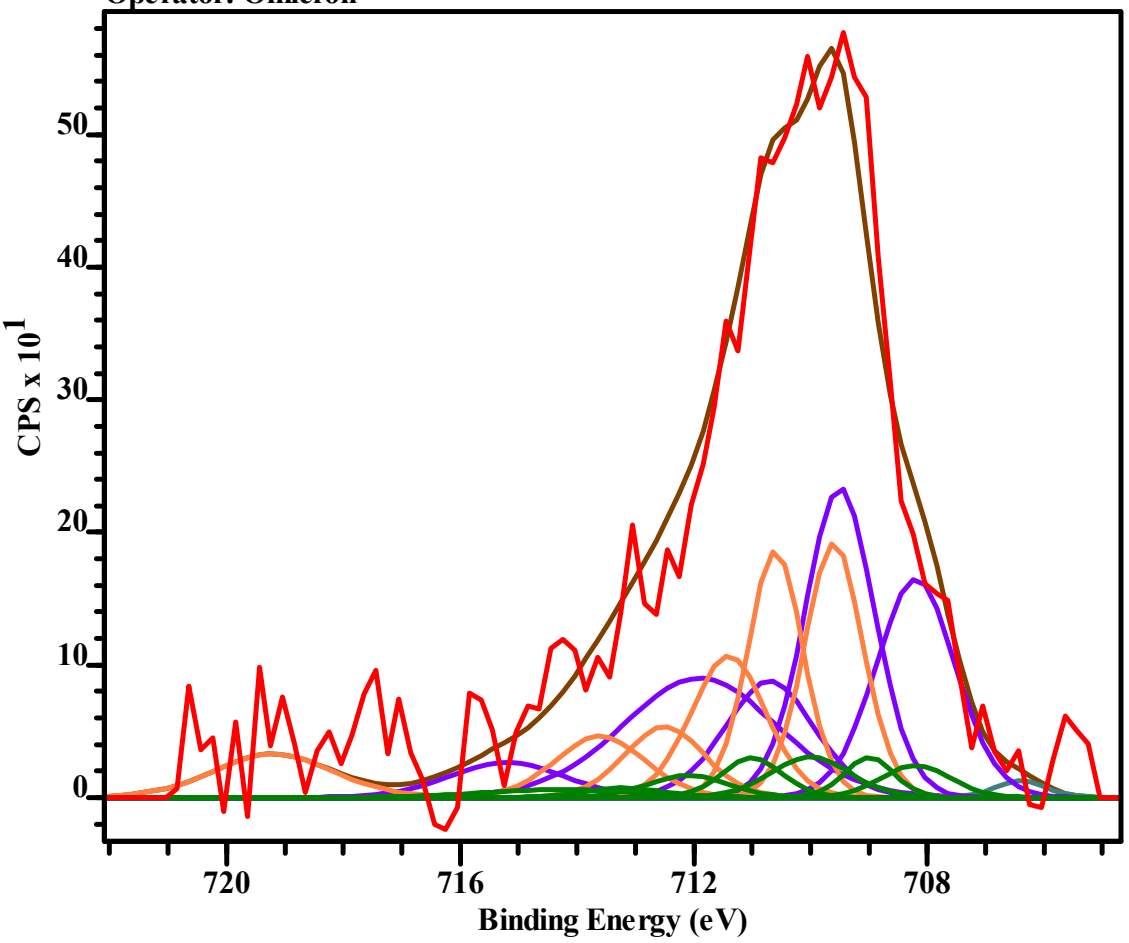

Fe 2p Region in Interface AFRL 2 Week Sample

Data Set 35 d

Pass Energy: 10 W.F.: 4.55 Energy Step 0.200 eV

Total Acqu Time 636 mins 40.000 s (200000.0 ms x 1 x 191)

Acquired On: 2018/ 1/14 10:25:34

Source: Al Ka 1486.7 eV normal (225 W)

Operator: Omicron

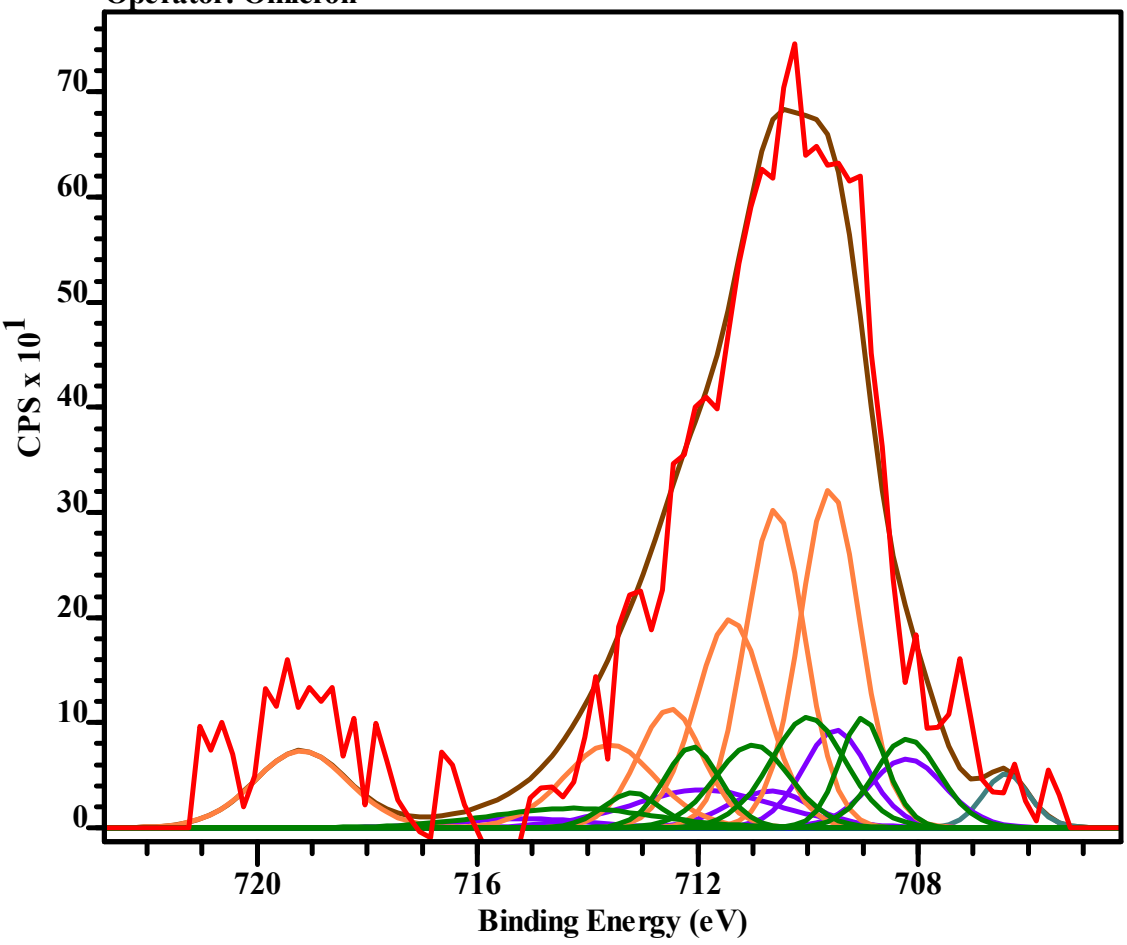

Fe 2p Region in Water Exposed AFRL 2 Week Sample
Data Set 38 d
Pass Energy: 10 W.F.: 4.55 Energy Step 0.200 eV
Total Acqu Time 636 mins 40.000 s (200000.0 ms x 1 x 191)
Acquired On: 2018/ 1/13 9:20:51
Source: Al Ka 1486.7 eV normal (225 W)
Operator: Omicron

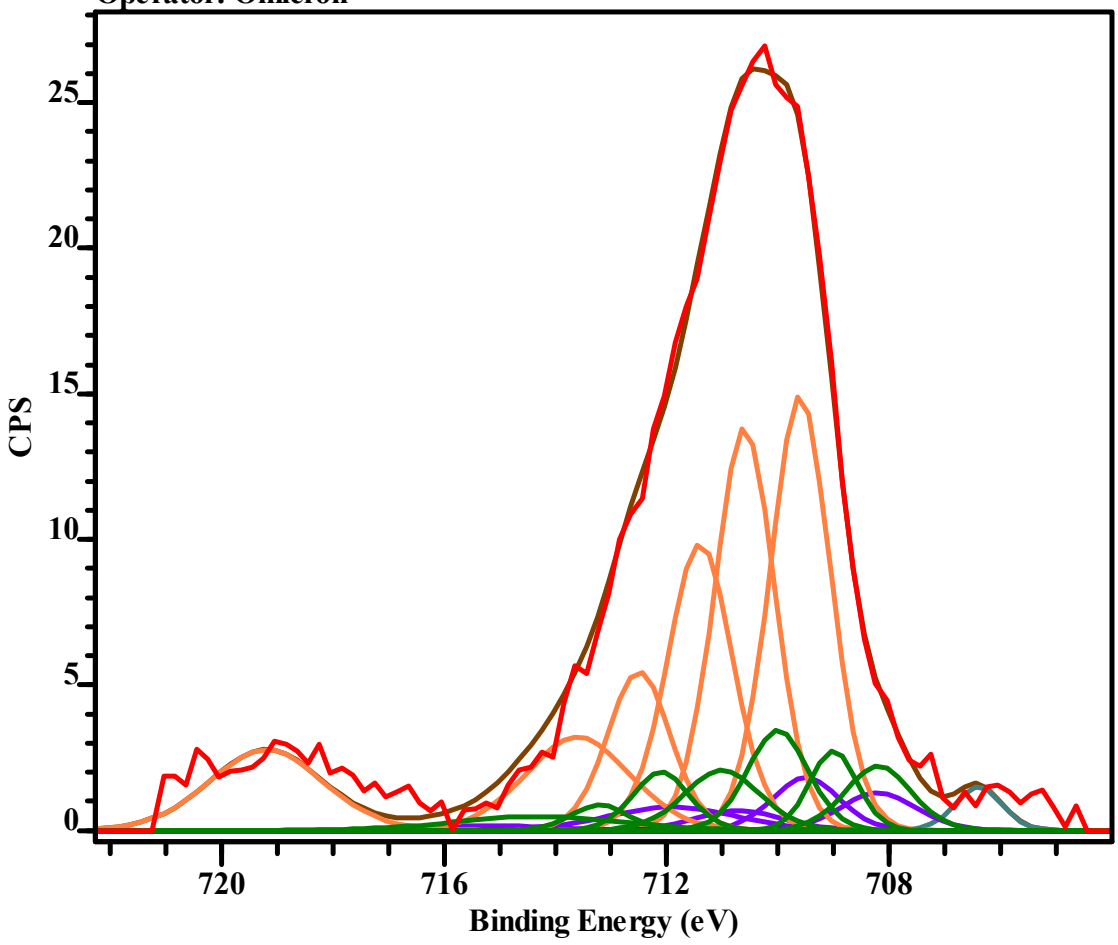

Bibliography

Beech, I. B., & Gaylarde, C. C. (1999). Recent advances in the study of biocorrosion: an overview. *Revista de Microbiologia*, *30*(3), 177–190. https://doi.org/10.1590/S0001-37141999000300001

Blake W. Stamps, Caitlin L. Bojanowski, Carrie A. Drake, Heather S. Nunn, P. F., Lloyd, James G. Floyd, Katelyn A. Berberich, Abby R. Neal, W. J. C.-G., & Stevenson, B. S. (2018). Linking Fungal and Bacterial Proliferation to Microbiologically Influenced Corrosion in B20 Biodiesel Storage Tanks. Retrieved from https://www.biorxiv.org/content/early/2018/08/25/399428.full.pdf+html

Blaney, L. (2007a). Magnetite (Fe3O4): Properties, Synthesis, and Applications. *Lehigh Review*, *15*(5), 33–81. https://doi.org/10.1016/j.ceramint.2011.11.027

Blaney, L. (2007b). Magnetite (Fe3O4): Properties, Synthesis, and Applications. *Lehigh Review*, *15*(5), 33–81. https://doi.org/10.1016/j.ceramint.2011.11.027

Briggs, D., & Grant, J. T. (2003). Surface Analysis by Auger and X-Ray Photoelectron Spectroscopy. In *Surface Analysis by Auger and X-Ray Photoelectron Spectroscopy* (pp. 31–56). https://doi.org/10.1016/0378-5963(78)90014-4

Bücker, F., Barbosa, C. S., Quadros, P. D., Bueno, M. K., Fiori, P., Huang, C. te, … Bento, F. M. (2014). Fuel biodegradation and molecular characterization of microbial biofilms in stored diesel/biodiesel blend B10 and the effect of biocide. *International Biodeterioration and Biodegradation*, *95*(PB), 346–355. https://doi.org/10.1016/j.ibiod.2014.05.030

Callister, W. D., & Rethwisch, D. G. (2009). *Materials science and engineering: An introduction (eight edition)*. *Materials & Design*. https://doi.org/10.1016/0261-

3069(91)90101-9

Casa software Ltd. (2009). CasaXPS Manual 2.3.15, 405.

Cornell, R. M., & Schwertmann, U. (2003). Crystal Structure. In *The Iron Oxides*. https://doi.org/10.1176/appi.neuropsych.17120351

Costello, J. A. (1974). Cathodic depolarization by sulphate reducing bacteria. *South African Journal of Science*.

Einstein, A. (1905). On a heuristic point of view concerning the creation and conversion of Light. *Annalen Der Physik*, *17*(132), 91. https://doi.org/10.1119/1.1973762

Eljuri, O. A. (2016). *Characterization of Fungal Contaminants in B20 Biodiesel Storage Tanks and Their Effect on Fuel Composition*. University of Oklahoma.

EPA. (2016). Investigation Of Corrosion-Influencing Factors In Underground Storage Tanks With Diesel Service, (EPA 510-R-16-001), 61.

Gaines, R. H. (1910). Bacterial activity as a corrosive influence in the soil. *Industrial and Engineering Chemistry*, *2*(4), 128–130. https://doi.org/10.1021/ie50016a003

Gerhardus H. Koch, M. P. H., & Brongers, and N. G. T. Y. P. V. J. H. P. (2002). Corrosion costs and preventive strategies in the United States. *Summary*, 1–12. https://doi.org/FHWA-RD-01-156

Grass, G., Rensing, C., & Solioz, M. (2011). Metallic copper as an antimicrobial surface. *Applied and Environmental Microbiology*, *77*(5), 1541–1547. https://doi.org/10.1128/AEM.02766-10

Grosvenor, A. P., Kobe, B. A., Biesinger, M. C., & McIntyre, N. S. (2004). Investigation of multiplet splitting of Fe 2p XPS spectra and bonding in iron compounds. *Surface and Interface Analysis*, *36*(12), 1564–1574. https://doi.org/10.1002/sia.1984

Gu, T. (2014). Theoretical Modeling of the Possibility of Acid Producing Bacteria Causing Fast Pitting Biocorrosion. *Journal of Microbial & Biochemical Technology*, *06*(02), 68–74. https://doi.org/10.4172/1948-5948.1000124

Hamilton, W. A. (2003). Microbially influenced corrosion as a model system for the study of metal microbe interactions: A unifying electron transfer hypothesis. *Biofouling*, *19*(1), 65–76. https://doi.org/10.1080/0892701021000041078

Herrera, L. K., & Videla, H. A. (2005). Microbiologically influenced corrosion : looking to the future. *INTERNATIONAL MICROBIOLOGY*, 169–180.

Hestrin, S., & Schramm, M. (1954). Synthesis of cellulose by *Acetobacter xylinum* . 2. Preparation of freeze-dried cells capable of polymerizing glucose to cellulose. *Biochemical Journal*, *58*(2), 345–352. https://doi.org/10.1042/bj0580345

Hussin, R., Ismail, N., & Mustapa, S. (2016). A study of foreign object damage (FOD) and prevention method at the airport and aircraft maintenance area. *IOP Conference Series: Materials Science and Engineering*, *152*(1). https://doi.org/10.1088/1757-899X/152/1/012038

Jenkin, J. G., Leckey, R. C. G., & Liesegang, J. (1977). The development of x-ray photoelectron spectroscopy: 1900-1960. *Journal of Electron Spectroscopy and Related Phenomena*, *12*(1), 1–35. https://doi.org/10.1016/0368-2048(77)85065-2

Johnson, D. B., & McGinness, S. (1991). Ferric iron reduction by acidophilic heterotrophic bacteria. *Applied and Environmental Microbiology*, *57*(1), 207–211.

Kip, N., & Van Veen, J. A. (2015). The dual role of microbes in corrosion. *ISME Journal*, *9*(3), 542–551. https://doi.org/10.1038/ismej.2014.169

Klassen, S. (2008). The Photoelectric Effect: Rehabilitating the Story for the Physics

Classroom. *Proceedings of the Second International Conference on Story in Science Teaching*, 1–18.

Landolt, D. (2007). *Corrosion and Surface Chemistry of Metals*. *EPFL Press*. New York.

Lee, J. S., Ray, R. I., & Little, B. J. (2010). An assessment of alternative diesel fuels: Microbiological contamination and corrosion under storage conditions. *Biofouling*, *26*(6), 623–635. https://doi.org/10.1080/08927014.2010.504984

Lee, W., Lewandowski, Z., Nielsen, P. H., & Allan Hamilton, W. (1995). Role of sulfate-reducing bacteria in corrosion of mild steel: A review. *Biofouling*. https://doi.org/10.1080/08927019509378271

Levine, I. N. (1983). *Physical Chemistry Second Edition*. *Mc Graw Hill*. https://doi.org/10.1017/CBO9781107415324.004

Mattsson, E. (2001). Basic electrochemical concepts. *Basic Corrosion Technology for Scientists and Engineers*, 204. Retrieved from http://books.google.com/books?id=l9JRAAAAMAAJ&pgis=1

McNamara, C., Perry, T., Leard, R., Bearce, K., Dante, J., & Mitchell, R. (2005). Corrosion of aluminum alloy 2024 by microorganisms isolated from aircraft fuel tanks. *Biofouling*. https://doi.org/10.1080/08927010500389921

Meyers, M. A., & Taylor Aimone, C. (1983). Dynamic fracture (spalling) of metals. *Progress in Materials Science*. https://doi.org/10.1016/0079-6425(83)90003-8

Ottow, G., Ottow, J. C., & Von Klopotek, a. (1969). Enzymatic Reduction of Iron Oxide by Fungi. *Applied Microbiology*, *18*(I), 41–43.

Prince, R. C., Haitmanek, C., & Lee, C. C. (2008). The primary aerobic biodegradation of biodiesel B20. *Chemosphere*, *71*(8), 1446–1451.

https://doi.org/10.1016/j.chemosphere.2007.12.010

Proctor, A., & Sherwood, P. M. A. (1982). Data Analysis Techniques in X-ray Photoelectron Spectroscopy. *Analytical Chemistry*, *54*(1), 13–19. https://doi.org/10.1021/ac00238a008

Rauch, M. E., Graef, H. W., Rozenzhak, S. M., Jones, S. E., Bleckmann, C. A., Kruger, R. L., … Stone, M. O. (2006). Characterization of microbial contamination in United States Air Force aviation fuel tanks. *Journal of Industrial Microbiology and Biotechnology*, *33*(1), 29–36. https://doi.org/10.1007/s10295-005-0023-x

Rutherford, E., Robinson, H., & Rawlinson, W. F. (1914). XXXIV. *Spectrum of the β rays excited by γ rays*. *The London, Edinburgh, and Dublin Philosophical Magazine and Journal of Science*, *28*(164), 281–286. https://doi.org/10.1080/14786440808635210

Sherwood, P. M. A. (1996). Curve fitting in surface analysis and the effect of background inclusion in the fitting process. *Journal of Vacuum Science & Technology A: Vacuum, Surfaces, and Films*, *14*(3), 1424–1432. https://doi.org/10.1116/1.579964

Sokolowski, E., Nordling, C., & Siegbahn, K. (1958). Chemical shift effect in inner electronic levels of cu due to oxidation [9]. *Physical Review*. https://doi.org/10.1103/PhysRev.110.776

Steinhardt, R. G., & Serfass, E. J. (1951). X-Ray Photoelectron Spectrometer for Chemical Analysis. *Analytical Chemistry*, *23*(11), 1585–1590. https://doi.org/10.1021/ac60059a019

Stuewer, R. H. (1983). The nuclear electron hypothesis. *Otto Hahn and the Rise of Nuclear Physics*, 19–67.

Suzuki, I., Masuko, N., & Hisamatsu, Y. (1979). Electrochemical properties of iron rust. *Corrosion Science*, *19*(7), 521–535. https://doi.org/10.1016/S0010-938X(79)80057-8

US Air Force. (2016). Air Force Manual. *32-1084*. United States Air Force.

Van Attekum, P. M. T. M., & Trooster, J. M. (1979). An X-ray photoelectron spectroscopy of PdSb, PtBi and AuSn. *Journal of Physics F: Metal Physics*. https://doi.org/10.1088/0305-4608/9/11/018

Videla, H. A., & Characklis, W. G. (1992). Biofouling and microbially influenced corrosion. *International Biodeterioration and Biodegradation*, *29*(3–4), 195–212. https://doi.org/10.1016/0964-8305(92)90044-O

WHOI. (1952). The History of the Prevention of Fouling. *Marine Fouling and Its Prevention*, (580), 211–222.

Xu, D., Li, Y., & Gu, T. (2016). Mechanistic modeling of biocorrosion caused by biofilms of sulfate reducing bacteria and acid producing bacteria. *Bioelectrochemistry*, *110*, 52–58. https://doi.org/10.1016/j.bioelechem.2016.03.003

Yuan, S. J., & Pehkonen, S. O. (2007). Microbiologically influenced corrosion of 304 stainless steel by aerobic Pseudomonas NCIMB 2021 bacteria: AFM and XPS study. *Colloids and Surfaces B: Biointerfaces*, *59*(1), 87–99. https://doi.org/10.1016/j.colsurfb.2007.04.020

Zimbro, M. J., Power, D. A., Miller, S. M., Wilson, G. E., & Johnson, J. A. (2009). *Difco & BBL Manual: Manual of Microbiological Culture Media*. *Citeseer*. https://doi.org/10.1002/1521-3773(20010316)40:6<9823::AID-ANIE9823>3.3.CO;2-C

REPORT DOCUMENTATION PAGE

Form Approved
OMB No. 074-0188

PLEASE DO NOT RETURN YOUR FORM TO THE ABOVE ADDRESS.

1. REPORT DATE *(DD-MM-YYYY)*	2. REPORT TYPE	3. DATES COVERED *(From – To)*
21-03-2019	Master's Thesis	Sept 2017- March 2019

4. TITLE AND SUBTITLE
Analysis of the Effect of Corrosion on the Surface Chemistry of Mild Steel Exposed to Biofuel

5a. CONTRACT NUMBER

5b. GRANT NUMBER

5c. PROGRAM ELEMENT NUMBER

6. AUTHOR(S)
Plourde, Timothy D., Captain, USAF

5d. PROJECT NUMBER
18V216

5e. TASK NUMBER

5f. WORK UNIT NUMBER

7. PERFORMING ORGANIZATION NAMES(S) AND ADDRESS(S)
Air Force Institute of Technology
Graduate School of Engineering and Management (AFIT/ENV)
2950 Hobson Way, Building 640
WPAFB OH 45433-8865

8. PERFORMING ORGANIZATION REPORT NUMBER
AFIT-ENV-MS-19-M-193

9. SPONSORING/MONITORING AGENCY NAME(S) AND ADDRESS(ES)
Air Force Research Laboratory
Biological Scientist Dr. Caitlin Bojanowski
AFRL/RXA 2179 12th Street
WPAFB, OH 45433-7718
(937)255-5180 DSN: 785-5180 Email: Caitlin.Bojanowski.1@us.af.mil

10. SPONSOR/MONITOR'S ACRONYM(S)
AFRL

11. SPONSOR/MONITOR'S REPORT NUMBER(S)

12. DISTRIBUTION/AVAILABILITY STATEMENT
DISTRIBUTION STATEMENT A. APPROVED FOR PUBLIC RELEASE; DISTRIBUTION UNLIMITED.

13. SUPPLEMENTARY NOTES
This work is declared a work of the U.S. Government and is not subject to copyright protection in the United States.

14. ABSTRACT
The use of biofuels in society is steadily becoming more prevalent. Through this proliferation a concern regarding the role of the fungus Byssochlamys nivea in microbially induced corrosion has surfaced. Through the use of X-ray Photoelectron Spectroscopy (XPS) and Scanning Electron Microscope (SEM) technology, this thesis focused on attempting to determine what effect, if any, Byssochlamys nivea has on the corrosion of mild steel. For this analysis, samples were placed in environments that simulated the conditions of fuel tanks containing the biofuel B20, water, and spores of Byssochlamys nivea for varying lengths of time. However, due to a variety of complicating factors involving the development of the samples analyzed in this thesis, no clear determination can be drawn about the influence of Byssochlamys nivea on mild steel. Some evidence may point towards microbially induced corrosion occurring in the form of iron reduction, however no conclusive statements on such a matter can be claimed, due to the lack of a comparable control. As such, the findings of this thesis ultimately describe the methods by which future researchers should carry out the preparation and execution of the experiment and analysis in order to identify microbially influenced corrosion in mild steel that results from Byssochlamys nivea.

15. SUBJECT TERMS
Biofuel, X-Ray Photoelectric Spectroscopy, Microbially Induced Corrosion, Biocorrosion

16. SECURITY CLASSIFICATION OF:			17. LIMITATION OF ABSTRACT	18. NUMBER OF PAGES	19a. NAME OF RESPONSIBLE PERSON
a. REPORT	b. ABSTRACT	c. THIS PAGE			Slagley, Jeremy M. Ph.D, USAF
U	U	U	UU	127	19b. TELEPHONE NUMBER *(Include area code)* (937) 255-3636, x 4632 (jeremy.slagley.1@afit.edu)